University of Minnesota
St. Anthony Falls Hydraulic Laboratory

Project Report No. 209

RESQUAL II: A DYNAMIC WATER QUALITY SIMULATION PROGRAM FOR A STRATIFIED SHALLOW LAKE OR RESERVOIR: APPLICATION TO LAKE CHICOT, ARKANSAS

by

Heinz G. Stefan, John J. Cardoni,

and Alec Y. Fu

Prepared for

U. S. DEPARTMENT OF AGRICULTURE
Water Quality and Watershed Research Laboratories
Durant, Oklahoma 74701

and

U. S. ARMY CORPS OF ENGINEERS
Vicksburg District
Vicksburg, Mississippi 39180

December, 1982

The University of Minnesota is committed to the policy that all persons shall have equal access to its programs, facilities, and employment without regard to race, creed, color, sex, national origin, or handicap.

ACKNOWLEDGEMENTS

This report summarizes the development of a water quality model primarily to predict post-construction turbidity of Lake Chicot, Arkansas. Overall responsibility of the Lake Chicot project lies with the Army Corps of Engineers, Vicksburg District. In the form described herein model RESQUAL II simulates water quality in a stratified or non-stratified shallow reservoir or lake with inflow and surface outflow. Specifically, the model predicts daily values of the following parameters:

- Lake stage
- Mixed layer depth
- Water temperature
- Suspended sediment concentration
- Phytoplankton chlorophyll-a concentration
- Dissolved orthophosphorus concentration
- Total phosphorus
- Secchi depth

Model development benefited from the earlier work done by S. Dhamotharan and inputs from Frank R. Schiebe, Charles M. Cooper, and Mark J. Hanson.

The USDA provided extensive field data and much other pertinent information. The study was conducted under cooperative agreement between the St. Anthony Falls Hydraulic Laboratory, University of Minnesota, and the USDA Water Quality and Watershed Research Laboratories, Durant, Oklahoma.

TABLE OF CONTENTS

LIST OF FIGURES

Figure No.

Figure No.

LIST OF TABLES

LAKE CHICOT, ARKANSAS--RESTORATION

AVAILABLE PUBLICATIONS
(July, 1982)

A. Subtopic Studies

St. Anthony Falls Hydraulic Laboratory
University of Minnesota

External Memorandum No. 152. Lake Chicot Field Study, by S. Dhamotharan and H. Stefan, 107 pages, Dec. 1977.

External Memorandum No. 174. A Model of Light Penetration in Lake Chicot, by H. G. Stefan, J. J. Cardoni, F. R. Schiebe, and C. M. Cooper, 52 pages, Feb., 1982.

External Memorandum No. 176. Lake Chicot Intensive Field Investigations: June 30 to July 10, 1981, by J. J. Cardoni and M. J. Hanson, 92 pages, Dec., 1981.

External Memorandum No. 177. A Model for Light and Temperature Controlled Primary Productivity in Lake Chicot, Arkansas, by J. J. Cardoni and H. G. Stefan, 46 pages, July, 1982.

External Memorandum No. 178. A Model of Phosphorus Available for Phytoplankton Growth in Lake Chicot, Arkansas, J. J. Cardoni, M. J. Hanson, and H. G. Stefan, 31 pages, July, 1982.

External Memorandum No. 179. User Instructions for RESQUAL II, A Dynamic Water Quality Simulation Model for a Stratified Shallow Lake or Reservoir, by A. Y. Fu, 174 pages, July, 1982.

Internal Memorandum No. 99. Concepts for a Nitrogen Cycling Model of Lake Chicot Arkansas, by L. Baker, 19 pages, July, 1982.

B. Papers Published

Dhamotharan, S., Stefan, H. G. and Schiebe, F. R.. Turbid Reservoir Stratification Modelling, Proc. 26th Annual Hydr. Div. Specialty Conf., ASCE, Univ. of Maryland, pp. 156-163, Aug., 1978.

Dhamotharan, S., Prediction of Post Construction Turbidity of Lake Chicot, Arkansas, Proc. Int'l Symp. on Environmental Effects of Hydraulic Engineering Works, TVA, IAHR, pp. 146-159, Sept., 1978.

Schiebe, F. R., Farell, J. O. and McHenry, J. R. Water Quality Improvement of Lake Chicot, Arkansas, Proc. Symp. on Surface Water Impoundments, ASCE, pp. 686-693, Oct., 1981

Dhamotharan, S. and Stefan, H. G. Mathematical Model for Temperature and Turbidity Stratification in Shallow Reservoirs, Proc. Symp. on Surface Water Impoundments, ASCE, pp. 613-623, Oct. 1981.

Cooper, C. M. and Bacon, E. J. Effects of Suspended Sediments on Primary Productivity in Lake Chicot, Arkansas, Proc. Symp. on Surface Water Impoundments, ASCE, pp. 1357-67, Oct., 1981.

Stefan, H. G., Schiebe, F. R. and Dhamotharan, S. Temperature/Sediment Model for a Shallow Lake, Proc. ASCE, Jour. Env. Engr. Div., Vol. 108, No. EE4, Aug., 1982.

Stefan, H. G., Cardoni, J. J., Schiebe, F. R., and Cooper, C. M. A Model of Light Penetration in Lake Chicot, Water Resources Research, AGU, accepted (1982).

C. Field Data Reports & Analysis

Bacon, E. J. Primary productivity, water quality, and limiting factors in Lake Chicot: Arkansas Water Resources Resesarch Center, Fayetteville, AR, Publ. No. 56, Resources Research center, 1978.

Bacon, E. J. Primary Productivy in Lake Chicot, Chicot County, Arkansas, Quarterly Progress Reports, University of Arkansas, Monticello, AR, Oct. 1977 to Sept. 1980.

Cardoni and Hanson. (External Memorandum M-176 in Section A)

Cooper and Bacon. (1981 - Paper in Section B)

Environmental Protection Agency. Report on Chicot Lake, Chicot County, Arkansas, EPA Region VI. National Eutrophication Survey, Environmental Monitoring and Support Laboratory, Las Vegas NV and Corvallis Environmental Research Laboratory, Corvallis, OR. Working Paper No. 484, 17 pages, 1977.

Swain, A. Material Budgets of Lake Chicot, Ph. D. Dissertation, University of Mississippi, Oxford, MS, 190 pages, 1980.

USDA-ARS. An Assessment and Evaluation of Hydrological, Chemical and Microbiological Regimes of Lake Chicot, Arkansas. Quarterly Progress Reports, Sedimentation Laboratory, USDA-ARS, Oxford, Miss., Oct. 1977 to Sept. 1980.

I. INTRODUCTION

The inflow of fine suspended sediment from Connerly Bayou into Lake Chicot, Arkansas (Figs. I-1 and I-2) has caused a profound change in the appearance, the ecology, and the recreational use of the lake. Before 1920, Lake Chicot, a large oxbow lake with limited drainage area along the Mississippi River, was attractive for recreation. A disastrous flood in 1927, construction of levees, clearing of the land for row crops, and other events have significantly increased the suspended solids content and thereby the turbidity of the lake. To reduce the turbidity and to stabilize the lake level, the U. S. Army Corps of Engineers has constructed a new lake outlet structure and a 6500 cfs pumping station to divert inflow from Connerly Bayou to the Mississippi River (Rothwell and Fletcher, 1979; Schiebe et al., 1981).

The present water quality of the lake has been documented in publications by the EPA (1977), Bacon (1978, 1980), Cooper and Bacon (1981), and Cardoni and Hanson (1981). The material and nutrient budgets of the lake have been studied by Swain (1980). Swain also examined correlation between hydrologic and water quality parameters in the lake. Since July 1976, the U. S. Department of Agriculture's Sedimentation Laboratory at Oxford, Mississippi, and since January, 1980, the USDA Water Quality Laboratory in Durant, Oklahoma, have been monitoring the lake's hydrological, chemical, and microbiological regimes. These studies have produced extensive baseline data as part of the preconstruction assessments, and they will be continued in order to document lake changes as a result of future inflow diversion and stage management. To assist in the interpretation of the data and ultimately in the selection of lake operational management alternatives, a process-oriented, dynamic model simulating several water quality parameters including transparency of the lake on a daily time scale, has been developed. Early stages of the model development were described at two symposia (Dhamotharan et al., 1978, 1981), and in a thesis (Dhamotharan, 1979). The model formulation will be summarized in this paper. The model is of interest not only for the solution of the Lake Chicot problem but has potential application in the design and operation of shallow detention basins and shallow reservoirs intended for the entrapment of suspended sediments.

Fig. I-1. LANDSAT image of Lake Chicot on 4/14/79, Band 7. High turbidity (light color) in lower lake and less turbidity in upper lake (dark color).

Fig. I-2. Aerial view of the dike separating the upper and lower basins of Lake Chicot. The lower and more turbid lake is on the right.

II. MODEL CONCEPT

Model RESQUAL II simulates lake stage, surface mixed layer depth, water temperature (T), suspended solids (SS), phytoplankton (Ch&a), available dissolved orthophosphorus (P_a), non-available particulate phosphorus (P_n), light attenuation coefficient (k) and Secchi depth (z_{SD}) in a shallow stratified reservoir. The primary objective is to simulate present and future transparency of the water. An earlier version of the model simulated only T and SS and was developed by Dhamotharan (1979).

The turbidity of Lake Chicot is the result of erosion and runoff from the watershed. It is for this reason that inflow diversion has been considered by the Corps of Engineers as a means to reduce turbidity in Lake Chicot. To simulate the response of the lake to any reduction in sediment loading all significant in-lake processes must be considered. These include stratification, turbulent diffusion, settling, resuspension, coagulation, growth kinetics in the case of phytoplankton, etc.(Fig. II-1). The mathematical model description of these processes uses the general flow chart shown in Fig. II-2. The elements shown in that flow chart will be described herein.

To account for the temperature and density stratification, a multilayer model (Fig. II-3) had to be formulated. To account for inflow and outflow, layers were chosen to be of variable thicknesses.

The mixing and density stratification dynamics of shallow reservoirs or lakes show a strong dependence on surface heat exchange and wind mixing at the air-water interface. A one-dimensional unsteady water temperature stratification and mixing model (MLTM) developed at the University of Minnesota (Ford, 1976; Stefan et al., 1975) for a daily timescale was used as a starting point for the RESQUAL model development. Additions and changes were made in the MLTM model to account for inflow, outflow, and the effects of suspended sediment on the heat transfer processes. Subsequently, an unsteady, mass-transport sub-model for suspended sediment was formulated. Results from the temperature stratification dynamics model are used as input to the suspended sediment model. Results from the suspended sediment distribution simulation are necessary in turn to specify attenuation and reflection of radiation in the heat transfer relationships in the dynamic temperature model. Subsequently, submodels for a density current inflow, for light attenuation, for phytoplankton, for phosphorus, and for Secchi depth were added.

The RESQUAL II model gives the water quality changes as a function of depth and on a day by day basis in response to real weather, also specified on a day by day basis. It is therefore possible to use the model

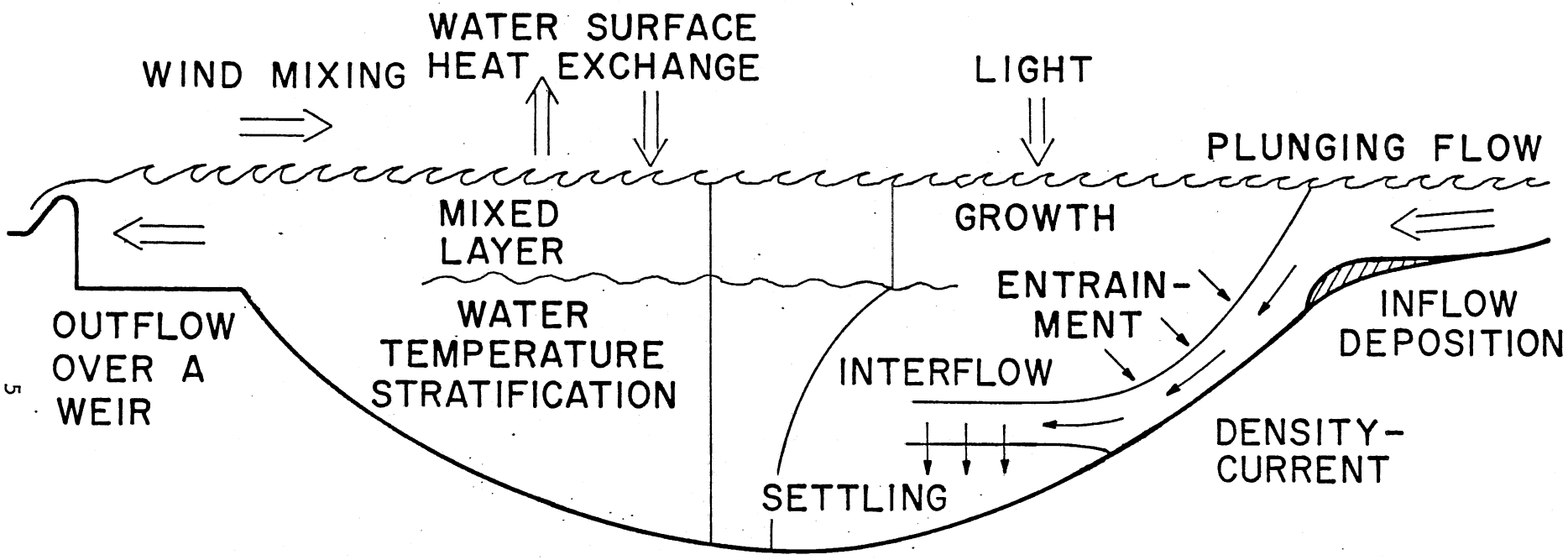

Fig. II-1. Schematic of physical processes represented by model RESQUAL

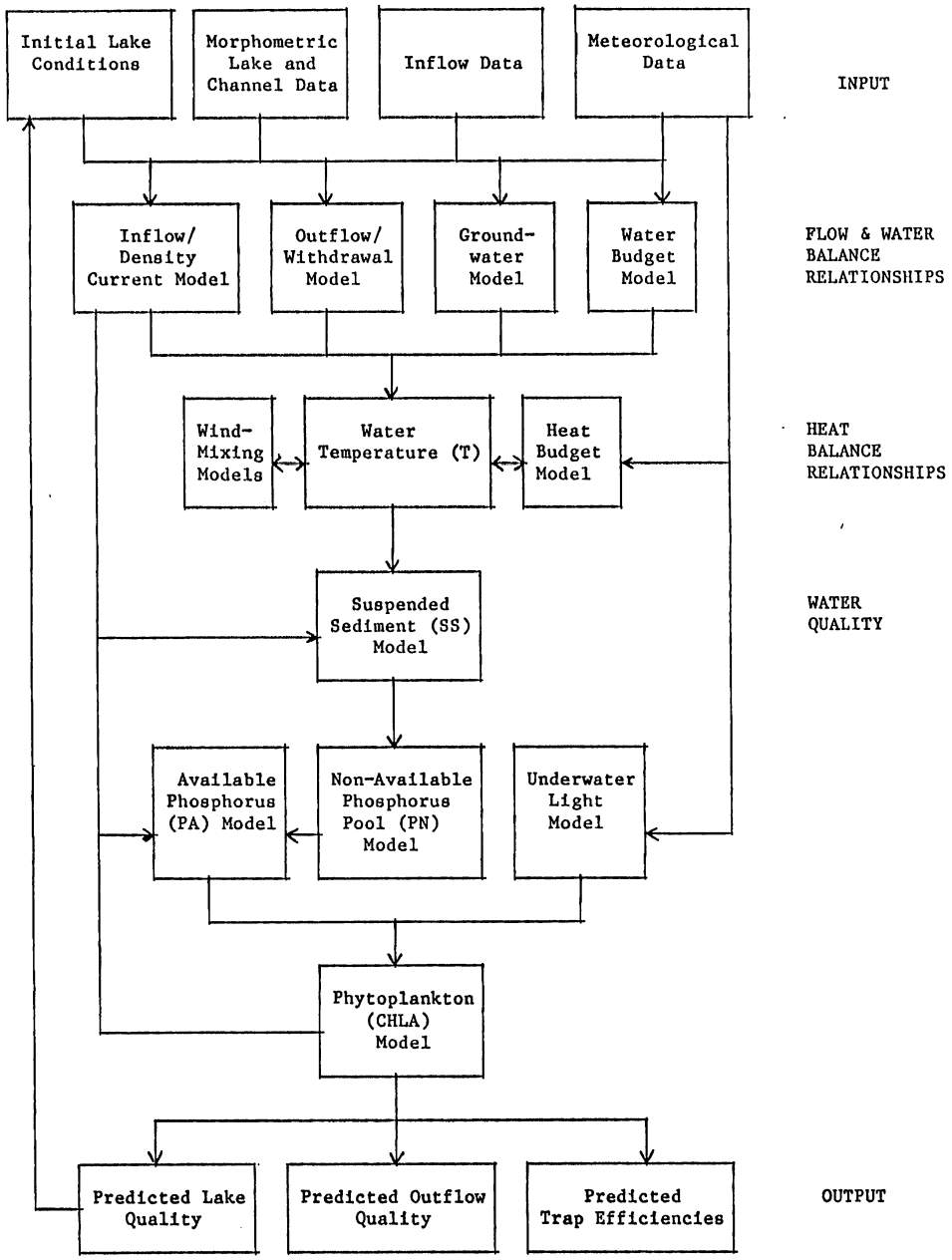

Fig. II-2. Information flow in RESQUAL II.

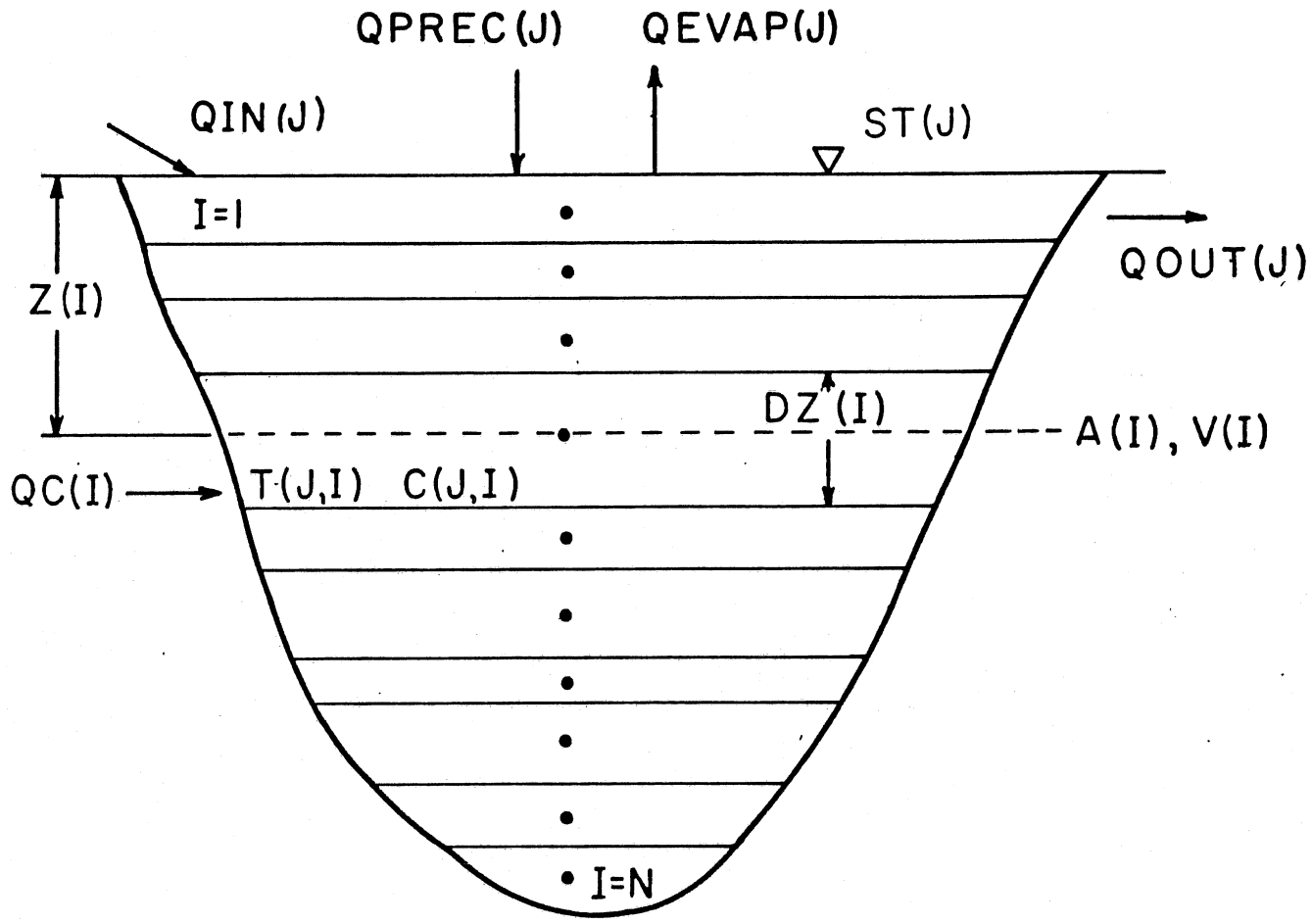

Fig. II-3. Schematic of reservoir subdivision and flow rates at timestep J.

(a) to simulate existing conditions by hindcasting with measured weather conditions,

(b) to predict conditions that would have existed had the inflow diversion been implemented, and

(c) to forecast conditions on a realtime basis for different diversion strategies.

III. INPUT DATA

A. Lake Morphology

Lake morphology is described by an equation developed by Dhamotharan (1979):

$$\frac{V}{V_{ref}} = \left(\frac{h}{h_{ref}} \right)^m \qquad \text{(III-1)}$$

where V = lake volume,

h = depth,

V_{ref} = reference volume at h_{ref}

h_{ref} = reference depth

m = 2.18 for lower lake

m = 1.57 for upper lake

A morphometric map of Lake Chicot is given in Fig. III-1. Some bathymetric data are summarized in Table III-1 and Fig. III-2.

From the above the following equations were developed for Volume V in (m^3)

$$V = 4046.8 \ (3.28^{m-1}) \ c \ h^m \qquad \text{(III-2)}$$

and projected horizontal area A in (m^2)

$$A = m \ c \ (3.28h)^{m-1} \qquad \text{(III-3)}$$

where c = 0.305 m/ft, and
h = depth in ft

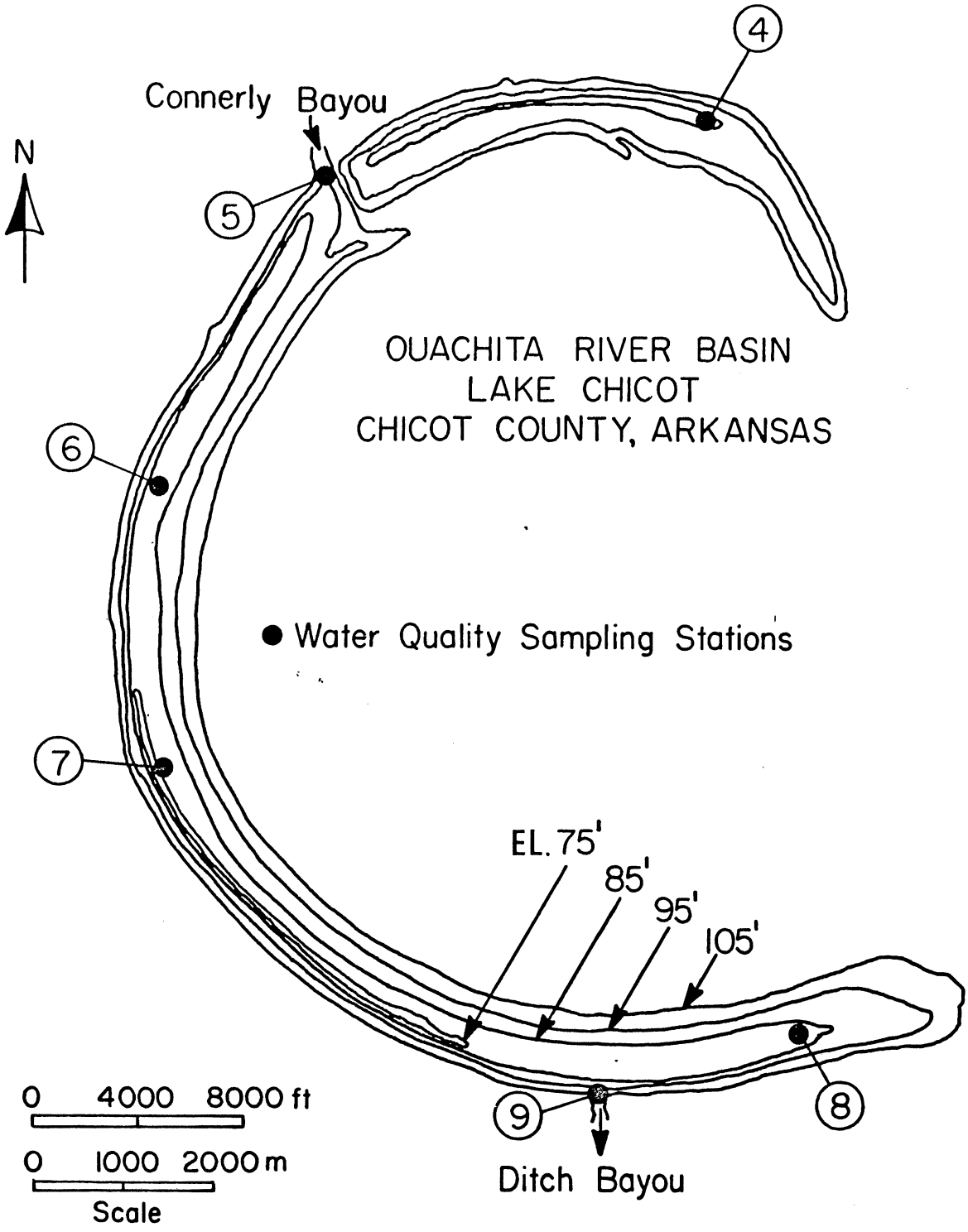

Fig. III-1. Morphometric map of Lake Chicot. (Bottom contour elevations in feet above MSL, 1 ft = 0.305 m).

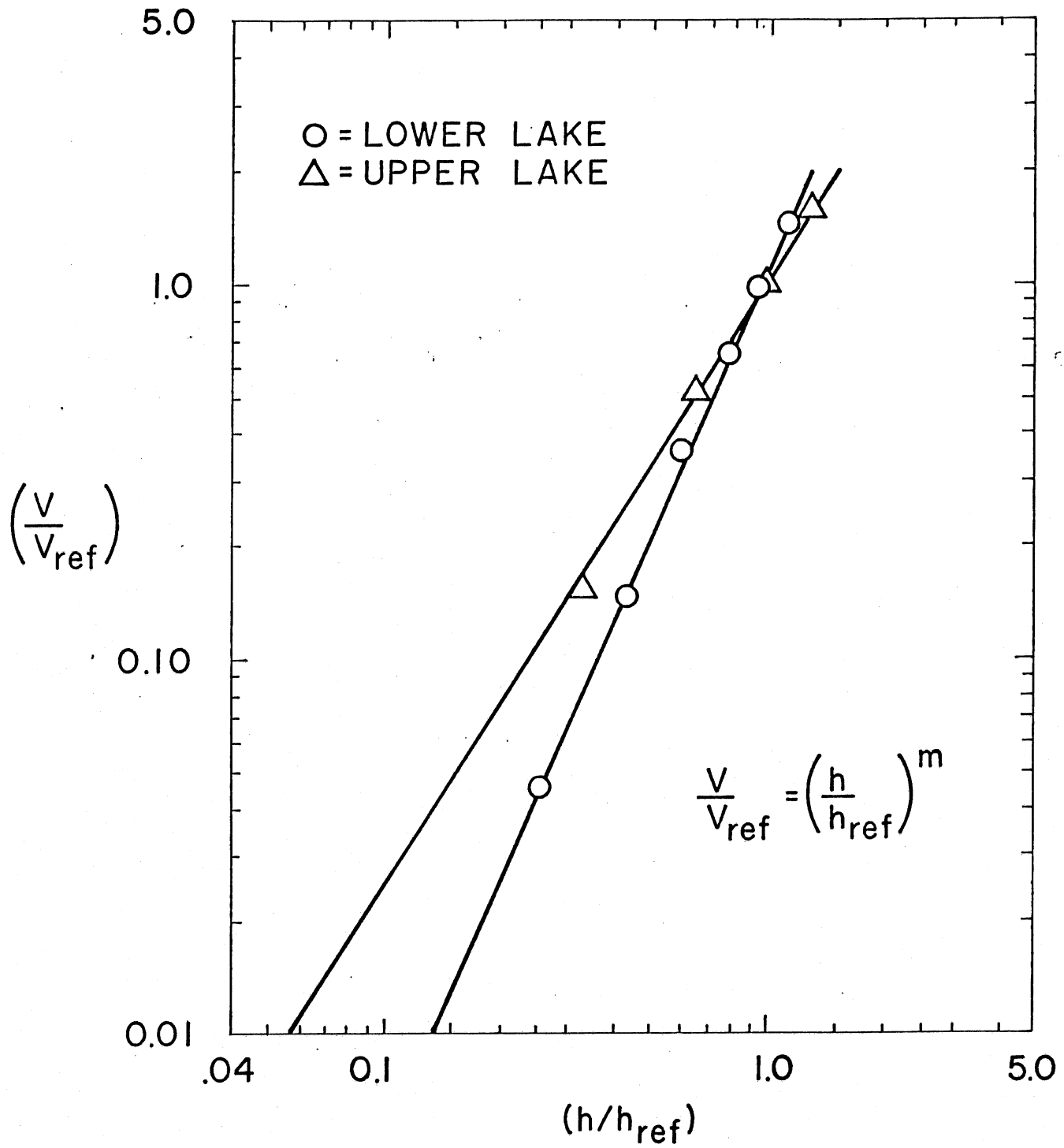

Fig. III-2. Plot of morphometric equation for upper and lower Lake Chicot.

TABLE III-1. BATHYMETRIC CHARACTERISTICS OF LAKE CHICOT

	Lower Lake	Upper Lake
Reference Pool Level	30.48 m above MSL (100 ft)	30.48 m above MSL (100 ft)
Maximum Effective* Depth (h_{ref})	8.29 m (27.2 ft)	4.52 m (15.5 ft)
Mean Depth (d_{ref})	3.8 m (12.5 ft)	3.0 m (9.9 ft)
Surface Area	13.63×10^6 m^2 (3369 ac.)	3.53×10^6 m^2 (873 ac.)
Volume (V_{ref})	51.85×10^6 m^3 (42036 ac. ft)	10.65×10^6 m^3 (8636 ac. ft)

*Effective refers to the deepest bed level 22.19 m.

B. Inflow

Inflow rates must be given. For Lake Chicot a stage/discharge relationship of the following form is used:

$$Q_C = 0.85\ Q_M^{0.99}$$

$$Q_M = 140.93\ (S_M - 105.63)^{1.72} \qquad \text{(III-4)}$$

where Q_C = discharge into Lake Chicot from Connerly Bayou

Q_M = discharge from Macon Lake

S_M = stage at Macon Lake in ft above MSL

The above equations were given by Swain (1980), Figs. III-3 and III-4. Water quality in the inflow (Connerly Bayou) is also specified by correlation functions given by Swain (1980) for suspended sediment:

$$SS_C = 6.55\ Q_{CAFD}^{.58} \qquad \text{(III-5)}$$

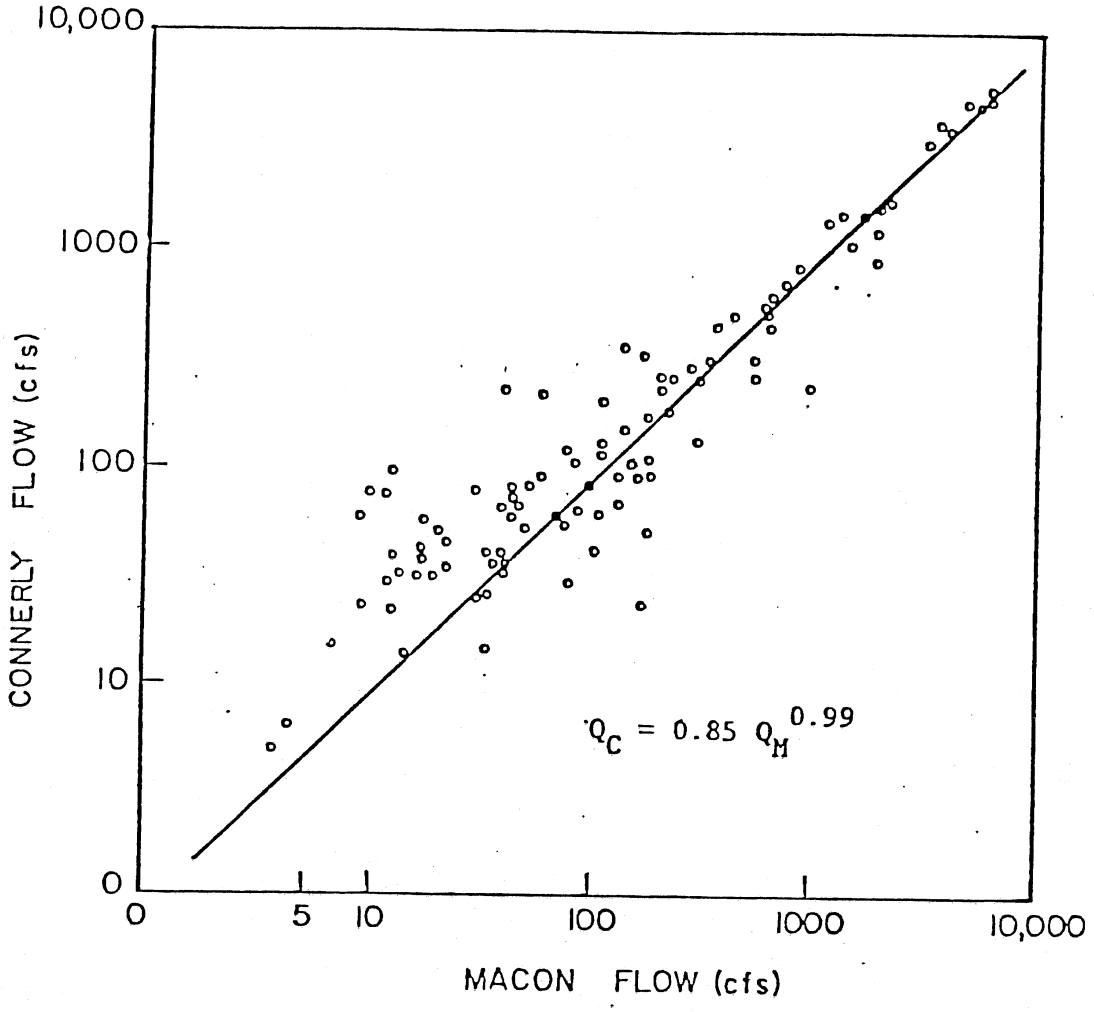

Fig. III-3. Macon Lake and Connerly Bayou Discharge Relationship. (Swain, 1980)

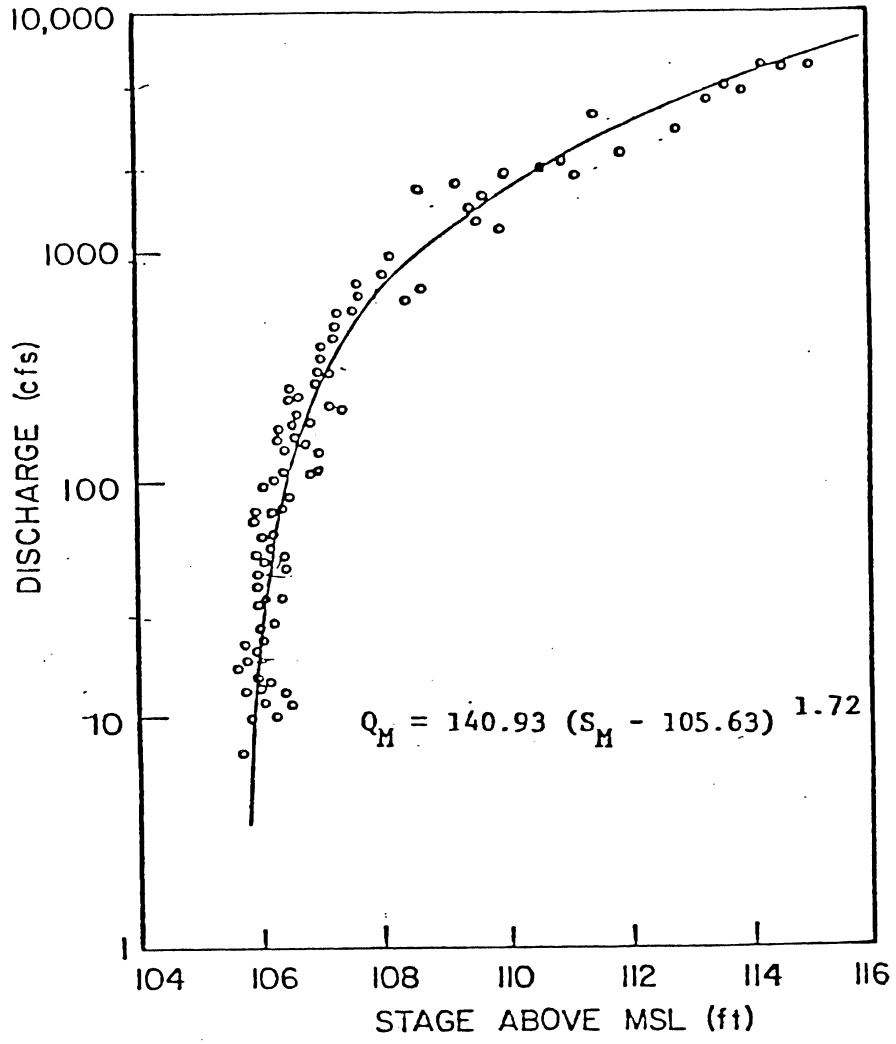

Fig. III-4. Stage Discharge Relationship for Macon Lake. (Swain, 1980)

where Q_{CAFD} = inflow from Connerly Bayou in acre ft per day, and for chlorophyll-a (Cardoni et al., 1982a and 1982b):

$$CHLA_C = 317(SS_C)^{-0.693} \qquad \text{(III-6)}$$

where $CHLA_C$ is in ppb and SS in ppm. For available dissolved orthophosphorus

$$P_{ac} = 100 \text{ ppb}^* \qquad \text{(III-7)}$$

and for non-available phosphorus:

$$P_{nc} = \eta\left[0.025(SS)^{.573} - \frac{CHLA_c}{Y_{ca}}\right] \qquad \text{(III-8)}$$

where Y_{ca} is the ratio of chlorophyll-a to phosphorus in the phytoplankton, and $^{ca}\eta$ is a specified fraction (see Section VIII-3).

The data from which the above relationships were derived are shown in Figs. III-5 through III-8. Additional measurements of available dissolved orthophosphorus in the inflow to Lake Chicot are desirable.

C. Weather

The weather station nearest Lake Chicot is at Stoneville, Miss.** Air temperature (TA) and total daily solar radiation (RAD) from that station were used in the model. Wind velocity (WIND) and dew point temperature (TD) were the arithmetic means of daily measurements at Memphis, Tenn., Jackson, Miss., and Shreveport, La. (see Fig. III-9 for locations). The three stations showed a good correlation and Lake Chicot is located at about the center of a triangle formed by these three stations. Daily precipitation data were from measurements at Stoneville, Mississippi. Additional information on weather stations and data is given by Dhamotharan (1979).

---

*As an alternative, combination of appropriate equations in Swain's thesis gives $P_{ac} = 0.015\ (Q_{in})^{0.26}$ where Q_{in} is the inflow in acre-ft/day. This equation has been tested in the model and provided comparable results, as in the cases when Eq. III-7 was used, with no significant improvement on the predictions.

**Midsouth Agricultural Weather Service Center, NOAA, P. O. Box 117, Stoneville, MS. 38776.

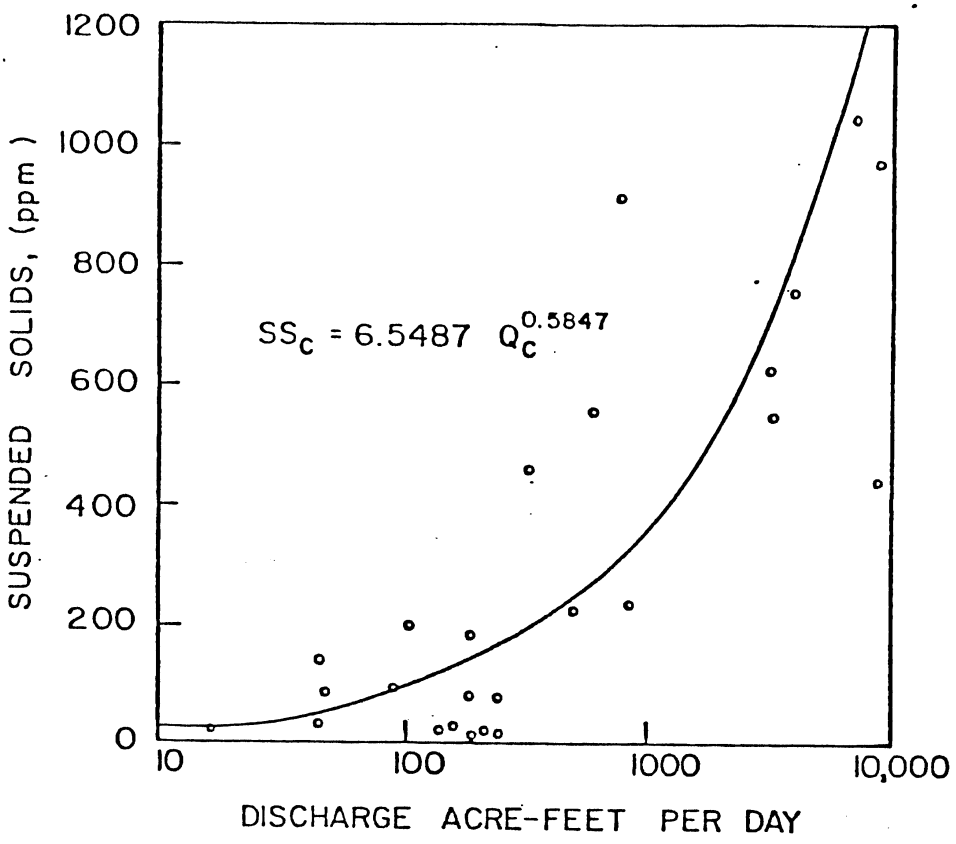

Fig. III-5. Relationship between suspended solids (sediments) and discharge at Connerly Bayou. (Swain, 1980)

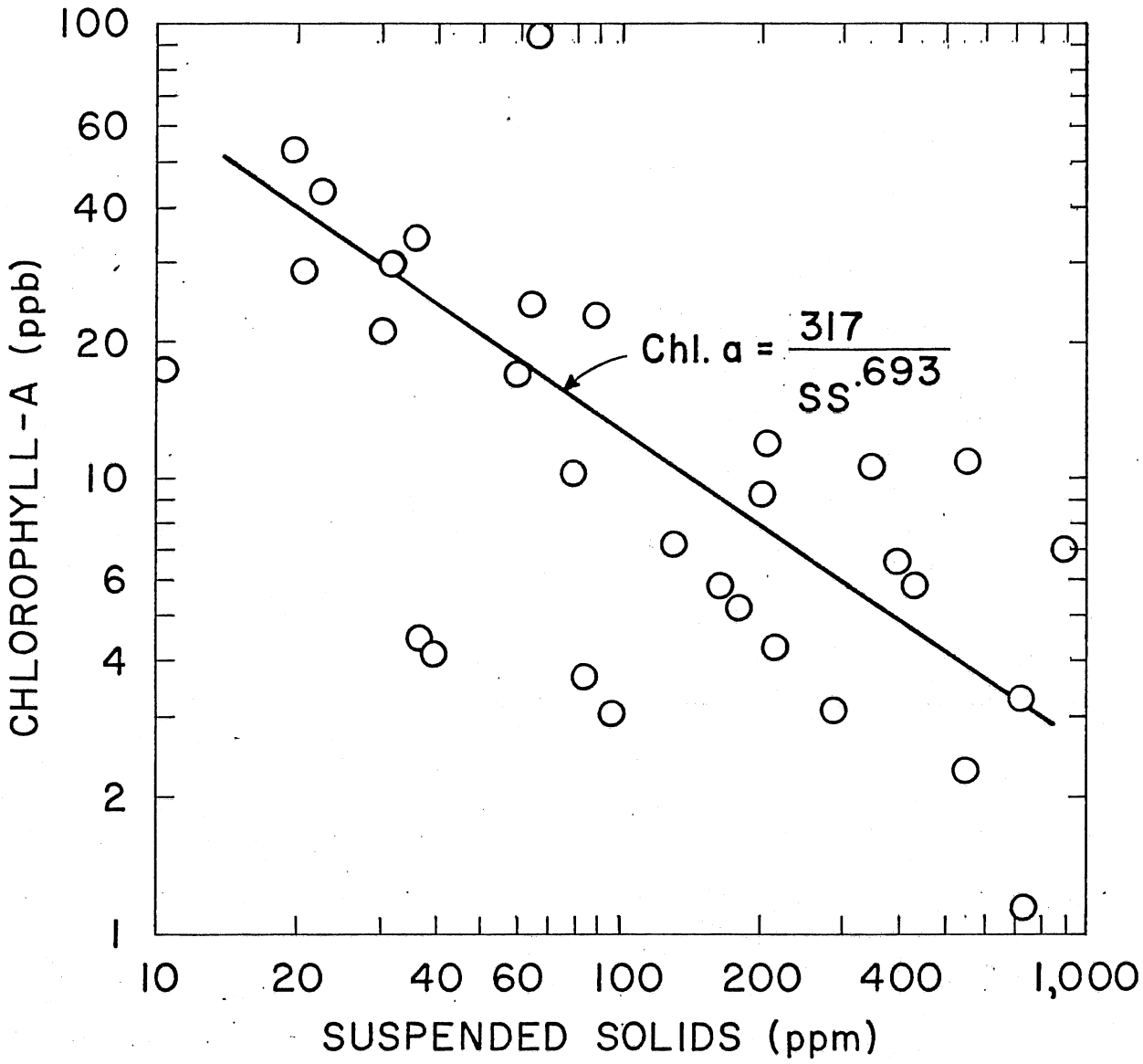

Fig. III-6. Chlorophyll-a versus suspended solids in inflow to Lower Lake Chicot, USDA Station C-5.

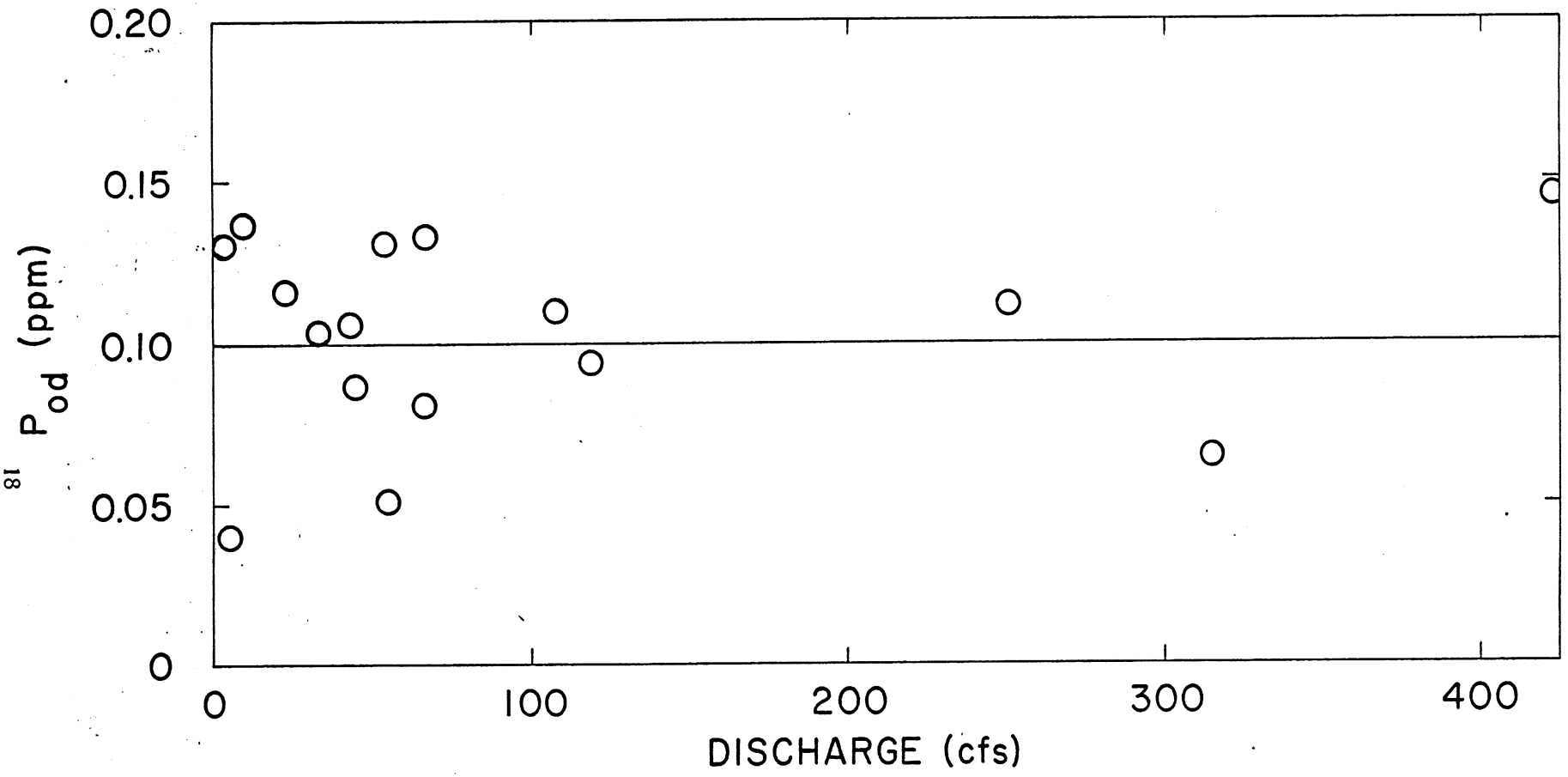

Fig. III-7. Dissolved orthophosphorus concentration versus discharge into Lower Lake Chicot, USDA Station C-5.

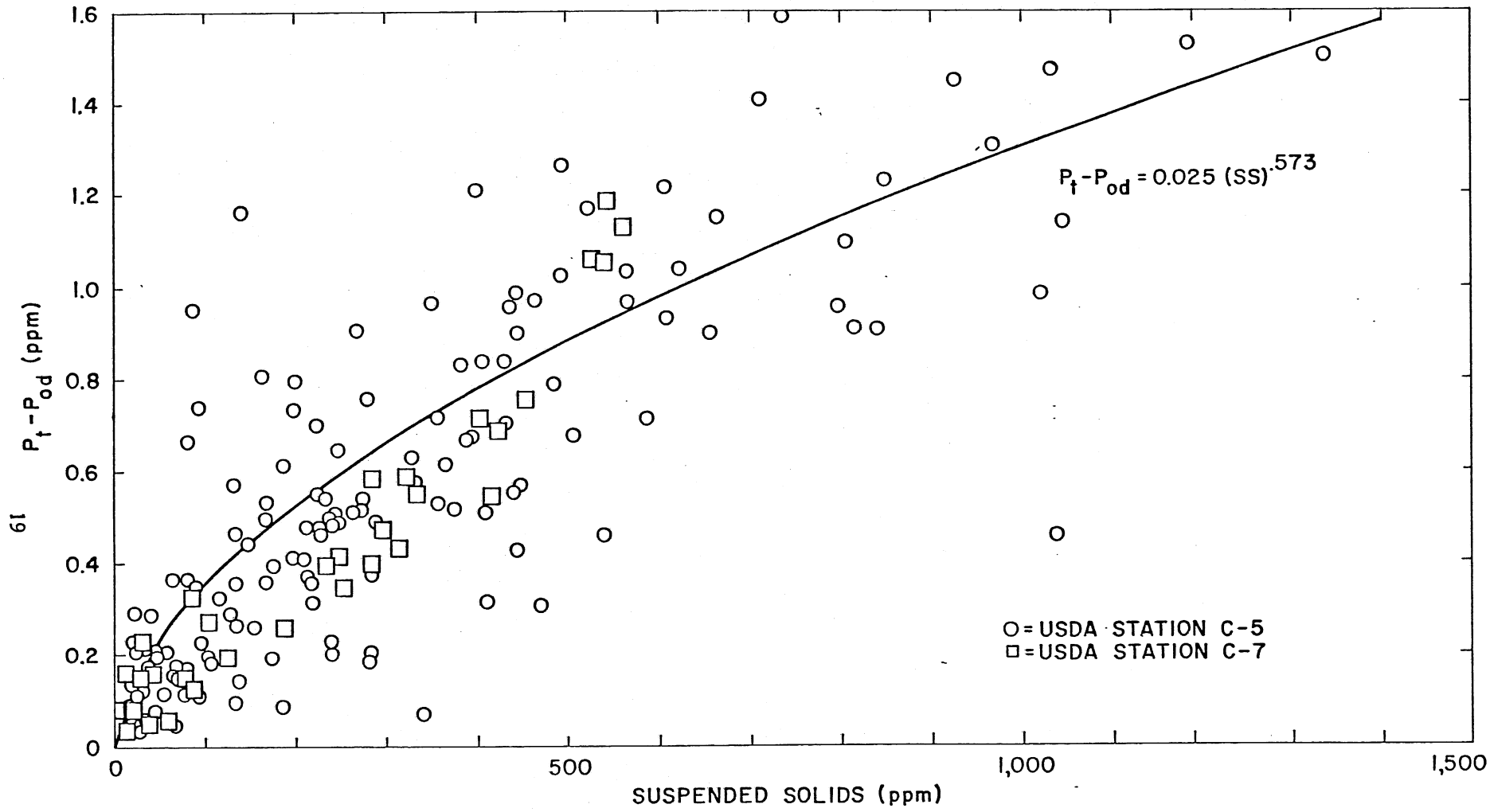

Fig. III-8. Total phosphorus (P_t) minus dissolved orthophosphorus (P_{od}) versus suspended solids, lower Lake Chicot.

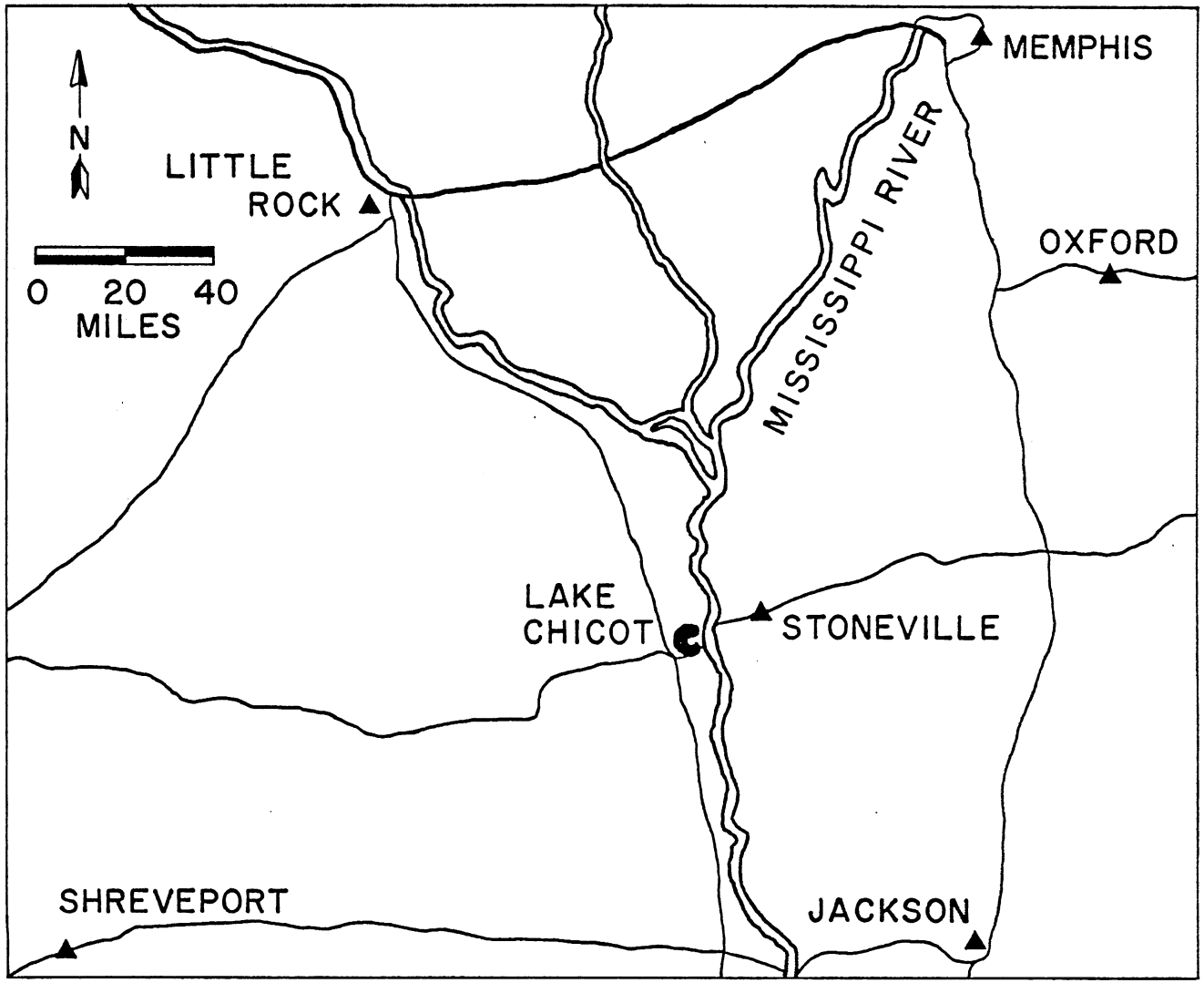

Fig. III-9. Map showing weather stations around Lake Chicot.

IV. ADVECTIVE FLOW MODEL/CONSERVATION OF VOLUME AND MASS

A. Advective Inflow/Outflow Mechanics in Stratified Reservoir

The lake or reservoir is considered to be composed of horizontal layers of variable thickness, and density (Fig. II-3). Each layer has a mean horizontal area and volume determined from the reservoir's morphometry.

The density of each layer of water in the reservoir is determined by its temperature, suspended sediment content, and dissolved solids content. The inflowing water will seek a layer with a density equal to its own. It will augment the volume of that layer and consequently all the layers above it will be displaced upward. As a layer rises, its horizontal area becomes larger and its thickness consequently diminishes.

The outflow from the reservoir can be considered in a similar way. Depending on the location and type of outlet, e.g. a weir versus a sluice gate, outflow is simulated by withdrawing water from the layers in front of the outlet.

Numerical computations can be kept simple by considering the reservoir as a stack of discrete volumes to which additions or subtractions are made in each timestep.

Some complicating factors need further consideration. As the inflow moves into the reservoir and towards its isopycnic layer, it entrains water from each layer it passes through. The amount of entrainment is a complex function of the flow rate, the density gradients, and other factors (Pedersen, 1980). If the inflow is into the surface mixed layer, entrainment can be ignored. Entrainment from deeper layers is specified in a density current subroutine. The characteristics of the density current, i.e. its temperature, suspended and dissolved solids content, are changed by dilution as the current passes from one layer to the next until it reaches its isopycnic layer. The temperature, suspended and dissolved solids contents of the isopycnic layer are recalculated, including the thermal energy and the mass of suspended and dissolved solids added by the density current.

B. Water Budget (Subroutine CONSMAS)

The water budget for the reservoir also includes precipitation, evaporation, and seepage to and from the surface layer. Evaporative losses are derived directly from the evaporative heat transfer term in the heat budget equation. Groundwater is calculated in subroutine GWATER.

Water balance equations for each layer and between timesteps j and j+1, typically one day apart, are

$$V(i, j+1) = V(i,j) - [Q_e(i) + Q_w(i) + Q_s(i)]\Delta t \qquad \text{(IV-1)}$$

where V = volume of layer

Q_e = flow entrained by density current from layer i

Q_w = withdrawal rate

Q_s = seepage rate

Δt = timestep

For the surface layer (i=1) the relationship is expanded to include $Q_{ev}(1)$ = evaporative water loss rate and $Q_p(1)$ = volumetric rate of water added by precipitation.

$$V(1,j+1) = V(1,j) - [Q_e(1) + Q_w(1) + Q_s(1) + Q_{ev}(1) - Q_p(1)]\Delta t \qquad \text{(IV-2)}$$

For the isopycnic layer, the mass balance equations are:

$$V(ip,j+1) = V(ip,j) - [Q_w(ip) + Q_s(ip) + Q_c]\Delta t \qquad \text{(IV-3)}$$

where Q_c = density current flow rate when it meets layer ip.

$$Q_c = Q_i + \sum_{i=1}^{ip-1} Q_e(i) \qquad \text{(IV-4)}$$

For the layers below the isopycnic layer ($ip < i < N$)

$$V(i,j+1) = V(i,j) - [Q_w(i) + Q_s(i)]\Delta t \qquad \text{(IV-5)}$$

In Lake Chicot seepage flow and withdrawal affect only the first layer.

C. Layer Thickness (Subroutine THICKNS)

Layer thicknesses are determined starting with the lowermost layer. A volume-versus-elevation curve derived from the reservoir morphology is used. The thickness of each layer is

$$\Delta z(i) = V(i)/A(i) \qquad \text{(IV-6)}$$

where A(i) is the horizontal area taken at the center of the layer i. A(i) is a function of the elevation of the center of the layer above the reservoir bottom and therefore dependent on $\Delta z(i)$. For this reason an iteration scheme described in more detail by Dhamotharan (1979) is used to derive the best estimates of $\Delta z(i)$. To safeguard against the accumulation of round-off errors, the sum of all layer thicknesses $\Delta z(i)$ is computed at the end of each timestep and compared to the total reservoir depth derived from a hydrologic water budget equation. To equalize the two values a correction factor is applied uniformly to all $\Delta z(i)$'s in each timestep.

Initial layer thicknesses are specified by the model user. After the initial timestep, layer thicknesses will keep changing. To avoid the development of anomalies, maximum and minimum layer thicknesses are specified. Selection of a maximum layer thickness is guided by total reservoir depth and affordable computation time. A value of 75 cm, 1/10 of the total reservoir depth was chosen. Layers exceeding the specified maximum value are divided into two or more layers (Subroutine SPLIT). Minimum layer thickness chosen was 15 cm, related to maximum possible withdrawal and to total reservoir depth. Depletion of more than one layer must not occur in any one timestep. If the thickness of any one layer falls below minimum value, it is added to the layer below it (Subroutine MERGE). Layers are renumbered and the pertinent morphometric values assigned as layers are generated or eliminated.

D. Outflow from Stratified Reservoir (Submodel OUTFLOW)

Outflow from Lake Chicot is through Ditch Bayou. A damaged rubble mound dam was replaced by a concrete weir in 1979. The following rating curves are used to calculate the volumetric outflow rate:

$$Q_w = 17.12\ (S - 101.42)^{2.42} \qquad \text{10/1/76 to 7/15/79}$$

$$Q_w = 146.67\ (S - 101.42)^{1.72} \qquad \text{7/15/79 to 9/30/79}$$

where Q_w = withdrawal flow rate in Ditch Bayou (cfs)
S = lake stage (ft)

The total depth in stratified Lake Chicot from which the withdrawal flow is taking place (Fig. IV-1) is calculated by subroutine WDEPTH as

$$z_w = d_w + \frac{\rho_w}{\rho_{zw} - \rho_w} \frac{V_w^2}{2g} \qquad \text{(IV-7)}$$

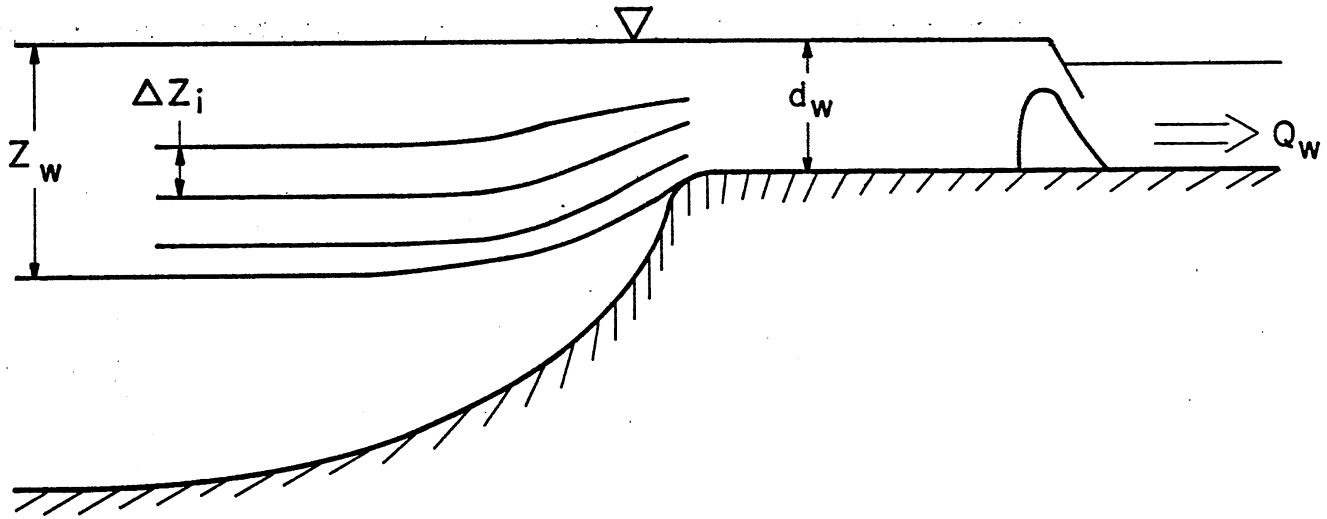

Fig. IV-1. Schematic of outflow (withdrawal) from stratified reservoir.

where z_w = withdrawal depth

d_w = S - 28.04 = water depth in outflow channel (m)

V_w = mean flow velocity in outflow channel = Q_w/A_w

A_w = cross section of the outflow channel

g = acceleration of gravity

ρ_w = density of the outflow

= depth weighted average density over the height of the withdrawal layer thickness z_w

$\Delta\rho_w = \rho_{zw} - \rho_w$

ρ_{zw} = density of the bottommost layer of the withdrawal layer.

The withdrawal from each individual layer within the withdrawal layer is apportioned according to individual layer thickness.

$$Q_w(i) = Q_w * \frac{\Delta z(i)}{z_w} \qquad \text{(IV-8)}$$

where $\Delta z(i)$ = thickness of an individual layer.

E. Inflow Density Current (Subroutine DCFLOW)

If the density of the inflowing water is higher than that of the first layer, the inflow plunges and continues as a density current. The submodel of the inflow density current follows the analysis by Akiyama and Stefan (1981).

In the analysis, it is assumed that inflow rate (q_o) inflow density (ρ_o), layer thicknesses (z), ambient density (ρ_a) and channel slope (S) are known, and that internal backwater effects in the case of flow over a mild slope channel are absent.

The analysis considers first the plunging region (plunging depth), then the dilution of the density current (underflow) as it progresses from layer to layer (Fig. IV-2).

1. Plunging Region

Following the detailed analysis of Akiyama and Stefan (1981), the plunging depth is evaluated as a function of channel slope (S), inflow rate per unit width of inflow channed (q_{in}), total friction factor (f_t) including bed friction and interfacial friction and buoyancy (ε_{in}). A distinction is made between a mild slope ($S < S_c$) and a steep slope ($S > S_c$). From analysis of reservoir data $S_c \approx 1/150$.

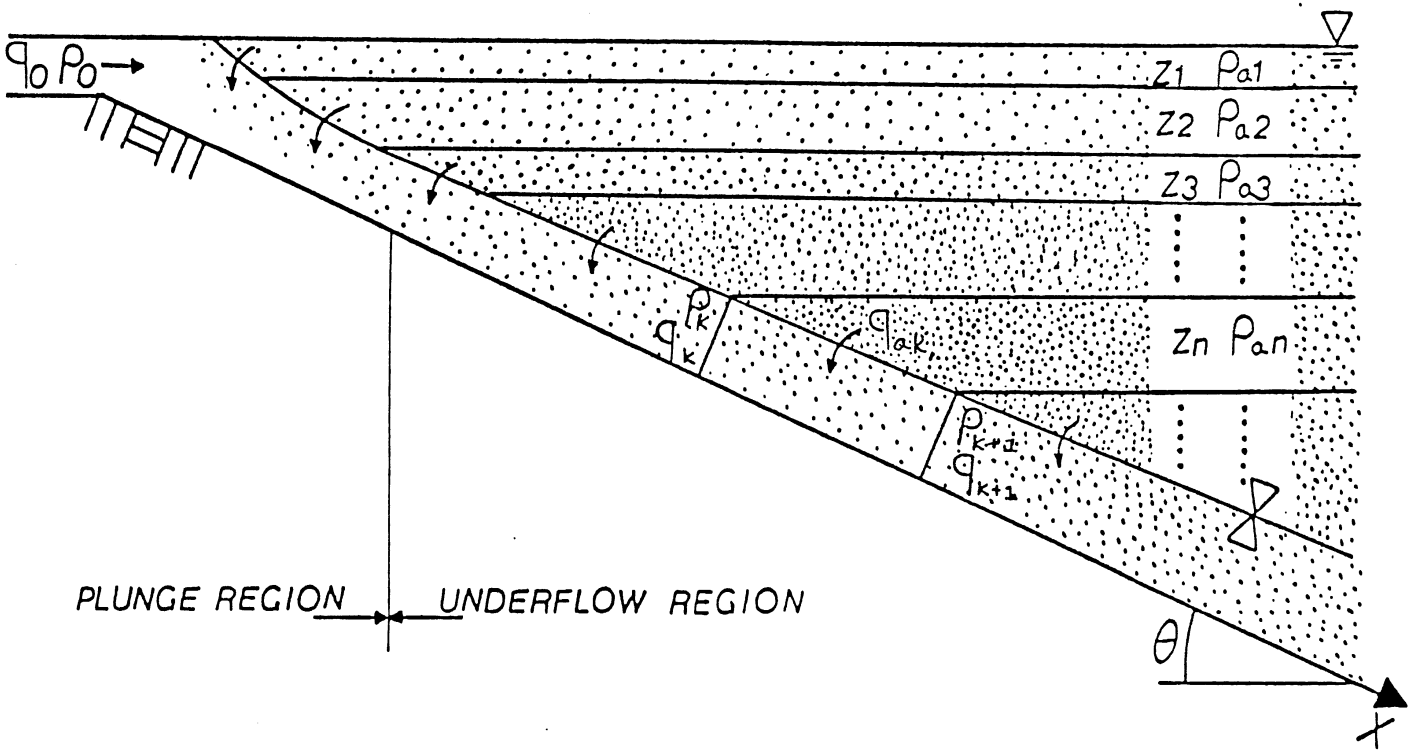

Fig. IV-2. Schematic of underflow in multi-layered reservoir.

Water depth at the plunge point h_p and initial dilution at the plunge point γ_{in} are found as follows.

On a mild slope:

$$h_p = 1.1 \left(\frac{f_t}{S} \right) \left(\frac{q_{in}^2}{\varepsilon_{in} g} \right)^{1/3} \qquad \text{(IV-9)}$$

$$\gamma_{in} = 0.15 \qquad \text{(IV-10)}$$

$f_t = 0.02$ for Lake Chicot

On a steep slope:

$$h_p = 1.6 \left(\frac{q_{in}^2}{\varepsilon_{in} g} \right)^{1/3} \qquad \text{(IV-11)}$$

$$\gamma_{in} = 1.8 \qquad \text{(IV-12)}$$

The buoyancy ε_{in} is defined as

$$\varepsilon_{in} = \frac{\rho_{in} - \rho_{\text{mixed layer}}}{\rho_{\text{mixed layer}}} \qquad \text{(IV-13)}$$

2. Underflow Region

In the underflow region beyond the plunging region the dilution of the flow by entrainment is calculated from the continuity equation (Fig. IV-2).

$$q_{i+1} = q_i + q_{ei} = q_i(1+\gamma_i) \qquad \text{(IV-14)}$$

The entrainment ratio for the underflow is

$$\gamma_i = \frac{\beta}{F_i^{1/3}} \left(\frac{g\,\varepsilon_i}{q_r^2} \right)^{1/3} \frac{\Delta z_i}{S} \qquad \text{(IV-15)}$$

with $$\varepsilon_i = \frac{\rho_{ci} - \rho_i}{\rho_i} \qquad \text{(IV-16)}$$

ρ_i = density of ambient layer i

ρ_{ci} = density of density amount upon entering layer i

F_i = normal densimetric Richardson number given by

$$F_n = \frac{\frac{1}{2} S_1 \beta + f_t + \sqrt{\left(\frac{1}{2} S_1 \beta + f_t \right)^2 + \Delta\beta\, S_2\, S}}{2 S_2\, S} \qquad \text{(IV-17)}$$

$$S_1 = \frac{1}{\varepsilon_c\, h_c^2} \int_o^\infty 2g \left(\frac{\rho_a - \rho(y)}{\rho_a} \right) y\, dy \qquad \text{(IV-18)}$$

$$S_2 = \frac{1}{\varepsilon_c\, h_c} \int_o^\infty g \left(\frac{\rho_a - \rho(y)}{\rho_a} \right) dy \qquad \text{(IV-19)}$$

h_c = depth of the density current

$\varepsilon_c = \frac{\rho_c - \rho_a}{\rho_a}$ = mean buoyancy of density current

Experimental observations indicate that $S_1 \approx 0.25$ and $S_2 \approx 0.75$.

The parameter β is an empirical coefficient in the expression for the entrainment coefficient

$$\gamma = \frac{\beta}{F} \quad , \tag{IV-20}$$

where F is the densimetric Richardson number defined as

$$F = \frac{\varepsilon\, g\, h_c^3}{q_c^2} \tag{IV-21}$$

An experimentally derived value $\beta = 0.0015$ is used. The theory behind the density current analysis has been given by Akiyama and Stefan (1981).

3. Determination of Initial Conditions (ρ_i, q_i) for Underflow Downstream from Plunge Point

Assume that ambient water is uniformly entrained during plunging (Fig. IV-3). The initial entrained flow from ambient water during plunging q_{ai} is

$$q_{ai} = \gamma_{in}\, q_{in} \tag{IV-22}$$

where q_{in} = inflow from the inlet channel to the reservoir,

γ_{in} = total initial dilution rate as computed earlier.

Conservation of volume and mass give, respectively:

$$q_{in} = q_{ai} = q_i \tag{IV-23}$$

$$\rho_{in}\, q_{in} \pm \overline{\rho}_a\, q_{ai} = \rho_i\, q_i \tag{IV-24}$$

where ρ_i = initial density for underflow,

q_i = initial flow rate for underflow, and

$\overline{\rho}_a$ = average density of entrained ambient water.

Equations IV-23 and IV-24 give

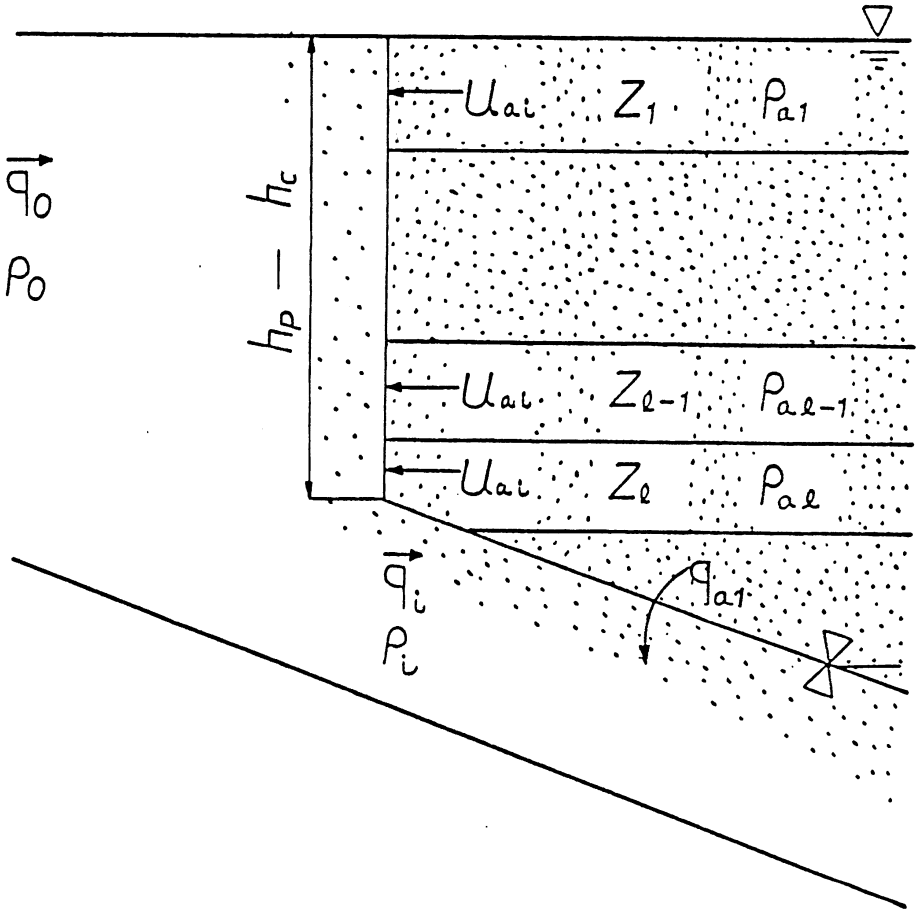

Fig. IV-3. Entrainment at plunge point in multi-layered reservoir.

$$q_i = (1+\gamma_{in})q_{in} \qquad \text{(IV-25)}$$

Equation IV-22, IV-24, and IV-25 give

$$\rho_i = (\rho_o + \overline{\rho}_a\ \gamma_{in})/(1+\gamma_{in}) \qquad \text{(IV-26)}$$

A relationship for $\overline{\rho}_a$ can be developed (Fig. IV-3)

$$\overline{\rho}_a(h_p - h_c)u_{ai} = \left[\sum_{j=1}^{\ell-1} \rho_{aj}\ z_j + \{(h_p - h_c) - \sum_{j=1}^{\ell-1} z_j\}\rho_{a\ell}\right] u_{ai} \qquad \text{(IV-27)}$$

where ℓ is the number of layer making up the height $h_p - h_c$ (see Fig. IV-3). Hence,

$$\overline{\rho}_a = \rho_{a\ell} + \frac{1}{h_p - h_c} \sum_{j=1}^{\ell-1} (\rho_{aj} - \rho_{a\ell})z_j \qquad \text{(IV-28)}$$

The above equation must satisfy the condition:

$$0 < (h_p - h_c) - \sum_{j=1}^{\ell-1} z_j \leq z_\ell \qquad \text{(IV-29)}$$

The total initial entrainment (dilution rate at the plunge point γ_{in} as used in Eqs. IV-22 and IV-26 is not well established. (S_2 = 0.75 and γ_{in} = 1.8 are used for Lake Chicot.

At the beginning of the subprogram DCFLOW subroutine PDEPTH is called to determine the plunging depth of a density current and the total volume of entrainment from layers lying within the plunging zone. Then the isopycnic layer is located by comparing the total density of the current with the total density of each layer as the density current flows down the slope. The volume, water temperature, suspended sediment concentration, dissolved solids concentration and chlorophyll-a concentrations of the density current are updated according to the volume of entrainment from each layer as the density current flows past as many layers as necessary until it joins the isopycnic layer.

F. Groundwater Inflow and Outflow (Subroutine GWATER)

The volume of groundwater going into or out of a lake must be evaluated on a case by case basis and incorporated in the model appropriately. The groundwater contribution to the Lake Chicot water budget is found to be dependent on the interaction between the lake and the Mississippi River stages. The groundwater flow rate is estimated by a relationship developed by Swain (1980). The groundwater is added or taken out at the surface mixed layer because studies by Winter (1978) have shown that seepage connections between a lake and an aquifer are usually most effective near the surface where contact areas and permeabilities are the largest.

The groundwater flow rate for Lake Chicot is calculated from the regression equation

$$Q_s(1) = \frac{K_s\, b}{\ell} \quad \frac{S_L^2 - S_{MR}^2}{2} - h(S_L - S_{MR}) \qquad \text{(IV-30)}$$

where $Q_s(1)$ = groundwater flow rate (cfs)

K_s = bulk soil permeability = 1.3 ft/day

b = projected length of lower Lake Chicot parallel to the Mississippi River = 5.5 miles

ℓ = mean distance between Mississippi River and Lake Chiot = 7 mi

S_L = Lake stage (ft)

S_{MR} = Mississippi River stage (ft)

h = aquifer thickness = 19 ft

The above relation combines expressions for 2-D flow in an unconfined aquifer and flow in a confined aquifer. Groundwater flow out of the lake is taken from the surface mixed layer. The volume of the mixed layer is adjusted in each timestep accordingly. Groundwater flow into the lake is routed to the isopycnic layer in the lake without dilution. Groundwater temperature is set equal to the annual average air temperature. Groundwater contains no sediments or nutrients in the simulation.

G. Precipitation

Water additions by precipitation are calculated by

$$Q_p(1) = A(1)\, p \qquad \text{(IV-31)}$$

where $Q_p(1)$ = inflow rate from precipitation

$A(1)$ = surface area of lake

p = precipitation intensity at Stoneville

H. Dilution of Water Quality Constituents

Associated with the advective transfer of water into and out of an individual layer is the transfer of heat, and suspended and dissolved materials. Water temperatures T and concentration C of individual layers are affected only if the advective flow is into the layer. For the isopycnic layer, T and C are therefore recalculated from the conservation equations:

$$T_{(ip,j+1)} = \frac{T(ip,j)\ V(ip) + T_c(i)\ Q_c(i)\ \Delta t}{V(ip) + Q_c(i)\ \Delta t} \qquad \text{(IV-32)}$$

$$C_{(ip,j+1)} = \frac{C(ip,j)\ V(ip) + C_c(i)\ Q_c(i)\ \Delta t}{V(ip) + Q_c(i)\ \Delta t} \qquad \text{(IV-33)}$$

where V = volume of a layer

Q_c = density current flow rate

Δt = time step of computation = 1 day.

where the concentrations C are those of suspended solids, SS, chlorophyll-a, Ch&a, available (dissolved ortho) phosphorus, P_a, or non-available phosphorus, P_n. Subscript c refers to the inflow density current as it arrives at layer (i).

Inter-layer density current flow and the temperature and concentrations of suspended and dissolved solids are calculated successively for each layer by considering the dilution due to entrainment at each step down; they are also used to compute water densities both in the lake and in the density current.

$$T_i = \frac{T_{i-1}\ Q_{i-1} + T_{i,j}\ Qe_i}{Q_{i-1} + Qe_i} \qquad \text{(IV-34)}$$

$$C = \frac{C_{i-1}\ Q_{i-1} + C_{i,j}\ Qe_i}{Q_{i-1} + Qe_i} \qquad \text{(IV-35)}$$

where T_i = temperature of density current after passing layer i

Q_i = volume of density current before reaching layer i

Qe_i = entrainment volume from layer i

C_i = concentration of suspended solids, dissolved solids, available and nonavailable phosphorus, chlorophyll-a.

Surface layer dilution by advection requires an expanded equation

$$T(1,j+1) = \frac{T(1,j)V(1) + [Q_s T_s + Q_p T_p + Q_{in} T'_{in}]}{V(1) + (Q_s + Q_p + Q'_{in})\Delta t} \qquad \text{(IV-36)}$$

for water temperature and a similar one for concentrations. Only if the inflows are positive does a dilution effect occur. Outflow does not change a layer's temperature or concentration.

V. WATER TEMPERATURE STRATIFICATION AND SURFACE ENERGY EXCHANGE MODEL

A. Concept

Because of the predominant influence of water temperature on the mid-summer density stratification and vertical mixing in Lake Chicot the dynamic, one-dimensional temperature prediction model developed by Stefan and Ford (1975) and Ford and Stefan (1980) was used as a starting point. The model uses a system of energy equations including wind energy input in addition to various forms of heat energy. It is a particularly suitable model for a shallow lake such as Lake Chicot since it can simulate vertical mixing dynamics using weather input at a timescale of a day or even shorter. Mixing is determined by a stability criterion that compares the total kinetic energy available for mixing with the incremental potential energy of the temperature profile. Thus, mixing is intermittent and occurs only when sufficient wind energy is available. The typical result of the simulation is a daily water temperature profile. The integral energy method emphasizes the net results of wind mixing and heat exchange between the lake and the atmosphere. Meteorological and morphometric data are the only required input data.

The suspended particles causing the objectionable turbidity in Lake Chicot are tiny flat clay particles about 1 micron average size. They increase the reflectivity and re-emergence from the water body of incoming radiation at the water surface and also the attenuation of radiation penetrating the water column. For use in the temperature model, the dependence of albedo and diffuse radiation attenuation coefficient on suspended sediment concentration had to be established.

The model considers the following:

- radiation heat transfer at the water surface and absorption in the water column.
- heat losses from the water surface by backradiation, evaporation and convection; and the surface mixed layer depth formed by natural convection.
- the surface mixed layer depth produced by wind mixing and natural convection during cooling.
- the heat transfer below the surface mixed layer by turbulent diffusion

B. Heat Transfer Equation (Submodel HEBUG)

The one-dimensional transient diffusion equation for heat in a water column is

$$\frac{\partial T}{\partial t} = \frac{\partial}{\partial z}\left(K_z \frac{\partial T}{\partial z} \right) + \left(\frac{S}{\rho c V} \right) \qquad \text{(V-1)}$$

where T = water temperature

t = time

K_z = vertical exchange coefficient

z = depth

S = solar radiation absorbed at depth z

ρc = specific heat per unit volume

V = volume of layer

Energy absorbed in the topmost layer is

$$S(1) = (1-r)\beta H_s + H_{an} - H_{br} - H_e - H_c \qquad \text{(V-2)}$$

where H_s = solar radiation received

β = near surface absorption coefficient, after Dake and Harleman (1969) = 0.4

r = reflectivity

H_{an} = net atmospheric radiation

H_{br} = backradiation

H_e = evaporative heat flux

H_c = convective heat flux

The remaining radiation $(1-\beta)(1-r) H_{sn}$ is attenuated exponentially with depth. The amount S absorbed at depth z is therefore

$$S(i) = k(1-\beta)(1-r)H_s e^{-kz} \qquad \text{(V-3)}$$

where k = attenuation coefficient (m^{-1}).

In the surface mixed layer water temperatures are first calculated layer by layer

$$T(j,i) = T(j-1,i) + \frac{S}{\rho\ c_p V(i)} \qquad (V-4)$$

Then the mixed layer depth due to natural convection is determined from

$$H_L = \sum_{i=1}^{N_m} [T(j-1,i) - T(j,N_m)]V_i\ \rho\ c_p \qquad (V-5)$$

where N_m = number of layers forming the surface mixed layer

H_L = total surface heat loss

$= H_{ev} + H_{br} + H_c$

The values of H_{an}, H_{ev}, H_{br} and H_c are calculated from empirical relationships.

C. Air/Water Energy Exchange

1. Solar Radiation

Solar radiation H_s is a measured total daily quantity. Values are from the Stoneville weather station. Both the reflectivity r and the attenuation coefficient η are functions of radiation wave length, angle of incidence of suspended sediment content, and color of the water. The dependence on suspended sediment concentation is shown in Figs. V-1 and V-2. Wave length was dependent only on natural radiation and assumed independent of season. Angle of incidence variations with season were expressed through radiation intensity. The following relationships were developed to fit Lake Chicot data by Dhamotharan (1979), Stefan et al. (1982a). Only measurements of incident and upwelling radiation from the water surface are available; therefore, reflectance and albedo had to be assumed as equivalent.

$$r = 0.087 - 6.76*10^{-5}\ RAD + 0.11[1 - \exp(-0.01\ SS)] \qquad (V-6)$$

where r = reflectance = H_r/H_{si}

H_r = reflected solar radiation

RAD = total daily incident solar radiation in cal cm^{-2} day^{-1}

SS = suspended sediment concentration in mg/ℓ

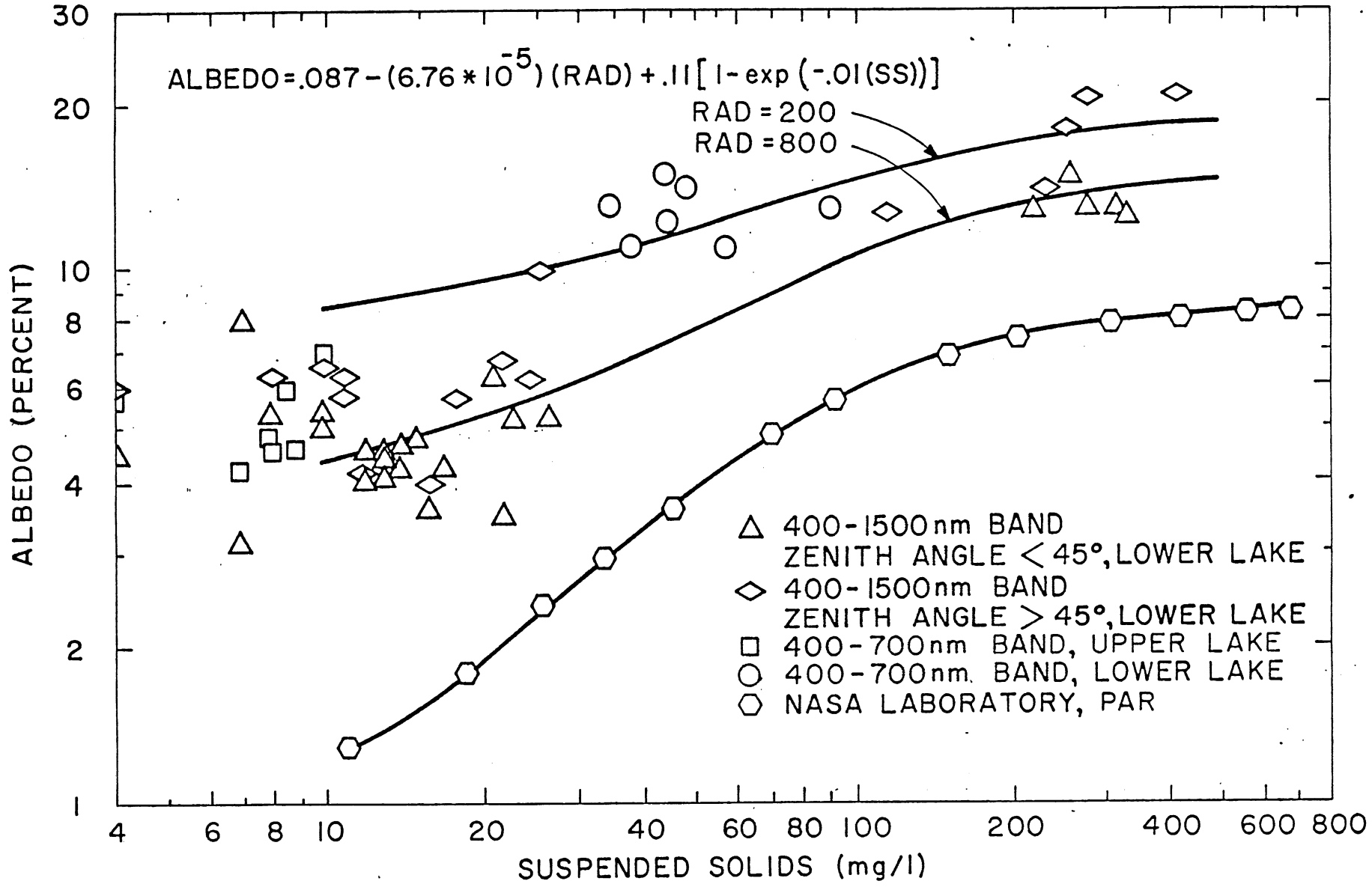

Fig. V-1. Albedo in Lake Chicot (400 - 1500 nm band).

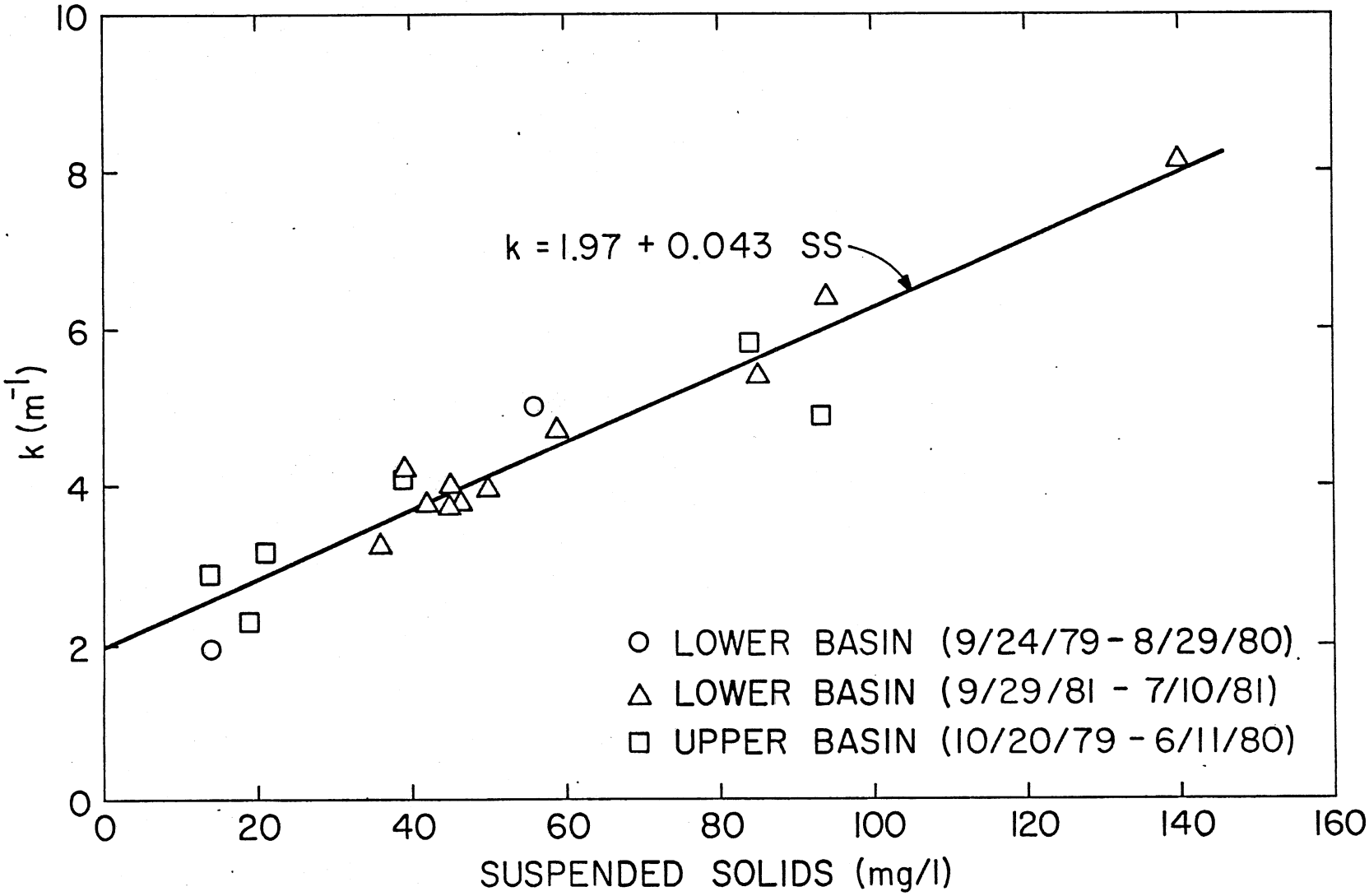

Fig. V-2. Suspended solids versus attenuation coefficient. ($k = k_{parsph}$)

The first two terms are for clear water, and the third term is from Lake Chicot data (Stefan et al., 1982a) and accounts for sediment effects. Reflectance must be adjusted for seasonal variation of the angle of incidence. This is done by the second term which was first introduced by Dingman (see Dhamotharan, 1979). Fig. V-1 shows the field data from Lake Chicot, and fitted equations for two levels of radiation.

Attenuation of radiation is calculated using the attenuation coefficient

$$k = 1.97 + 0.043\ SS + 0.025\ Ch\ell a \qquad (V\text{-}7)$$

where SS = suspended sediment concentration, (mg/ℓ)

Chℓa = chlorophyll-a concentration (μg/ℓ)

The above equation was actually derived for photosynthetically active light from Lake Chicot data by Stefan et al. (1982a), but can also be applied to the entire solar spectrum since much of the longwave components have been taken out in the surface layer.

2. Atmospheric radiation H_{an}

Net atmospheric (longwave) radiation is expressed as

$$H_{an} = \sigma\ \varepsilon_a\ T_a^4 \qquad (V\text{-}8)$$

where σ = Stefan-Boltzman const. = $1.171*10^{-7}$ cal cm^{-2} $°K^{-4}$

T_a = air temperature in °K

ε_a = atmospheric emissivity

For atmospheric emissivity without cloud cover, ε_{ac}, the Idso and Jackson (1969) formula will give accurate results for air temperatures above and below the freezing point

$$\varepsilon_{ac} = 1 - 0.261\ \exp\left[-0.74x10^{-4}\ T_a(°C)^2\right] \qquad (V\text{-}9)$$

The Bolz formula is then used to find ε_a.

$$\varepsilon_a = \varepsilon_{ac} (1 + K C_c^2) \qquad \text{(V-10)}$$

where C_c = fraction cloud cover, and
K = a coefficient which depends upon cloud height

The coefficient K varies between 0.04 and 0.25. A TVA (1968) study recommends an average value of $K = 0.17$.

3. Back Radiation

Back radiation is the atmospheric long wave radiation emitted by the water surface.

$$H_{br} = \sigma \varepsilon_w (T_w)^4 \qquad \text{(V-11)}$$

where ε_w = emissivity of water = 0.97
T_w = water surface temprature in °K

4. Evaporative transfer H_e

Evaporative heat transfer from a water surface is expressed by the relation

$$H_e = \rho L (Wftn)_z (e_{sw} - e_{az}) \qquad \text{(V-12)}$$

where e_{az} = vapor pressure of the air at height z
e_{sw} = saturated vapor pressure at water surface temperature
$Wftn_z$ = a wind function using wind velocity at height z
L = latent heat of vaporization for water (E/M)
ρ = density of water (M/L^3).

Saturation vapor pressure at any air temperature T(°K) over water is computed by the Magnus-Tetons formula, (see Murray, 1967).

$$e_s(mb) = 6.1078 \exp \frac{17.269(T - 273.16)}{T - 35.86} \qquad \text{(V-13)}$$

Atmospheric vapor pressure is computed from relative humidity, RH

$$e_a = \frac{RH}{100} e_{sa} \tag{V-14}$$

The latent heat of vaporization is

$$L = 597.31 - 0.5631\ T_s \tag{V-15}$$

with L in cal/g and T_s in °C

5. Convective Heat Transfer H_c

The convective heat transfer from an air-water interface, when evaluated according to Bowen (1926) may be expressed as

$$H_c = 0.61 \frac{P_a(mb)}{1000} \rho L\ Wftn_z(T_s - T_{az}) \tag{V-16}$$

where T_{az} is air temperature at a height z above the water surface, P_a is in mb and $Wftn_z$ is the same as that for evaporative heat transfer.

A number of empirical wind function formulas $(Wftn)_z$ have been developed for various conditions. A formula used by many investigators, e.g. Marciano and Harbeck (1954), for natural water bodies is

$$(Wftn)_z = a + b\ W_z \tag{V-17}$$

where W_z = wind velocity at elevation z above the water surface

a,b = empirical constants

Using U. S. Geological Survey data for Lake Hefner and Lake Mead, (Dake, 1972), the wind speed function is given by

$$\rho L(Wftn) = 25.617\ U \tag{V-18}$$

where U = windspeed in m/s

$\rho L(Wftn)$ = wind speed function in kcal m^{-2} mb^{-1}

Below the surface mixed layer the complete diffusion equation with an annual average value K_z = 1 m^2/day is solved.

The above heat transfer scheme ignores seasonal heat storage in the lake bed.

D. Wind Mixing

The deepening of the surface mixed layer by wind shear is considered by a stability criterion as described by Stefan and Ford (1975) and Ford and Stefan (1980a).

$$\frac{\rho_a u_*^3 A(1)\Delta t}{V(m)\ \Delta\rho g(z_m - z_g)} = \sigma \qquad \text{(V-19)}$$

where ρ_a = air density

u_* = wind shear velocity

$V(m)$ = volume of the surface mixed layer

$\Delta\rho = \rho(m) - \rho(m+1)$

z_m = depth of the surface mixed layer

z_g = center of gravity of the surface mixed layer

$$z_g = \frac{\sum_{i=1}^{m} z(i)\ A(i)\ \Delta z(i)}{\sum_{i=1}^{m} A(i)\ \Delta z(i)} \qquad \text{(V-20)}$$

The surface mixed layer depth is attained where $\sigma < 1$.

The effect of wind on vertical diffusivities in the surfaced mixed layer and below the surface mixed layer is described by an equation of the form

$$K_z = aW^b \qquad \text{(V-21)}$$

where K_z = vertical diffusivity (m^2/day)

a,b = coefficients

W = wind velocity (mph)

This empirical equation was proposed by Filatov et al. (1981). For shallow Lake Ladoga, coefficient b varied from 1.2 to 1.4. The average value b = 1.3 was chosen for Lake Chicot.

Coefficient a was estimated by using the seasonal mean values K_z = 400 m^2/day for the mixed layer and $K_z \approx 1$ m^2/day for all layers below, as previously applied by Dhamotharan (1979). For an average annual wind velocity W = 7.73 mph, a = 28 for the mixed layer and a = 0.1 for the hypolimnion. Thus,

$$K_z = 28\ W^{1.3} \qquad \text{in mixed layer} \qquad \text{(V-22)}$$

$$K_z = 0.1\ W^{1.3} \qquad \text{below mixed layer} \qquad \text{(V-23)}$$

VI. SUSPENDED SEDIMENT (MODEL RESSETL)

In stratified lakes and reservoirs of moderate size, including Lake Chicot, advection in the horizontal direction is rapid, relative to vertical mixing. This had been verified in Lake Chicot by measurements of longitudinal temperature gradients (Dhamotharan, 1979), and hence only vertical gradients in suspended sediment concentration C were simulated. Biweekly suspended sediment measurements in the lake also showed that one-dimensionality was an acceptable assumption for Lake Chicot. A relationship among suspended sediment concentration profiles, vertical mixing intensity, rate of deposition, and time is

$$A \frac{\partial(C)}{\partial t} + \frac{\partial(WAC)}{\partial z} - WC \frac{\partial A}{\partial z} - \frac{\partial C}{\partial z}\left(AK_z \frac{\partial C}{\partial z}\right) = 0 \qquad \text{(VI-1)}$$

where C = suspended sediment concentration

W = fall velocity of suspended sediment in quiescent water

A = surface area of x-section

K_z = vertical turbulent diffusivity

The first term in this equation represents the change in sediment content with time, the second term is the rate of transfer by settling from one layer to another, the third term is the rate of deposition on the lake bed, and the fourth term is the vertical turbulent mixing rate.

The particle fall velocity was determined after Gibbs et al (1971).

$$W = \frac{-3d_{vs} + \sqrt{9d_{vs}^2 + gr_s^2 \rho_f(\rho_s - \rho_f)(0.015476 + 0.19841r_s)}}{\rho_f(0.011607 + 0.14881\ r_s)} \qquad \text{(VI-2)}$$

$$0.1\mu \leq 2r_s \leq 6\text{mm}$$

where d_{vs} = dynamic voscosity of fluid in poises

r_s = sediment sphere radius in cm

ρ_f = density of fluid in g/cm^3

ρ_s = density of sediment sphere in g/cm^3

$$d_{vs} = \frac{1.79 \cdot 10^{-6} \rho}{(1 + 0.03368\ T + 0.000221\ T^2)}$$

where d_{vs} is in kg/m-sec
ρ is in kg/m^3
T is in °C

For Lake Chicot a mean particle size was determined as $r_s \approx 1\ \mu$ by Schiebe (1980) and confirmed by model calibration. The sediment transport equation accounts for deposition on the shelf. The equation is solved over the entire depth. Solution of the equation requires two boundary conditions which are:

(i) no suspended sediment transfer at the water surface, i.e.

$$K_z \frac{\partial C}{\partial z} - WC = 0 \qquad \text{at } z = 0 \qquad \text{(VI-3)}$$

(ii) no resuspension at the bottom, i.e.

$$K_z \frac{\partial C}{\partial z} = 0 \qquad \text{at } z = h \qquad \text{(VI-4)}$$

condition (i) is usually well satisfied while condition (ii) requires field verification. In Lake Chicot no resuspension was observed after storms. A uniform concentration distribution $C = C_o$ is specified as the initial condition at $t = 0$ (Oct. 1, 1976, after the fall overturn).

Equation VI-1 describes a balance between advective transport by settling and diffusive transport by vertical mixing. In a stratified reservoir, vertical exchange coefficients are strongly dependent on depth and wind on the surface. For the Lake Chicot simulation annual average values of $K_z = 400$ m^2/day for the surface mixed layer, and $K_z = 1$ m^2/day were used for all layers below (see Section V-D). The depth of the surface mixed layer was variable and simulated by the temperature stratification model. The two values of K_z which were also used in the temperature model were established by calibrating the model against field measurements of water temperature profiles. Daily variations in K_z were computed from Eqs. V-22 and V-23.

The model also computes a suspended sediment budget and determines the amount of sediment deposited in the reservoir. The apparent trap efficiency is defined as

$$ATE = \frac{\Sigma \text{ Sediment Inflow} - \Sigma \text{ Sediment Outflow}}{\Sigma \text{ Sediment Inflow}} \qquad \text{(VI-5)}$$

The trap efficiency ATE is meaningful only when computed over long time periods. It does not take into account the change in storage of suspended sediment in the lake.

The RTE real trap efficiency is the apparent trap efficiency ATE minus the change in storage in the lake. It is calculated from

$$RTE = ATE - \frac{\text{Change in Storage}}{\Sigma \text{ Sediment Inflow}} \qquad \text{(VI-6)}$$

Change in storage is the amount of suspended sediment in the lake at the beginning of the time interval minus the amount at the end.

VII. PHYTOPLANKTON MODEL

A. Concepts

Lake Chicot is divided into an upper and lower basin. The lower basin receives turbid inflow from Connerly Bayou, while the upper basin receives primarily local overland runoff. As a result, the two basins represent distinctly different systems in terms of suspended solids concentration and primary productivity. The lower basin is highly turbid due to inorganic suspended solids, and biological productivity in this basin in substantially lower than in the upper basin (Cooper and Bacon, 1981). The upper basin is high in primary productivity, and much of the turbidity there is due to organic material. Observed seasonal variations in chlorophyll-a and suspended solids (Cooper and Bacon, 1981) are shown in Fig. VII-1 and indicate that primary productivity in the lower basin is limited by the amount of available light, while in the upper basin both available light and nutrients most likely limit productivity. In the lower and upper basins Secchi depths rarely are greater than 0.50 and 0.70 meters, respectively.

Surges in phytoplankton populations occur whenever inorganic sediment concentrations and turbidity have diminished (Fig. VII-1). If flow diversion effectively reduces inorganic sediment concentrations and turbidity in the future, phytoplankton will grow more substantially. It is for this reason that phytoplankton was modelled.

Phytoplankton concentrations can be described by a suspended sediment equation except that fall velocities are smaller than for clay and terms for biological growth and loss kinetics must be added. At present growth of nuissance algae in Lake Chicot is prediminantly controlled by the light available for photosynthesis. Losses of phytoplankton are due to settling and respiration. Grazing by zooplankton was not included separately because the observed species (Bacon, 1978; Cooper and Bacon 1981; and EPA, 1977) are not desirable food sources.

In this chapter a relationship between productivity rate, light intensity, and temperature developed from available field measurements by Cardoni and Stefan (1982b) is presented. Nutrient limitation was not considered in this first analysis. A light limited situation occurs frequently in lower Lake Chicot (EPA, 1977). An extension of this analysis, including a nutrient limitation (phosphorus), was also given by Cardoni et al. (1982b) and will be summarized in the next chapter.

B. Basic Equation

The goal is to predict the concentration of phytoplankton that will be present in the future. The parameter used to indicate algal abundance is

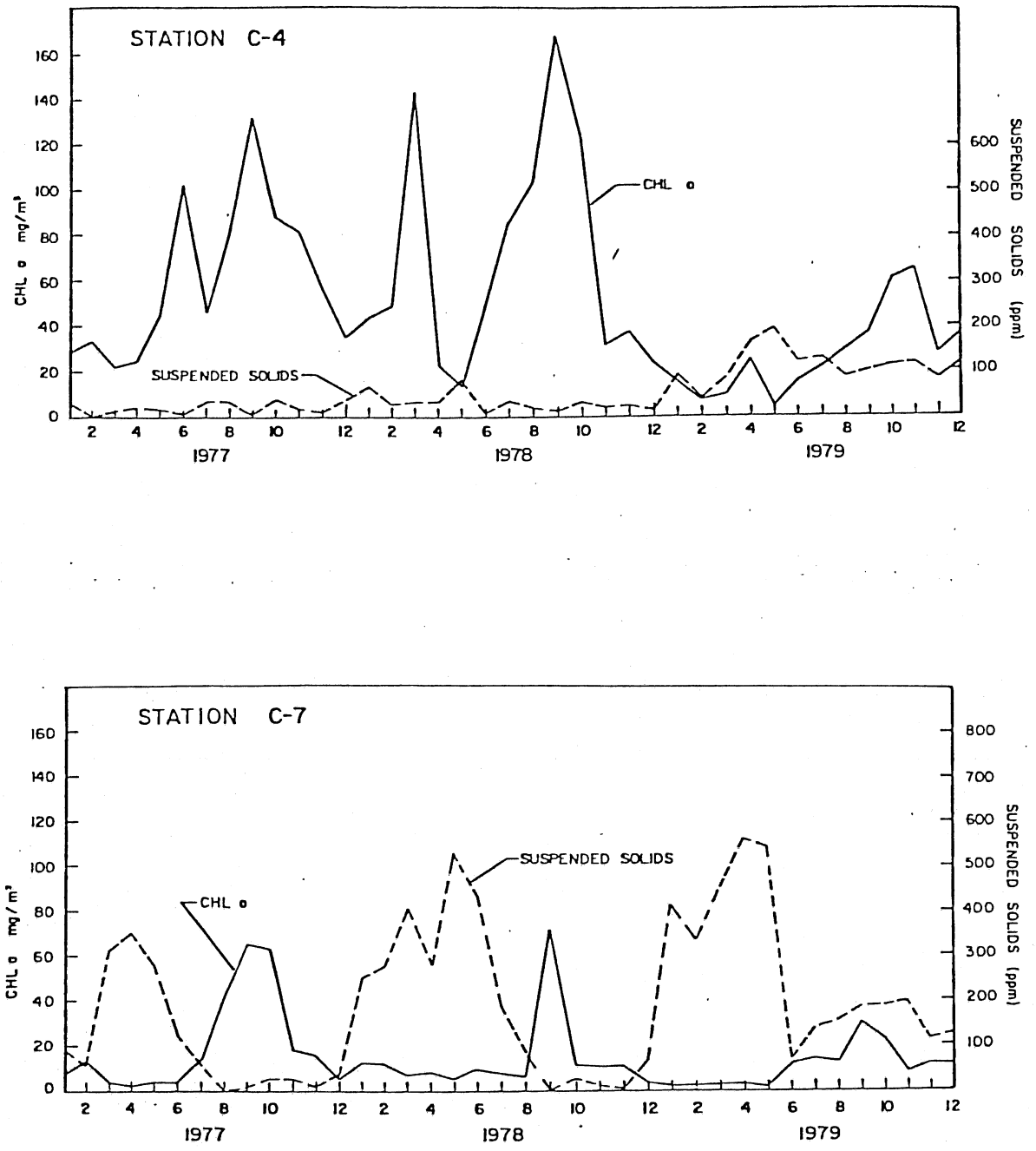

Fig. VII-1. Monthly (28 days) surface chlorophyll-a (mg/m^3 and suspended sediment values for the north (C-4) and south (C-7) basins of Lake Chicot, 1977-1979. (After Cooper and Bacon, 1981.)

chlorophyll-a concentration [Chℓa]. The model is for use on a daily time scale. The most important input parameters to the chlorophyll-a model are above water surface light intensity, suspended solids concentration, and water temperature, each on a daily time basis. The basic dynamic equation is

$$\frac{\partial[Ch\ell a]}{\partial t} + \frac{1}{A}\frac{\partial(AW_c[Ch\ell a])}{\partial z} - \frac{W_c[Ch\ell a]}{A}\frac{\partial A}{\partial z} - \frac{1}{A}\frac{\partial}{\partial z}\left(A K_z \frac{\partial[Ch\ell a]}{\partial z}\right)$$

$$+ K_2 T[Ch\ell a] - P'[Ch\ell a] = 0 \qquad \text{(VII-1)}$$

where [Chℓa] = chlorophyll-a concentration, mg/m^3

A = area at center of layer, m^2

W_c = Chℓa fall velocity in quiescent water, m/day

K_z = vertical turbulent diffusivity, m^3/day

K_2 = respiration/mortality loss coefficient, day^{-1} °C

T = water temperature, °C

P' = productivity rate, day^{-1}

Equation VII-1 is of the same form as Eq. VI-1 for the concentration of suspended solids but includes the additional source and sink terms, P' and K_2. Also, the fall velocity W_c is different for algal particulates than for the suspended sediment particulates (mostly clay).

C. Primary Productivity

Productivity of Lake Chicot was measured by Bacon (1978), using the carbon-14 uptake method, and reported in part by the USDA (1977-1980). Bacon's data was converted to a specific growth rate by dividing measured rates of carbon-14 uptake by the concentration of chlorophyll-a present in the lake (Schiebe, 1980) thus obtaining productivity in units of mg carbon/mg Chℓa/hr. Unfortunately carbon uptake and chlorophyll-a were never measured in the same water samples.

A relationship between productivity rate, light intensity, and temperature was developed by Cardoni and Stefan (1982a) from all available field measurements.

All light intensity data used in the productivity rate analysis were from the National Weather Service Station in Stoneville, Mississippi, and attenuated with depth in the lake using relationships developed by Stefan et al. (1982a).

Example of the P(I) data are shown in Figs. VII-2, 3, and 4. All available data are listed by Cardoni and Stefan (1982a). The data display the expected characteristic relationship between productivity and light: (1) An approximately linear increase in growth rate with light intensity at low values of light, and (2) plateau of maximum growth rate at the light intensity. Photoinhibition, i.e. the decrease of growth rate of excessive light exposure of plant, was not observed. This is not unexpected, since light intensity in Lake Chicot is usually quite low due to rapid attenuation with depth.

The shape of the P(I) curve can be described by a variety of mathematical and mostly empirical formulations. Some include the effect of photoinhibition. Comparisons of some of the equations to sets of measured data have given inconclusive results (Field and Effler, 1982; Jassby and Platt, 1976). All empirical equations for the P(I) curve require the use of coefficients, usually P_{max} and the initial slope of the curve. The selection of a mathematical equation for the P(I) curve may not be as critical as the determination of the coefficients used in the equation.

A Michaelis-Menten type equation was selected.

$$P = P_{max} \left(\frac{I}{K_{I+I}} \right) \qquad \text{(VII-2)}$$

where P = productivity rate at light intensity,

P_{max} = minimum productivity at optimum light intensity,

I = light intensity

K_I = half saturation coefficient

This equation is simple and is sufficient to describe the basic shape of the P(I) curves calculated from Lake Chicot field measurements.

1. Maximum Growth Rate, P_{max}

In the P(I) growth rate expression (VII-2) an optimum growth rate P_{max} is needed. Light intensity is considered to be the limiting factor in primary productivity; the maximum growth rate is found at optimum light conditions. Growth inhibition occurs only at low light intensity in Lake Chicot at present because of the high turbidity. The maximum growth rate also varies with temperature. An expression relating growth rate to temperature is derived from the Arrhenius equation and given in the form

$$P_{max} = P_{20}\, \Theta^{T-20} \qquad \text{(VII-3)}$$

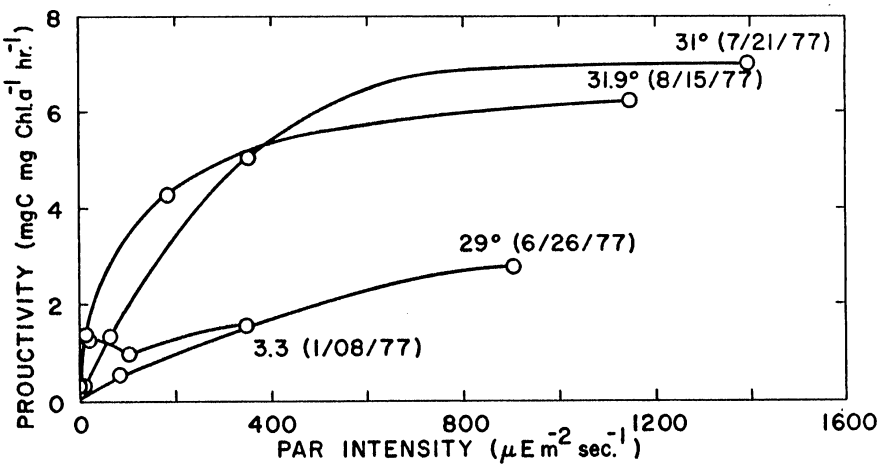

Fig. VII-2. Productivity rate versus photosynthetically active radiation (PAR) intensity, Bacon Station 4, lower Lake Chicot.

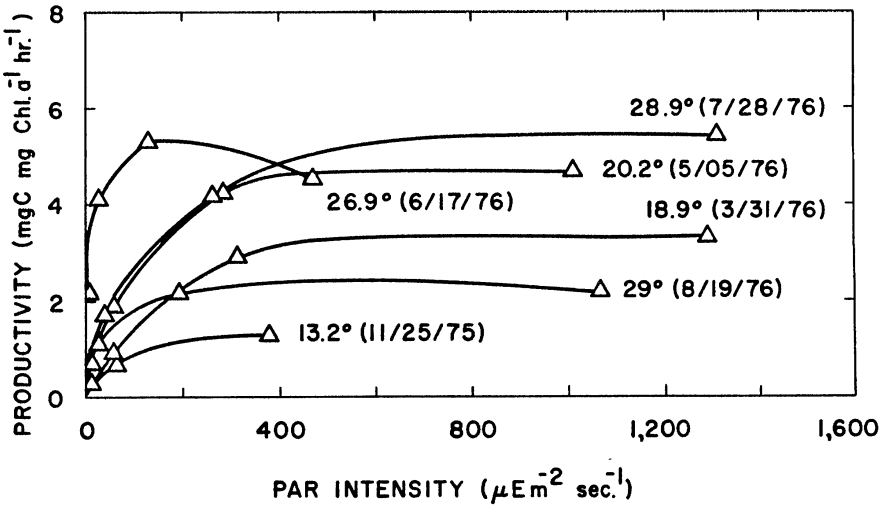

Fig. VII-3. Productivity rate versus photosynthetically active radiation (PAR) intensity, Bacon Station 2, upper Lake Chicot.

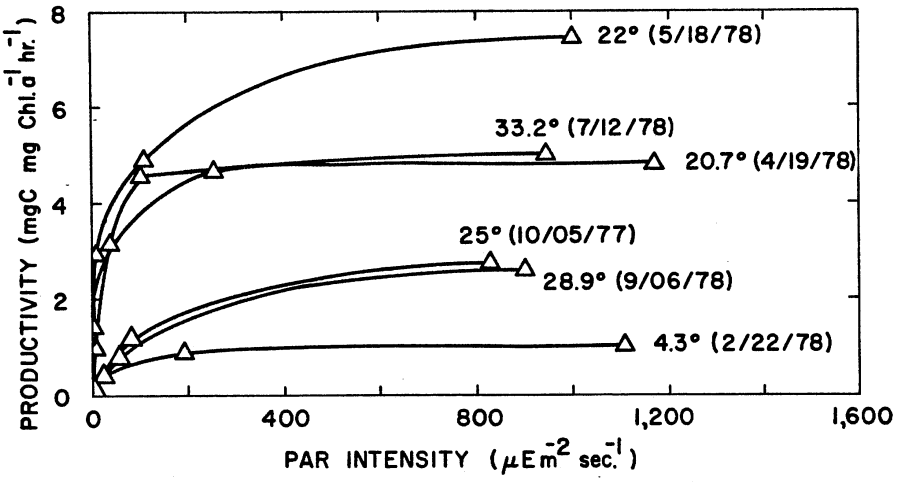

Fig. VII-4. Productivity rate versus photosynthetically active radiation (PAR) intensity, USDA Station C-4, upper Lake Chicot.

where P_T = growth rate at temperature T, P_{20} = growth rate at 20°C, and Θ = a temperature coefficient. Figure VII-5 shows a plot of maximum measured growth rate versus temperature for the upper and lower basins of Lake Chicot. This productivity rate will not exceed the optimum rate at the measured temperature. Therefore, an envelope of the highest measured growth rates should give an approximate relationship between temperature and maximum growth rate. The data yielded the coefficients $\Theta = 1.043$ and $P_{20} = 4.7$. P_{max} represents the maximum growth rate, mg C/mg Chℓa/hr, at temperature T under optimum light conditions.

A linear envelope fits the data equally well and is also shown in Fig. VII-5.

$$P_{max} = 1.2 + 0.187\ T \quad (T < 32°C) \qquad \text{(VII-4)}$$

An apparent retardation of the growth rate occurs at very high temperatures. From the data in Fig. VII-5 it has been estimated that temperature retardation begins at 32°C, and a linear envelope has been extended to a growth rate of zero at 37°C. This upper envelope represents the maximum growth rate under optimum light conditions but with temperature inhibition. The equation for this upper envelope is

$$P_{max} = 52.86 - 1.43\ T \quad (37 > T > 32°C) \qquad \text{(VII-5)}$$

In summary, it is considered that Eq. VII-4 is appropriate for determination of P_{max} for temperatures less than 32°C, and Eq. VII-5 is applicable for temperatures greater than 32°C. In the analysis made, no seasonal variation in the P_{max} versus temperature relationship was apparent, although the dominant phytoplankton species in the lake vary. Bacon (1978) reports that the flora of Lake Chicot is dominated by chlorophyta (green algae), chrysophyta (primarily diatoms), or cyanophyta (blue-green algae), depending on season. An extensive literature review of the effect of temperature on phytoplankton growth rate (Canale and Vogel, 1974) indicates that P_{max} is a function of species as well as temperature. It should be noted also that there is considerable variation in the growth rates reported for the same species at the same temperature. For a dynamic model of gross phytoplankton standing crop, a relationship of the form of Eq. VII-4 is expected to be adequate.

The productivity rates measured in Lake Chicot are reported in mg $C/m^3/hr$. Since phytoplankton concentration is to be expressed as Chℓa, it is necessary to have a yield coefficient of carbon to Chℓa.

Equation VII-4 can be divided by the ratio of carbon to chlorophyll-a to give the maximum productivity rate in units of $time^{-1}$.

$$P'_{max} = 24(1.2 + 0.187\ T)/\phi \qquad \text{(VII-6)}$$

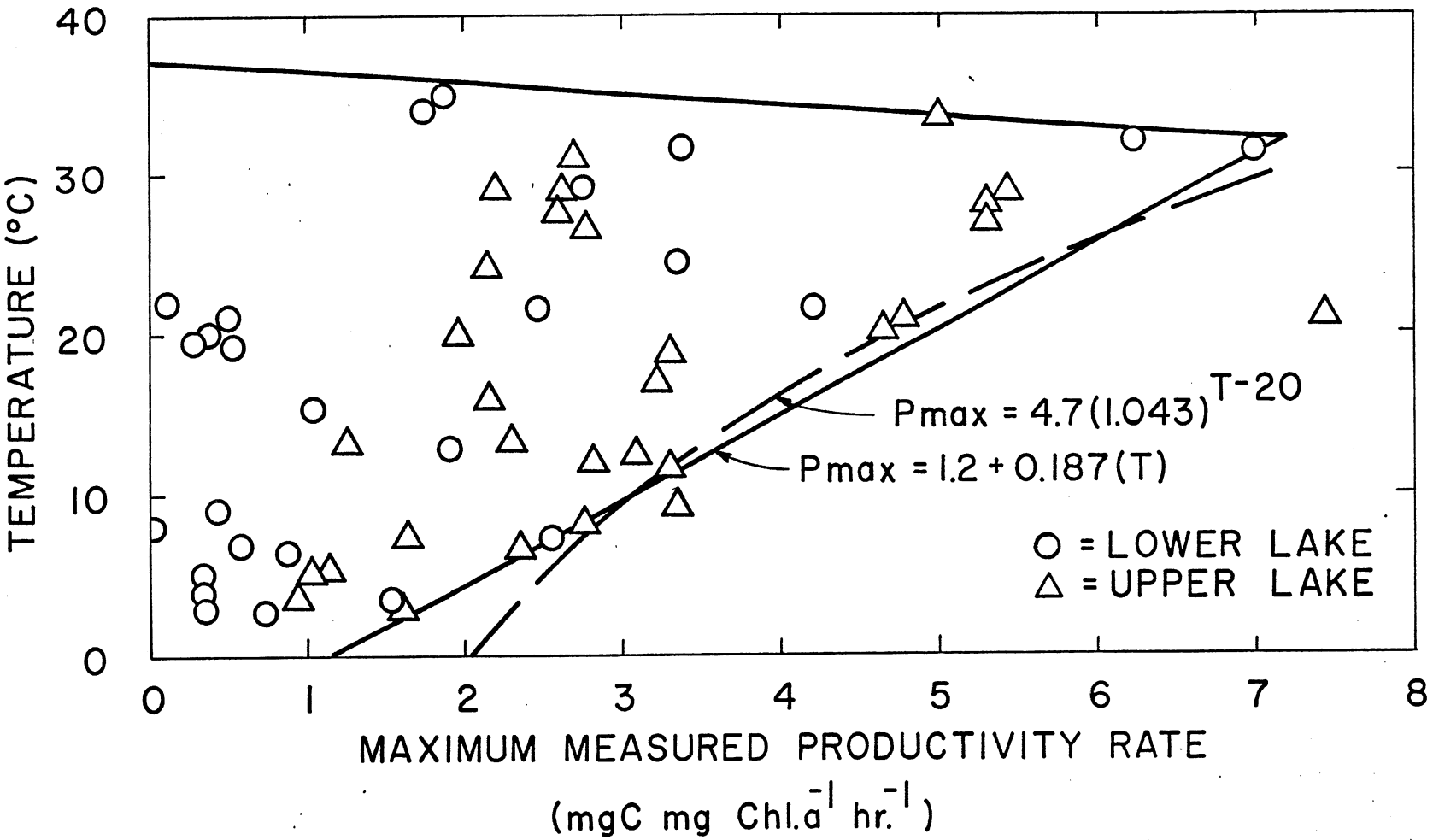

Fig. VII-5. Maximum productivity rate versus temperature, Lake Chicot data.

P'_{max} = maximum growth rate, day^{-1} , and ϕ = ratio of carbon to chlorophyll-a in the algae cells, mg C/mg Chℓa. The coefficient ϕ has been found to vary considerably. Smith (1980) contends that the amount of chlorophyll per cell increases (ϕ decreases) with decreasing light intensity and much of the variability in the coefficient ϕ is due to adaptive changes rather than taxonomic diversity. Listed below are several values of ϕ from the literature:

65 mg C/mg Chℓa	Canale and Vogel (1974)
25 mg C/mg Chℓa	Nyholm (1978)
50 mg C/mg Chℓa	Jorgensen (1981)
13-135 mg C/mg Chℓa	Smith (1980)
33 mg C/mg Chℓa	Metro Waste Control Comm (1978)

A preliminary model calibration with Lake Chicot Chℓa measurements gave a value of ϕ on the order of 45.

As stated by Goldman and Carpenter (1974) and Smith (1980), Eppley (1972) reviewed temperature effects on marine algae and proposed the following relationship for maximum specific growth rate:

$$P'_{max} = 0.693 \exp(0.06325T - 0.161) \qquad \text{(VII-7)}$$

Goldman and Carpenter (1974) compared data for maximum growth rate and temperature from continuous culture studies with marine and freshwater algae. The relationship they found is given by the equation

$$P'_{max} = (5.35 \times 10^{9}) \exp[-6472/T(°K)] \qquad \text{(VII-8)}$$

where $T(°K)$ is temperature in degrees Kelvin.

In a water quality modeling study of the upper Mississippi River using the computer program AESOP (Metro Waste Control Comm., 1978) the following equation was used for the maximum growth rate:

$$P'_{max} = 3.5\ (1.066)^{T-20} \qquad \text{(VII-9)}$$

Equation VIII-6 using values of θ = 40, 45, and 50 is compared with Eqs. VII-7, VII-8, and VII-9 in Fig. VII-6.

2. Half Saturation Coefficient, K_I

The parameter K_I was estimated directly from the productivity versus light intensity curves. K_I was taken as the light intensity at one-half the maximum productivity rate measured. No relationship between K_I

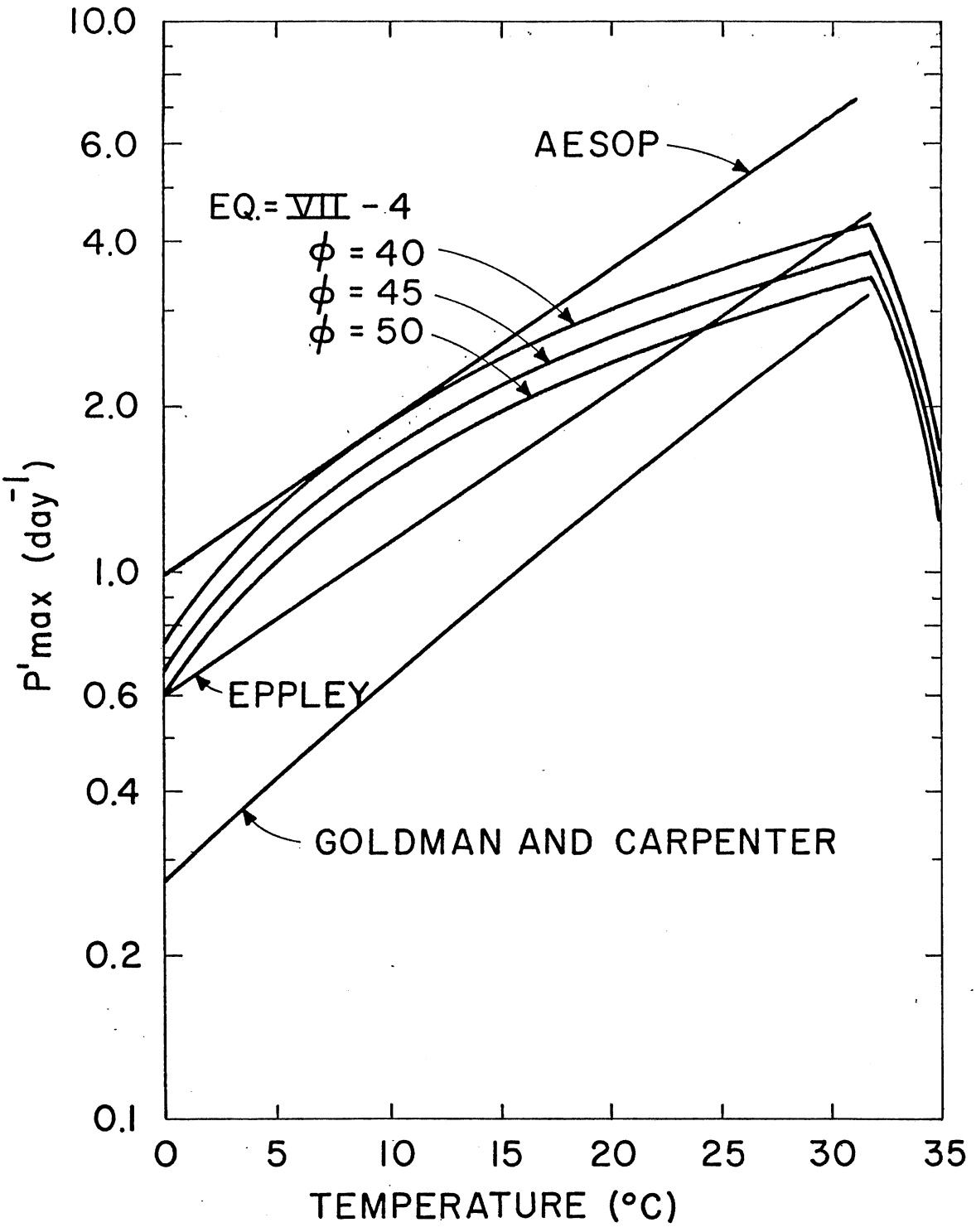

Fig. VII-6. Comparison of equations for maximum productivity rate as a function of temperature.

and temperature was found from the Lake Chicot data. A constant value K_I = 100 μEm^{-2} sec^{-1} was the best estimate. Jorgensen (1978) quotes Gargas (1975) as using K_I = 400 $Kcal/m^2$-day, which is equivalent to 45 $\mu E\ m^{-2}$ sec^{-1} using the conversion of Combs (1977).

3. Composite Relationship

The relationships retained for simulation of light and temperature controlled primary productivity rates in Lake Chicot are:

$$P = (1.2 + 0.187T)\frac{I}{100+I} \quad \text{for } 0 < T < 32°C \qquad \text{(VII-10a)}$$

$$P = (52.9 - 1.43T)\frac{I}{100+I} \quad \text{for } 32 < T < 37°C \qquad \text{(VII-10b)}$$

$$P' = 24P/\phi \qquad \text{(VII-10c)}$$

where P = primary productivity rate (mg C mg Chℓa^{-1} hr^{-1}),
P' = primary productivity rate (day^{-1}),
I = light intensity ($\mu E\ m^{-2}\ S^{-1}$), and
T = water temperature (°C).

Sample plots of the relationship VII-10a between productivity, light intensity, and temperature are shown in Fig. VII-7.

4. Underwater Light Penetration Model (Submodel LIGHT)

To apply the P(I) relationships to the prediction of daily photosynthesis in a stratified lake it is necessary to describe the variation of underwater irradiance as a function of depth and time over the course of a day. A model for underwater irradiance in Lake Chicot was developed by Stefan et al. (1982a). The input to the model is terrestrial (above water) total daily solar radiation measurements as available, e.g. from the Stoneville, Mississippi, weather station. Using empirical equations for albedo (Fig. V-1) and attenuation (Eq. V-7), and a conversion from energy units to quantum units, a composite relationship is derived for photosynthetically active radiation (PAR) under water.

Radiation available with depth is calculated as

$$I(t) = I_s(1 - \text{albedo})e^{-k(z)z} \qquad \text{(VII-11)}$$

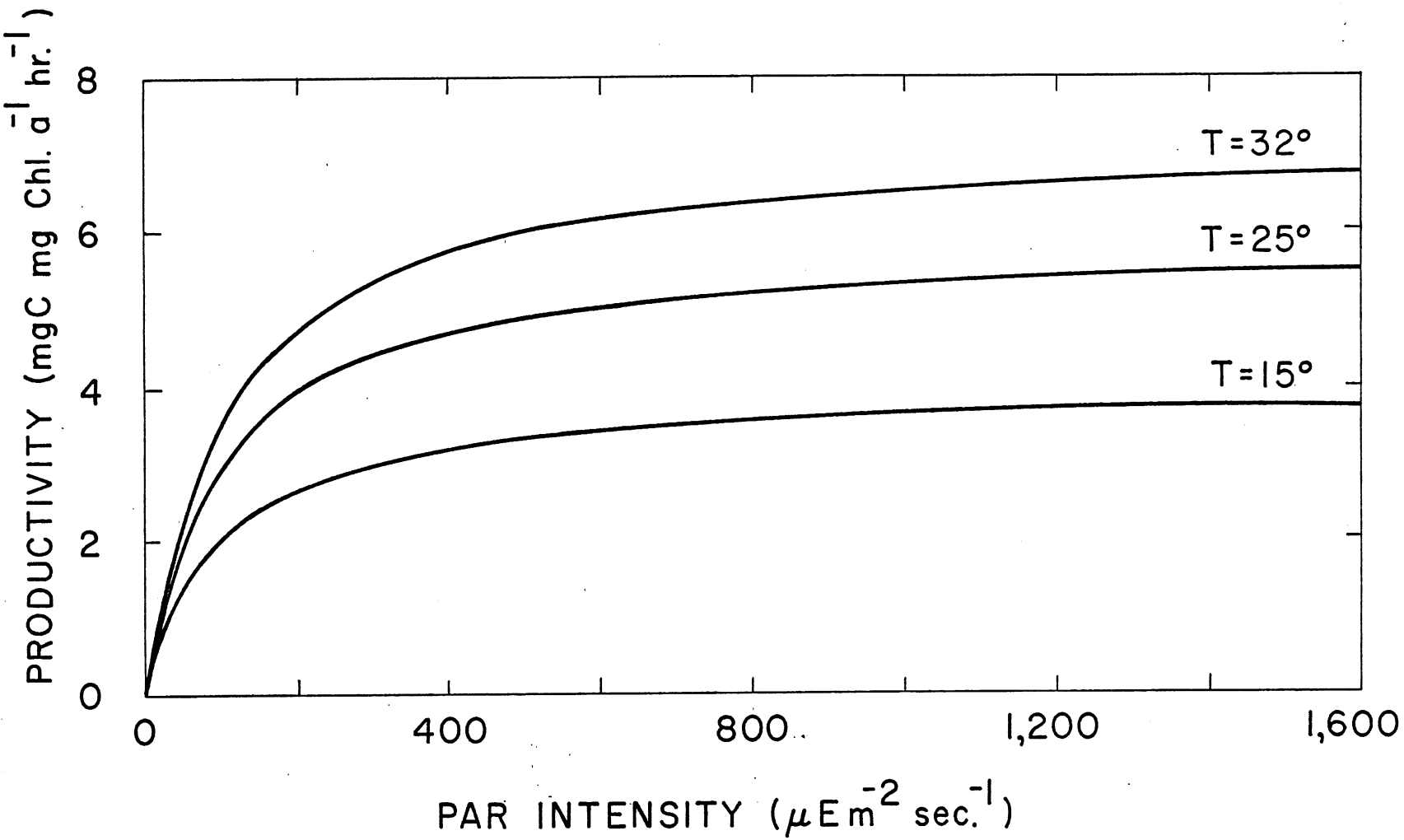

Fig. VII-7. Productivity rate versus PAR intensity and temperature relationship used in model.

Total daily solar radiation measurements are converted to average PAR values by

$$I_s = \frac{27.25}{t_d} H_s \qquad \text{(VII-12)}$$

where I_s = average photosynthetically active radiation over daylight period, above surface ($\mu E\ m^{-2}\ sec^{-1}$)

H_s = measured total daily radiation above water surface ($cal\ cm^{-2}\ day^{-1}$)

$$t_d = 12.16 + 2.36 \cos \left[\frac{2\pi}{365} (172-D) \right] \qquad \text{(VII-13)}$$

t_d = length of daylight (hrs), at latitude 35°N (U. S. Naval Obs., 1977)

D = number of days of year (Jan. 1:D=1)

The variation of irradiance over the length of the daylight is described by a cosine function:

$$I(t) = I_{max} \cos \left(\frac{\pi t}{t_d} \right) \qquad \text{(VII-14)}$$

I(t) = PAR intensity at time t ($\mu E/m^2$-sec)

I_{max} = maximum PAR intensity ($\mu E/m^2$-sec)

t = time of day starting with t=0 at solar noon (hours)

which is transformed to

$$I(t) = I_s \frac{\pi}{2} \cos \left(\frac{\pi t}{t_d} \right) \qquad \text{(VII-15)}$$

For the numerical computation, the daylight period is divided into eight subperiods. Productivity is calculated for each period and averaged over a day. This procedure is repeated for each layer (depth z). The details of the computation are given by Cardoni and Stefan (1982a).

D. Loss Rate And Settling Rate

Loss rate represents the decrease in phytoplankton mass due to normal endogenous respiration and other factors causing plytoplankton mortality (e.g. zooplankton grazing, toxic pesticides, etc.). Endogenous respiration rate is the rate at which phytoplankton oxidize their organic carbon to carbon dioxide per unit weight of phytoplankton organic carbon. Respiration is the reverse of the photosynthetic process. Loss rate of mortality is taken to be a combination of all processes that cause a decrease in phytoplankton mass, except settling. Zooplankton grazing has not been considered independently since there is not sufficient data to make this distinction. Several values from the literature for loss rate in phytoplankton mass modeling are listed below:

.096 day^{-1}	Di Giano (1978)
.05-.25 day^{-1}	Schnoor (1980)
0.1 day^{-1}	Imboden (1978)
(.005 ± .001) * T(°C) day^{-1}	O'Connor et al. (1973)

The relationship proposed by O'Connor et al. (1973) is for endogenous respiration rate. Since endogenous respiration represents a significant portion of the total loss rate, a temperature dependence of the form used by O'Connor is used in the model:

$$\text{loss rate} = K_2 T(°C) \qquad \text{(VII-16)}$$

The coefficient K_2 was determined by calibration with Lake Chicot Chl*a* measurements to be on the order of .005 $°C^{-1}$ day^{-1}.

The settling rate of phytoplankton is a highly variable parameter dependent on species, season, nutrient concentration, age of the population, time of day, and relative brightness of the day (Burns and Rosa, 1980). Jorgensen et al. (1981) quote the settling velocity of Scenedesmus as ranging from 0.1 to 0.6 meters per day, based on literature values. Burns and Rosa (1980) measured settling velocities of ten species of phytoplankton, and found values ranging from 0.07 ± .21 m/day to 0.32 ± 0.32 m/day.

No direct measurements of phytoplankton settling velocities from Lake Chicot are available. Due to the highly variable nature of this parameter and the difficulty associated with measuring it accurately, the model was calibrated by varying the settling rate within the range of values reported in the literature. By comparison of measured in-lake chlorophyll-a concentrations with those predicted by the simulation model, a settling rate on the order of .04 m day^{-1} was determined.

E. Chlorophyll Model Formulation

To predict the concentration of phytoplankton that will be present in the future, Eq. VII-1 must be solved with appropriate boundary and initial conditions. The parameter to indicate algal abundance is chlorophyll-a concentration [Ch&a]. The model is set up for use on a daily time basis, with the lake divided into a number of layers as determined by the model RESQUAL II. The input parameters to the chlorophyll-a model will be incident (above surface) light intensity, suspended solids concentration, and water temperature, each on a daily basis. The boundary conditions are the same as for the suspended sediment model (Eq. VI-3 and VI-4). Based upon these input parameters and an initial value of [Ch&a], the model predicts [Ch&a] for each layer in the lake. The dynamic Eq. VII-1 in numerical form is applied to each layer derived in the temperature model and the suspended sediment model. Inflow of chlorophyll from Connerly Bayou is accounted for by the concentration Eq. III-6. The transport of incoming chlorophyll to the appropriate isopycnic layer is handled by a density current submodel as described in Section IV. Outflow through Ditch Bayou uses the analogy to suspended sediment transport.

Equation VII-1 is of the same form as Eq. VI-1 for the concentration of suspended solids in the lake. Equation VII-1 includes additional source and sink terms. The chlorophyll equation can be solved in the same manner as the suspended solids equation (Dhamotharan et al., 1981).

A flow chart outlining the procedure for predicting chlorophyll-a concentration is shown in Fig. VII-8.

Daily measurements of total solar radiation at the National Weather Service Station at Stoneville, Mississippi, are input to the model. Daily measurements are used because the dynamic model RESQUAL II uses a one-day time step. The total radiation measurements are converted to quantum units of photosynthetically active radiation (PAR) using the conversion of Combs (1977). The productivity versus light intensity relationship is not linear. It is therefore not possible to use the daily average PAR to determine the daily average productivity rate. Instead, the total daily photosynthetically active radiation is distributed throughout the daylight period using the cosine function (Eq. VII-15). The daylight period is divided into eight subsegments, and the average PAR incident at the water surface is computed for each subsegment. This procedure is executed by a subroutine called LIGHT.

The euphotic depth of a lake is defined as the depth at which one percent of the surface irradiance remains. This is the depth at which primary productivity ceases for lack of light. Model RESQUAL II divides the lake into a number of layers, and computes the suspended solids concentration, volume, temperature, and depth boundaries for each layer of the lake. The attenuation coefficient for each layer and the euphotic depth can be computed from this information by Eq. V-7. This is accomplished by subroutine EUPHZ.

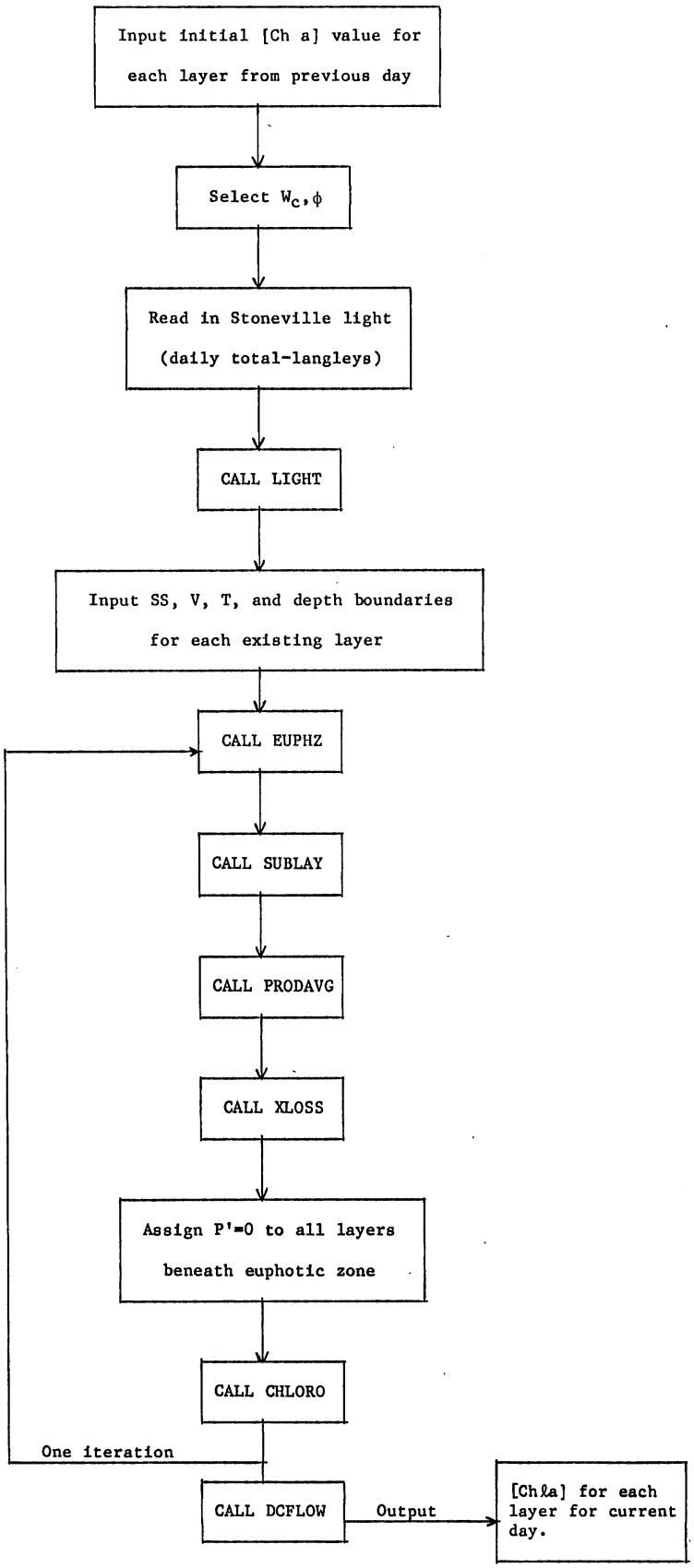

Fig. VII-8. Flow chart of chlorophyll-a model.

Light is attenuated rapidly in Lake Chicot due to the high level of turbidity commonly present. The existing layering system in RESQUAL II uses layer thicknesses up to a maximum of 0.75 m. This is not fine enough to account for the rapid change in light intensity in the euphotic zone. Thus, each of the existing layers in the euphotic zone is subdivided into sublayers of 0.20 m maximum thickness (Subroutine SUBLAY).

The average light intensity in each of these sublayers is computed for each of the eight subsegments of the daylight period. With this information a productivity rate for each sublayer during each subsegment of the day is defined.

Since it is necessary to maintain the existing layering system in RESQUAL II when solving the governing equations (Eq. VII-1), it is also necessary to determine a time and spatially averaged productivity rate for each of the existing layers (in the euphotic zone). To do this, the average productivity rate for the entire daylight period is computed for each sublayer using an arithmetic averaging procedure. Then, the average daily productivity rate for each existing layer is computed from the volume weighted average of each of the sublayers' daily average productivity rates. This procedure is executed by subroutine PRODAVG.

After the system of equations (Eq. VII-1) has been solved once by the subroutine CHLORO, a preliminary value of the new chlorophyll-a concentration for each layer of the lake has been obtained. Then a new attenuation coefficient for each layer is computed using the average of the newly computed value of chlorophyll-a concentration and the value from the previous day. Subroutine CHLORO is then called again to solve Eq. VII-1 for the chlorophyll-a concentrations in all existing layers of the lake using the newly computed attenuation coefficient. This iteration procedure is necessary because attenuation and, hence, light intensity and productivity P are dependent on the chlorophyll-a concentration which changes from day to day.

Any chlorophyll-a in the inflow to Lake Chicot is handled by the subroutine DCFLOW. This subroutine uses a density current approach to determine which layer of the lake receives the inflow, and adds the water and Ch&a from the inflow to this layer. The Ch&a in the inflow is determined as a function of the suspended solids concentration in the inflow.

After the inflow has been added to the lake, the chlorophyll-a concentration for each layer of the lake has been determined. This scheme of calculations is repeated for each day of the simulation.

More details on this procedure are provided by Cardoni and Stefan (1982a).

VIII. NUTRIENT MODEL

At present phytoplankton growth in Lake Chicot is most often controlled by available light. Nutrient concentrations in the lake are generally high and primary productivity is not significantly inhibited by lack of nutrients. The Lake Chicot restoration project is designed to reduce the amount of water and suspended sediment entering the lake. The input of nutrients will therefore also be significantly reduced. A nutrient limitation in the growth model is desirable for future conditions when lower nutrient levels may restrict phytoplankton growth.

Phosphorus and nitrogen are the most likely limiting nutrients. Both have been considered, but only phosphorus is at present represented in the model. Phosphorus was chosen because it is most often the only limiting nutrient for algal growth in fresh waters. EPA (1977) suggested that phosphorus may be more significant in controlling growth in Lake Chicot. Baker (1982) reviewed more recent Lake Chicot nutrient data and came to the conclusion that nitrogen may also be an important nutrient controlling phytoplankton growth.

The framework and general approach to the modeling of phosphorus and nitrogen cycles and interactions with phytoplankton growth in Lake Chicot have been given by Cardoni, Hanson and Stefan (1982b) and Baker (1982), respectively. The cycles of both elements are quite complex and their dynamic modeling requires substantial numbers of rate coefficients and field and laboratory data presently not available. It is for this reason that only a phosphorus model of a relatively simple form has been incorporated into RESQUAL II.

A. Phosphorus Model Formulation

In-lake measurements of phosphorus were made from 1976 through 1980. Available data include total (P_t), total dissolved (P_{td}), ortho- (P_o), and ortho-dissolved (P_{od}) phosphorus. Measurements were made at the water surface; the time interval between measurements varied from one day to one month. While there are several different forms of phosphorus in lake water, only forms of immediate influence on the phytoplankton growth were selected for the model: phosphorus tied up in the phytoplankton cell-mass, available dissolved phosphorus (dissolved orthophosphorus), and a pool of "non-available" phosphorus that may become available phosphorus. Figure VIII-1 shows schematically these three phosphorus compartments and the associated inputs and outputs.

Available phosphorus corresponds to dissolved orthophosphorus, which is immediately available for uptake by planktonic algae. Non-available phosphorus represents phosphorus that is not immediately available but can

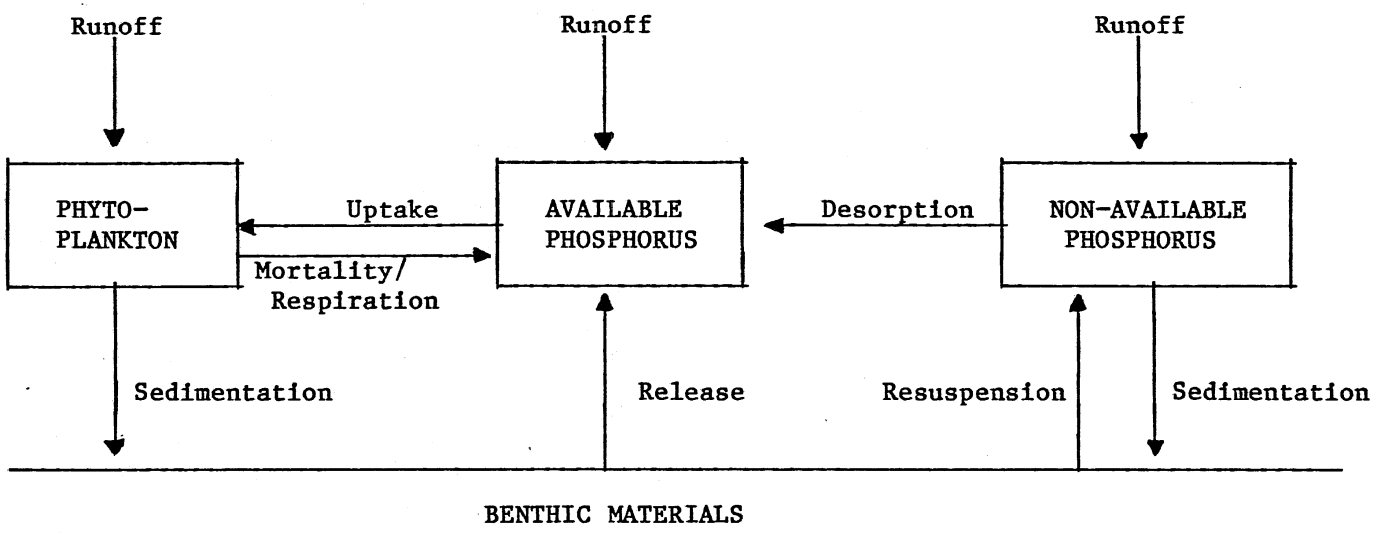

Fig. VIII-1. Phosphorus Submodel - RESQUAL II.

be converted to the available form. Much of this quantity is associated with the inorganic suspended solids in the lake. Phytoplankton represents both a source and a sink of available phosphorus. Available phosphorus is taken up during algal growth. Planktonic mortality and respiration releases organic phosphorus to the available form.

The actual phosphorus cycle in a lake is much more complex than that shown in Fig. VIII-1. In particular, organic detritus and zooplankton have not been modelled as specific compartments. The available data do not allow accurate calculation of the required coefficients for a complex phosphorus cycling system. The simplified cycle shown in Fig. VIII-1 includes the most important components of the system. The exchange coefficients will be calibrated to suite lower Lake Chicot.

The equations governing the phosphorus cycle depicted in Fig. VIII-1 are:

Available phosphorus:

$$\frac{\partial P_a}{\partial t} - \frac{1}{A}\frac{\partial}{\partial z}\left(AK_z \frac{\partial P_a}{\partial z} \right) - K_2 Tr \frac{Ch\ell a}{Y_{ca}} + \mu_m \left(\frac{I}{K_I + I} \right)\left(\frac{P_a}{K_p + P_a} \right) \frac{Ch\ell a}{Y_{ca}}$$

$$- \left[\frac{K_r A}{V} \right]_{\text{bottom layer}} = 0 \qquad \text{(VIII-1)}$$

Non-available phosphorus:

$$\frac{\partial P_n}{\partial t} + \frac{1}{A}\frac{\partial}{\partial z}\left(A W_n P_n \right) - \frac{W_n P_n}{A}\frac{\partial A}{\partial z} - \frac{1}{A}\frac{\partial}{\partial z}\left(A K_z \frac{\partial P_n}{\partial z} \right)$$

$$- \left[\frac{K_{rr} A}{V} \right]_{\text{bottom layer}} = 0 \qquad \text{(VIII-2)}$$

Phytoplankton:

$$\frac{\partial Ch\ell a}{\partial t} + \frac{1}{A}\frac{\partial [AW_c(Ch\ell a)]}{\partial z} - \frac{W_c(Ch\ell a)}{A}\frac{\partial A}{\partial z} - \frac{1}{A}\frac{\partial}{\partial z}\left[AK_z\frac{\partial(Ch\ell a)}{\partial z}\right]$$

$$+ K_2T(Ch\ell a) - \mu_m\left(\frac{I}{K_I+I}\right)\left(\frac{P_a}{K_p+P_a}\right)(Ch\ell a) = 0 \qquad \text{(VIII-3)}$$

These equations are solved for each layer of the lake on a daily time scale. The variables and coefficients used in these equations are:

P_a = available phosphorus, ppb

P_n = non-available phosphorus, ppb

A = projected (horizontal) lake area, m^2

K_z = vertical turbulent diffusivity ($m^2 day^{-1}$)

K_2 = respiration/mortality loss coefficient ($day^{-1} {}^\circ C^{-1}$)

T = water temperature (°C)

r = available phosphorus release fraction

$Ch\ell a$ = chlorophyll-a concentration (ppb)

Y_{ca} = yield coefficient, chlorophyll-a to phosphorus

I = light intensity ($\mu E\ m^{-2}\ sec^{-1}$)

K_I = half saturation coefficient for light ($\mu E\ m^{-2}\ sec^{-1}$)

μ_m = maximum phytoplankton growth rate (day^{-1})

K_p = half saturation growth coefficient for phosphorus (ppb)

K_r = bottom release rate of available phosphorus from sediments (mg P_a m^{-2} day^{-1})

W_n = fall velocity of non-available phosphorus (m day^{-1})

K_r = resuspension rate of non-available phorphorus from the lake bottom (mg suspended solids m^{-2} day^{-1})

W_c = fall velocity of chlorophyll-a (m day^{-1})

B. Determination of Model Coefficients

1. Plankton - Available Phosphorus Link

Models which use the limiting nutrient concept assume that the yield of phytoplankton will in part be determined by the concentration of the limiting nutrient when the nutrient concentration is low. Since yield is a function of growth, growth rate is often substituted. The classical Monod growth rate for phosphorus limitation is described by

$$\mu = \mu_m \frac{P_a}{K_p + P_a} \qquad \text{(VIII-4)}$$

where μ = specific growth rate for phytoplankton (day^{-1}) and the other terms are as previously defined.

The most straightforward approach to formulating a growth rate expression involving both nutrient and light limitation is to multiply the maximum growth rate by the reduction factors for both the limiting nutrient and available light. This approach has been suggested by Chen (1970) and O'Connor et al (1973). The resulting growth expression, using the light limited term and maximum growth rate μ_m developed earlier is

$$\mu = \mu_m \left(\frac{I}{K_I + I} \right) \left(\frac{P_a}{K_p + P_a} \right) \qquad \text{(VIII-5)}$$

An alternative is to calculate the fractions $I/(K_I+I)$ and $P_a/(K_a+P_a)$ separately, and to retain only the smaller of the two.

Plytoplankton growth usually requires available phosphorus uptake. Equation VIII-5 can be used to represent this uptake:

$$u = \mu \frac{Ch\ell a}{Y_{ca}} \qquad \text{(VIII-6)}$$

where u = specific rate of available phosphorus uptake (mg P_a m^{-3} day^{-1}), μ in day^{-1}, Chℓa in mg m^{-3}, and Y_{ca} = the Chℓa to P_a ratio. Equation VIII-5 and VIII-6 are incorporated in Eq. VIII-1. Nyholm (1978) states that the yield coefficient Y_{ca} may vary from 1.19 to 16.3. Measurements in the upper basin of Lake Chicot during July, 1981, (Cardoni and Hanson, 1981) indicate a value of Y_{ca} equal to from about 0.2 to 0.75 (Fig. VIII-2).

Many values have been given in the literature for the half-saturation growth coefficient for phosphorus, K_p, e.g.

.003 - .0015 mg/ℓ	DiToro (1980)
.0031 mg/ℓ	Walters (1980)
.01 - .1 mg/ℓ	Lewis and Ni (1978)
.01 mg/ℓ	O'Connor et al. (1973)

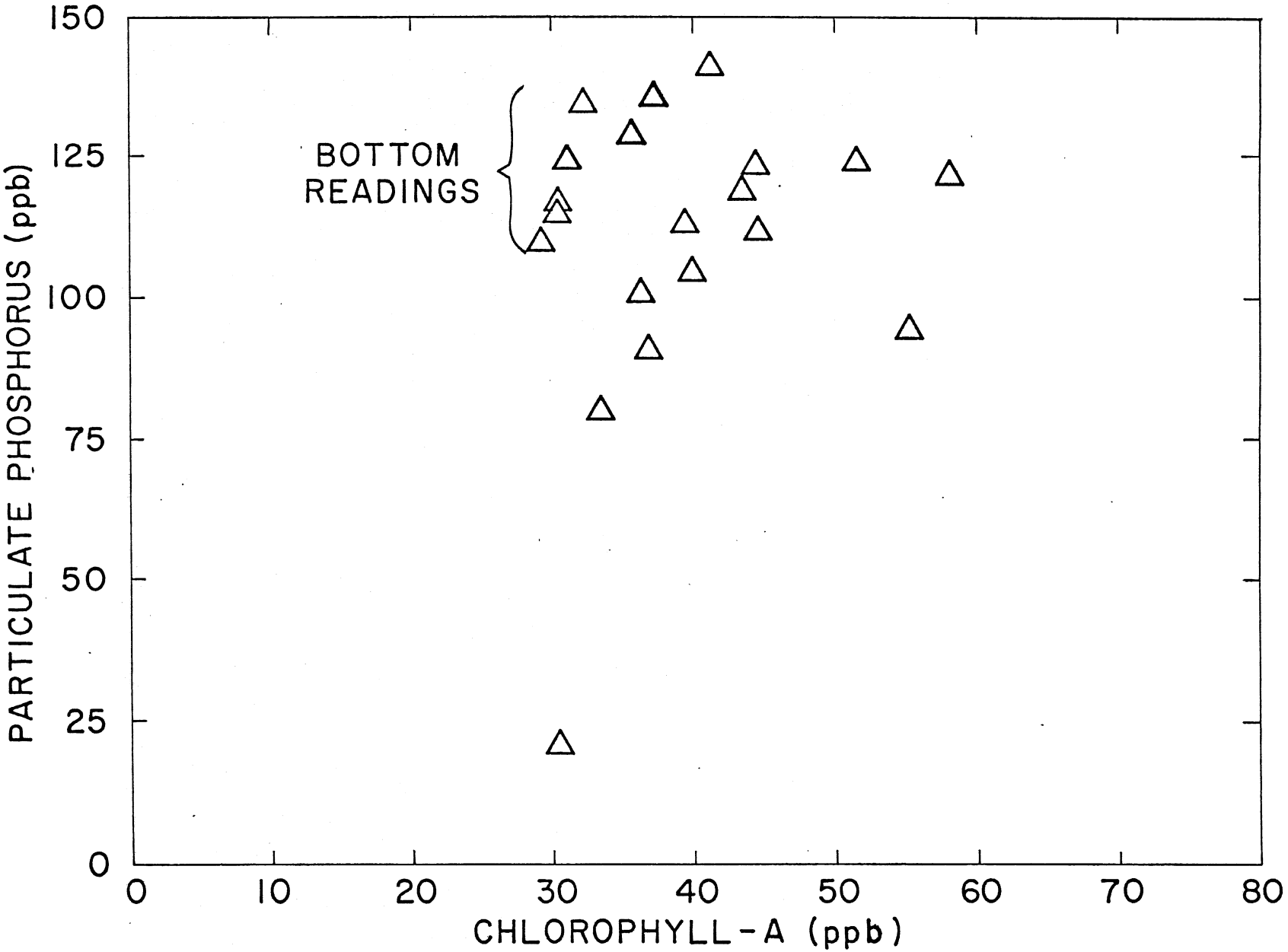

Fig. VIII-2. Particulate phosphorus concentration versus chlorophyll-a concentration, USDA Station C-4, Upper Lake Chicot.

During phytoplankton respiration and decay of dead plankton mass, cellular organic phosphorus is converted to the available form. Several coefficients for the phytoplankton loss rate due to mortality and respiration were listed in Section VII.D.

Using a temperature dependent loss rate of the form of O'Connor et al (1973), the release of available phosphorus from the phytoplankton can be formulated as

$$R = K_2 \, Tr \, \frac{Ch\ell a}{Y_{ca}} \qquad \text{(VIII-7)}$$

where R = specific rate of available phosphorus release (mg $P_a \, m^{-3} \, day^{-1}$)

K_2 = respiration/mortality loss coefficient ($day^{-1} {}^{\circ}C^{-1}$)

r = the fraction of cellular phosphorus converted immediately to available phosphorus

and the other terms are as previously defined. Nyholm (1978) used a value for r of 0.6. Equation VIII-7 is included in Eq. VIII-1.

To account for available phosphorus release during phytoplankton decay beyond the fraction released immediately during respiration, a higher value of r is proposed for the hypolimnion. The phytoplankton in the mixed layer will settle to the hypolimnion, where most decay occurs. The result is that two values of r will be employed, r_m for the mixed layer and r_h for the hypolimnion, where $r_h > r_m$.

2. Available - Non-available Phosphorus Link

Non-available phosphorus is the phosphorus pool that is not in a form immediately available to plant growth but can be converted in time to available phosphorus. Lee et al. (1978) estimated that roughly 20 percent of the difference between the total phosphorus and the soluble orthophosphorus will be available in addition to the soluble orthophosphorus. McDowell et al. (1980) indicate that this percentage could range from 5 to 40 percent.

Lower Lake Chicot generally has a high suspended solids concentration. It is proposed that much of the non-available phosphorus entering the lake is associated with the suspended solids. It was at first considered that desorption from the solid phase will control the conversion from non-available to available phosphorus.

The suspended sediment entering Lake Chicot is most likely neither saturated with nor completely free of adsorbed phosphate. The sediments entering the lake are partially from erosion in the upstream drainage basin

and partially from growth processes in Macon Lake and Connerly Bayou. About 13 percent by weight of the incoming sediments has been determined to be organic material. The solution phosphate concentration in the lake is expected to be somewhat different from that in the tributary, but the difference will most likely not be large. For these reasons, it is not expected that an initial, rapid adsorption or desorption reaction will occur when the sediment enters the lake.

The literature indicates that the bulk of the phosphate adsorption-desorption reaction is complete within a 24-hour time span, and that equilibrium is approached within this period. The Model RESQUAL II is on a daily time scale; therefore accuracy will not be sacrificed by using an equilibrium rather than a kinetic approach to estimate the magnitude of the phosphate adsorption-desorption reaction.

In the governing equations of non-available and available phosphorus (Eqs. VIII-1 and VIII-2) the desorption process is not included. This process will instead be included by a "partitioning" in the following way. Equations for non-available and available phosphorus will be solved numerically. Then the concentration of available phosphorus (P_a) in each layer will be compared with an equilibrium concentration of available phosphorus ($P_{a,eq}$). The value of ($P_{a,eq}$) can be determined by a laboratory experiment (see Cardoni et al., 1982b). If available phosphorus concentration is greater or equal to ($P_{a,eq}$), nothing further needs to be done. If $P_a <$ ($P_{a,eq}$), two cases have to be considered.

(i) if $(P_{a,eq} - P_a) < P_n$ (non-available phosphorus)

then, $P_a = P_{a,eq}$

and $P_{n_{new}} = P_{n_{old}} - (P_{a,eq} - P_a)$

(ii) if $(P_{a,eq} - P_a) > P_n$

then, $P_{a_{new}} = P_{a_{old}} + P_n$

and $P_{n_{new}} = 0$

This "partitioning" will be done after the solution of the two governing equations and before advancing to the next time step.

3. Inflow, Settling, and Resuspension Rates

The inflow to Lake Chicot contains available phosphorus and non-available phosphorus. The concentration of available phosphorus in the inflow is fairly consistent, with an average value of 100 ppm over the period of data collection (Section III-B).

The inflow of convertible non-available phosphorus is estimated from Eq. III-8.

$$P_n(\text{inflow}) = \eta \left[.025(SS)^{.573} - Ch\ell a/Y_{ca}\right] \qquad \text{(VIII-8)}$$

where SS = suspended solids concentration in the inflow (ppm)

η = fraction of the non-available phosphorus that may become available.

This equation is based on the data in Fig. III-8.

Non-available phosphorus is assumed to be associated with the suspended solids in the lake. Thus, non-available phosphorus will have a settling velocity W_n equivalent to that of the suspended solids.

Resuspension of non-available phosphorus from the lake bottom would be in the form of suspended solids resuspension. In Lake Chicot, solids resuspension does not seem to be significant at present.

Release of available phosphorus from the bottom sediments requires anoxic conditions at the sediment-water interface. This condition may be attained during a stratified period with much organic decay at the lake bottom. Under the present conditions anoxic conditions occur rarely and this term is neglected.

Table VIII-1 summarizes the coefficients required for the phytoplankton/phosphorus submodel, and their respective values.

4. Total Phosphorus Concentration

Total phosphorus concentration in Lake Chicot is modeled as a function of the suspended solids concentration in the lake. The data in Fig. III-8 relates suspended solids concentration to the difference between total phosphorus and dissolved orthophosphorus, both in the lake and at the inlet to the lake. Equation VIII-8, without subtraction of the phosphorus associated with the plankton and without the η reduction is used to predict the total phosphorus concentration in the lake.

$$P_t = 0.025(SS)^{.573} + P_a \qquad \text{(VIII-9)}$$

TABLE VIII-1. PHYTOPLANKTON MODEL COEFFICIENTS

Symbol	Meaning of Symbol	Value	Reference Source	Calib. Value	Comments
K_2T	Plytoplankton Mortality/ Respiration Rate	0.096 day^{-1} .05-.25 day^{-1} .005*T(°C)day^{-1} 0.1 day^{-1}	DiGiano (1978) Schnoor (1980) O'Connor et al (1973) Imboden (1978)	.005T(°C) day^{-1}	Mineralization coefficient Endogenous Respiration Mineralzation rate
K_I	Half saturation coefficient for light	100 $\mu E/m^2$-sec 400 k cal/m^2-day	Lake Data Jorgensen (1978); Gargas (1975)	100 μE m^{-1} sec^{-1}	400 K cal/m^2-day ≈ 45 $\mu e/m^2$-sec (Combs conversion)
K_p	Half saturation growth coefficient for phosphorus	.0003-.0015 mg/ℓ ≈ .01 mg/ℓ ≈ .01-.1 mg/ℓ	DiToro (1980) O'Connor et al. (1973) Lewis & Nir (1978)	.015 mg/ℓ	Variable cell nutrient quota constant cell nutrient quota
K_r	Bottom release rate from sediments	.704 mg P/m^2-day	Golterman (1975)	0	Great Lakes, Oxygenated, winter
K_{rr}	Resuspension rate of non-available phosphorus (at bottom layer, gm SS/m^2-day)			0	
$P_{a_{equil}}$	Equilibrium concentration of available phosphorus			0.08 mg/ℓ	
r_h	Phosphorus release fraction (hypolimnion)	> 0.6		1.0	
r_m	Phosphorus release fraction (mixed layer)	0.6	Nyholm (1978)	0.8	
W_c	Settling velocity of chlorophyll-a	0.1-0.6 md^{-1} .08-1.87 md^{-1} < .1 md^{-1} 1-3 md^{-1} .1-1.0 md^{-1} .1-5 md^{-1}	Jorgensen et al. (1981) Schnoor (1980) Schnoor (1980) Schnoor (1980) Schnoor (1980) Lewis & Nir (1978)	0.4	Literature range, SCENEDESMUS From Titman & Kilham (1976) Bluegreens & phytoflagellates Geen algae Diatoms
Y_{ca}	Yield coefficient (in cell) (chlorophyll-a to phosphorus)	0.3 1.19 to 16.3 1.0	Lake Data (1981) Nyholm (1978) Metro Waste Control Comm. (1977)	0.6	
η	Fraction of difference between P_{total} and $P_{ortho\text{-}dissolved}$ that may become available phosphorus	.20 .05-.40	Lee et al. (1978) McDowell et al. (1980)	.20	
ϕ	Yield coefficient (carbon to chlorophyll-a)	65 25.2 50 13-135	Canale & Vogel (1974) Nyholm (1978) Jorgensen (1981) Smith (1980)	30	Assumed average for optimal light nutrients

IX. SECCHI DEPTH MODEL

Secchi depth is a comprehensive measurement of water transparency. Lay people can easily relate to the meaning of Secchi depth.

Secchi depths in upper and lower Lake Chicot were analyzed and related to attenuation coefficients in an extensive study by Stefan et al. (1982b). Secchi depths in the lower lake were related to total suspended solids (Fig. IX-1) and Secchi depths in the upper lake were related to Chℓa (Fig. IX-2). Equations IX-1 and IX-2 describe the data in Figs. IX-1 and IX-2, respectively.

$$z_{SD} = \frac{3.67}{(SS)^{.625}} \qquad \text{(Lower Lake)} \qquad \text{(IX-1)}$$

$$z_{SD} = \frac{1.37}{Ch\ell a^{.258}} \qquad \text{(Upper Lake)} \qquad \text{(IX-2)}$$

z_{SD} is the Secchi depth in meters, (SS) is the suspended solids concentration in ppm and (Chℓa) is the chlorophyll-a concentration in ppb.

Development of a predictive model of Secchi depth requires incorporation of the cumulative effects of inorganic suspended solids and phytoplankton on transparency. Two methods for predicting Secchi depth in Lake Chicot were developed.

The first method involves linear relationships between the inverse of Secchi depth and suspended solids and chlorophyll-a concentrations. The effects of suspended solids and Chℓa have been isolated by considering the lower and upper basins of Lake Chicot during periods when inorganic suspended solids (SS) and phytoplankton, respectively, dominated turbidity. Figures IX-3 and IX-4 show the measured relationships between $1/z_{SD}$ and SS and Chℓa. The data from the upper lake were obtained when suspended solids concentrations were less than approximately 45 mg/ℓ. The equations of best fit to the measured data in Figs. IX-3 and IX-4 are, respectively,

$$1/z_{SD} = 2.16 + 0.0265(SS) \qquad \text{(IX-3)}$$

$$1/z_{SD} = 1.66 + 0.0083\ (Ch\ell a) \qquad \text{(IX-4)}$$

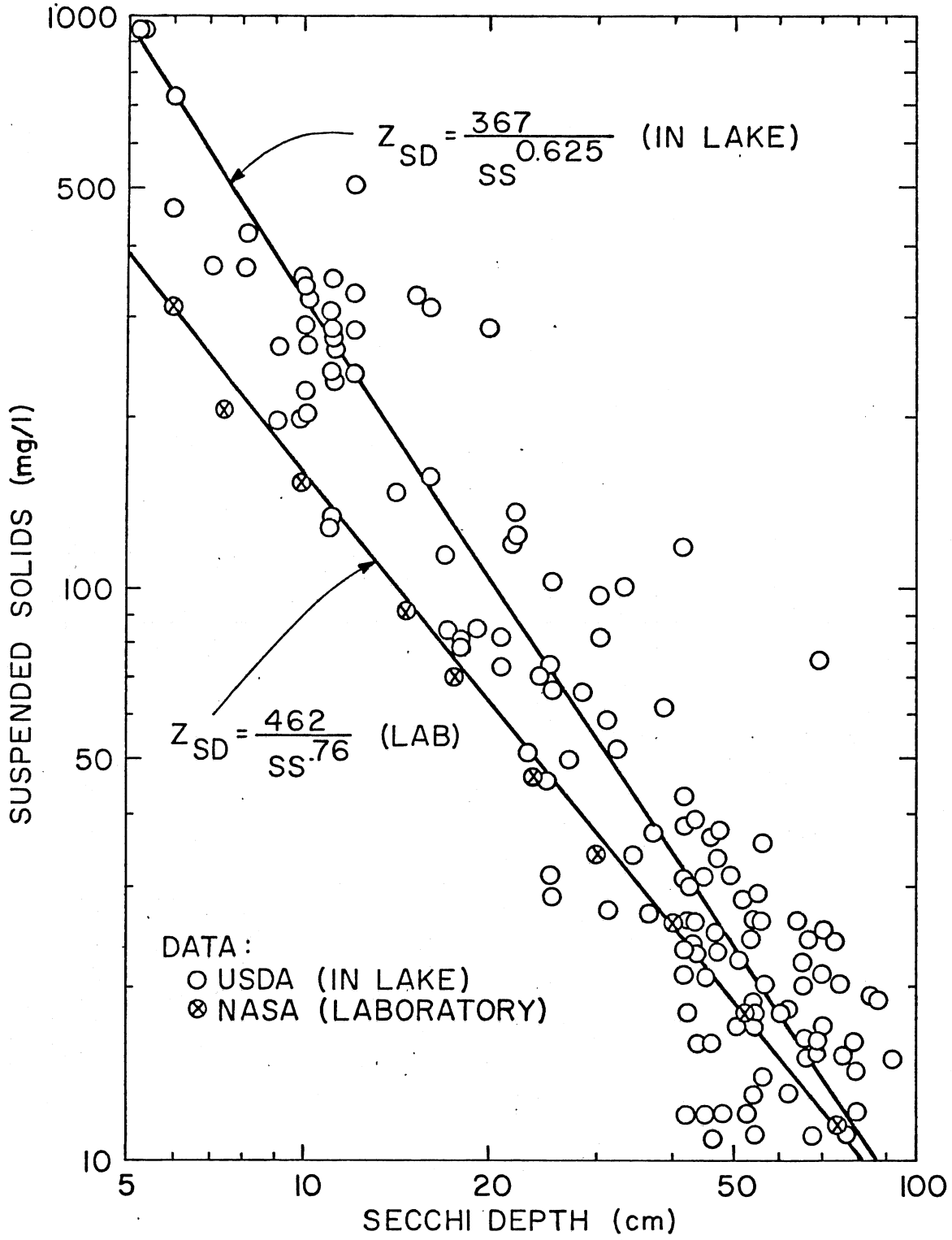

Fig. IX-1. Secchi depth versus suspended sediment concentration in Lake Chicot. Fitted line: $C_{SS} = 8\ d^{-1.6}$, with C_{SS} in mg/ℓ and d in meters.

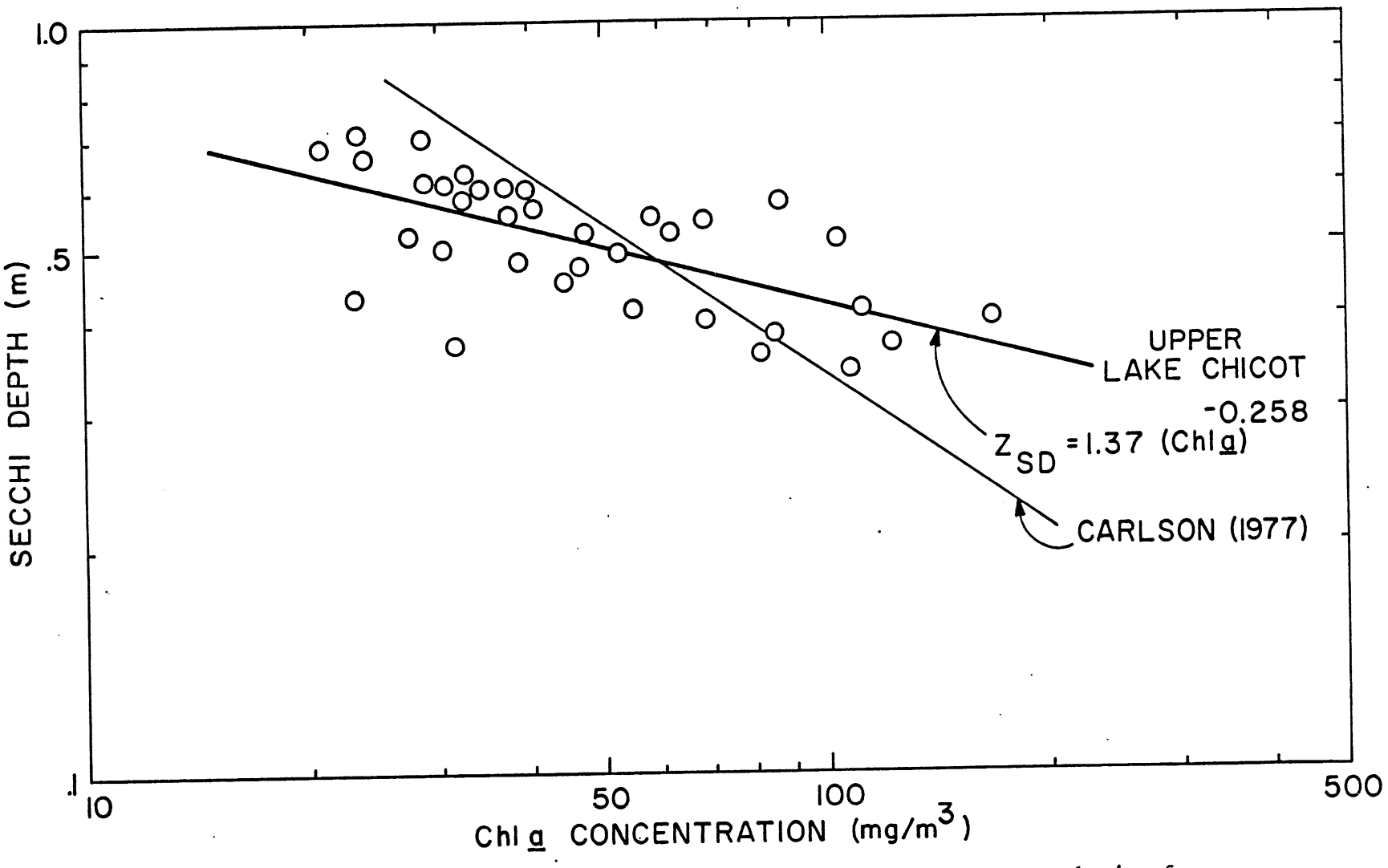

Fig. IX-2. Chlorophyll-a concentration versus Secchi depth in the upper basin of Lake Chicot, when SS < 45 ppm.

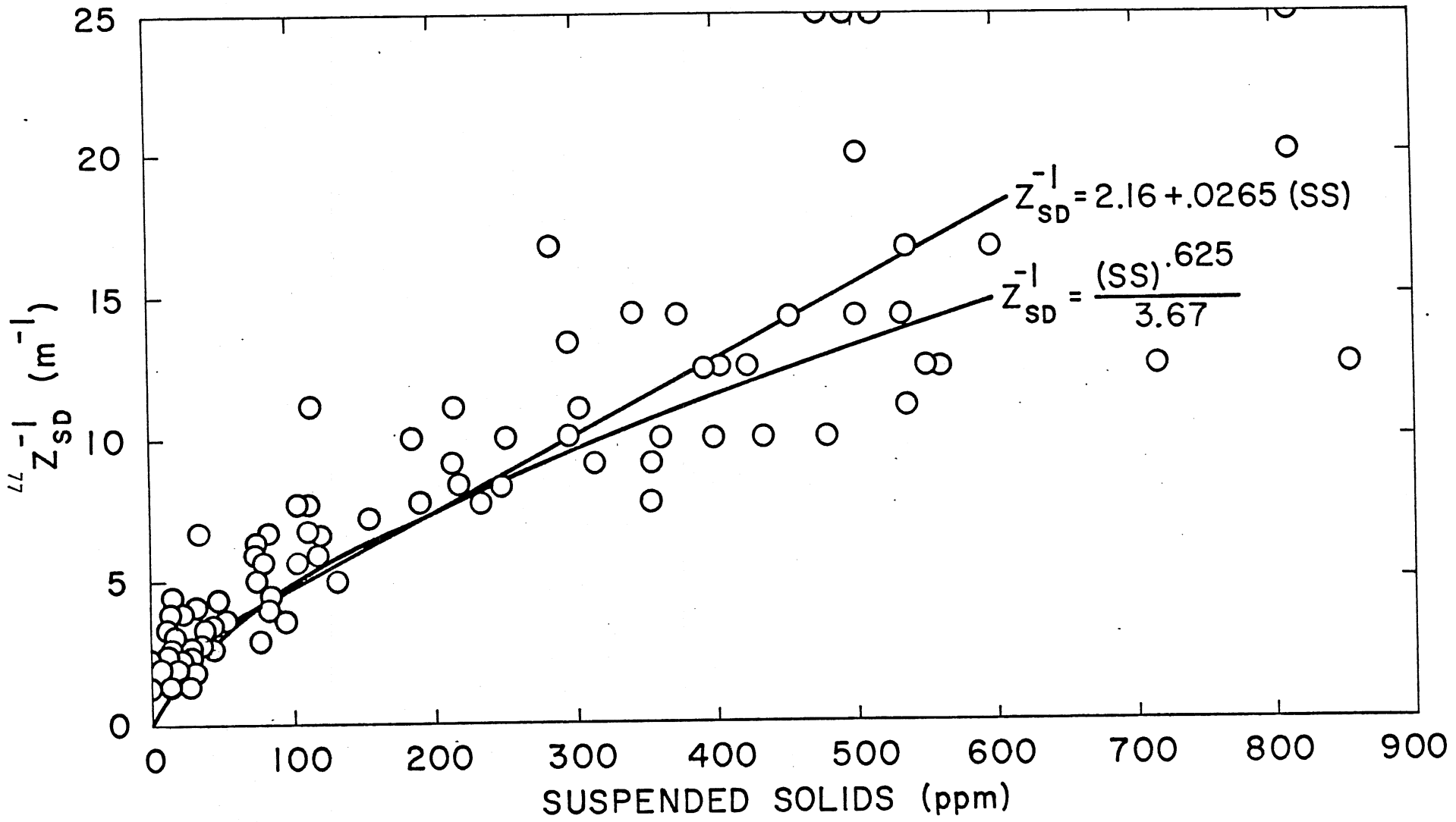

Fig. IX-3. Inverse of Secchi depth versus suspended solids concentration, Lower Lake Chicot.

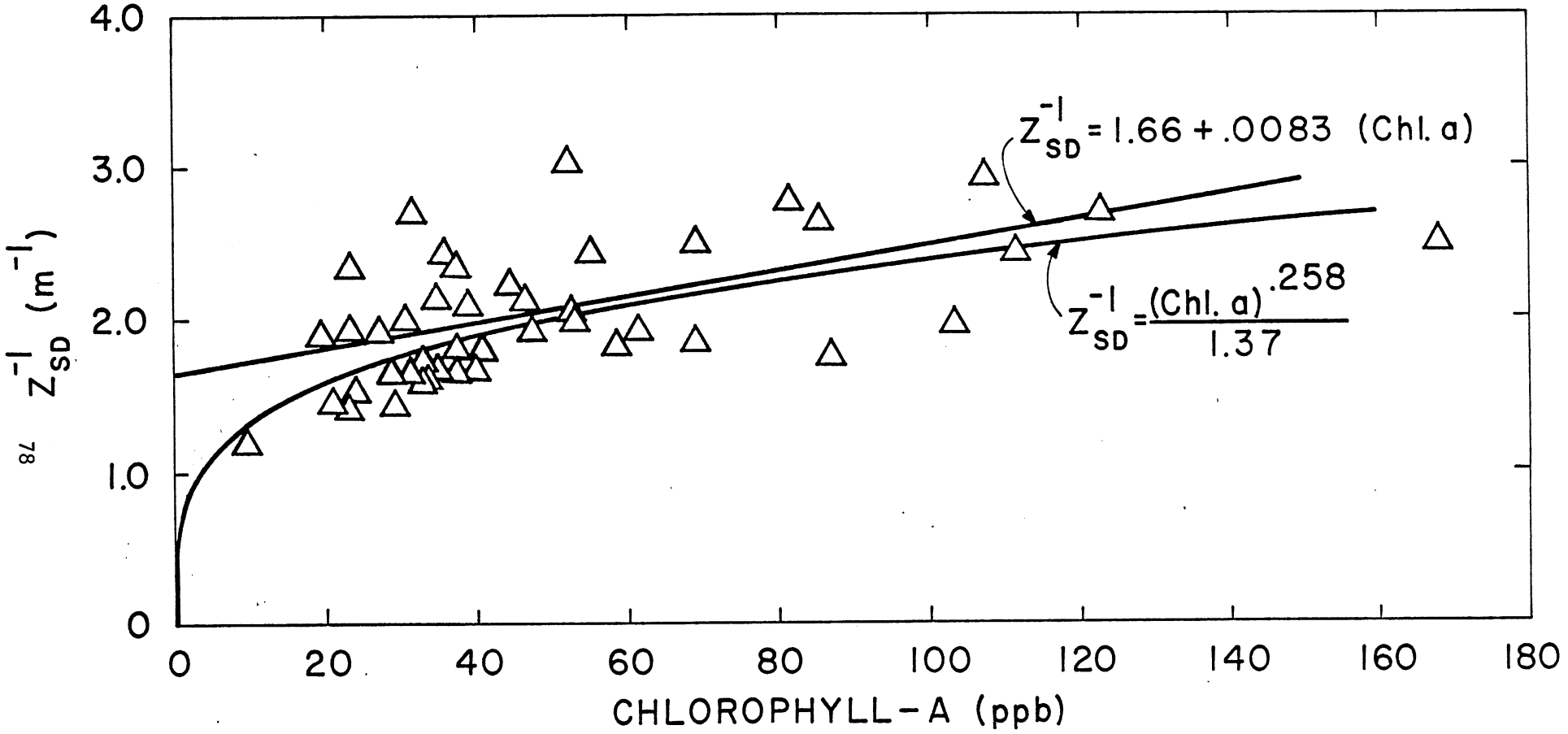

Fig. IX-4. Inverse of Secchi depth versus chlorophyll-a concentration, Upper Lake Chicot (SS concentration < ≈ 45 ppm).

where SS is in ppm and Chℓa is in ppb. The coefficient for the effect of Chℓa, 0.0083, is lower than those presented by Brezonik (1978) (≈ .03) and Shapiro (1982)(.0146). Brezonik's data is from 55 Florida lakes, and Shapiro's data is from Minnesota lakes. To combine Eqs. IX-3 and IX-4, the effects of SS and Chℓa are considered additive. The intercept value is not the same in both basins, indicating that factors other than SS and Chℓa in each of the respective basins were not the same. Using an average of the intercept values, the composite relationship for Secchi depth is

$$1/z_{SD} = 1.9 + 0.00265(SS) + 0.0083(Ch\ell a) \qquad \text{(IX-5)}$$

The second approach to formulating a Secchi depth model involves a combination of the logarithmic and the linear relationships for Secchi depth presented here. Equations IX-1 and IX-2 have been added to Figs. IX-3 and IX -4, respectively. Equation IX-2 provides a better fit than Eq. IX-4 to the data in Fig. IX-4. The effect of suspended solids on the Secchi depth is adequately described by Eq. IX-3. Combining Eqs. IX-2 and IX-3, the following composite relationship is proposed.

$$\frac{1}{z_{SD}} = \frac{(Ch\ell a)^{.258}}{1.37} + 0.0265(SS) \qquad \text{(IX-6)}$$

The SS term in Eq. IX-6 isolates the effect of SS alone, and does not include other factors influencing transparency since the intercept from Eq. IX-3 is not included. The Chℓa term from Eq. IX-2 does not have an intercept that isolates other factors affecting z_{ZD}, and thus they are included in this term. To prevent the Secchi depth from going to infinity at zero Chℓa and SS concentrations, a minimum Chℓa concentration of 3 ppb will be imposed. This sets the maximum possible Secchi depth at 1.03 meters, which is slightly deeper than the maximum Secchi depth measurement from the available Lake Chicot data. Equation IX-6 is graphically presented in Fig. IX-5. Equation IX-6 is used to predict Secchi depth in the model RESQUAL II.

The shading of phytoplankton by inorganic suspended sediment produces an inverse correlation between Chℓa and SS, as shown by the data in Fig. IX-6. Therefore, only the range of the Chℓa values to the left of the dotted line in Fig. IX-5 is of practical interest.

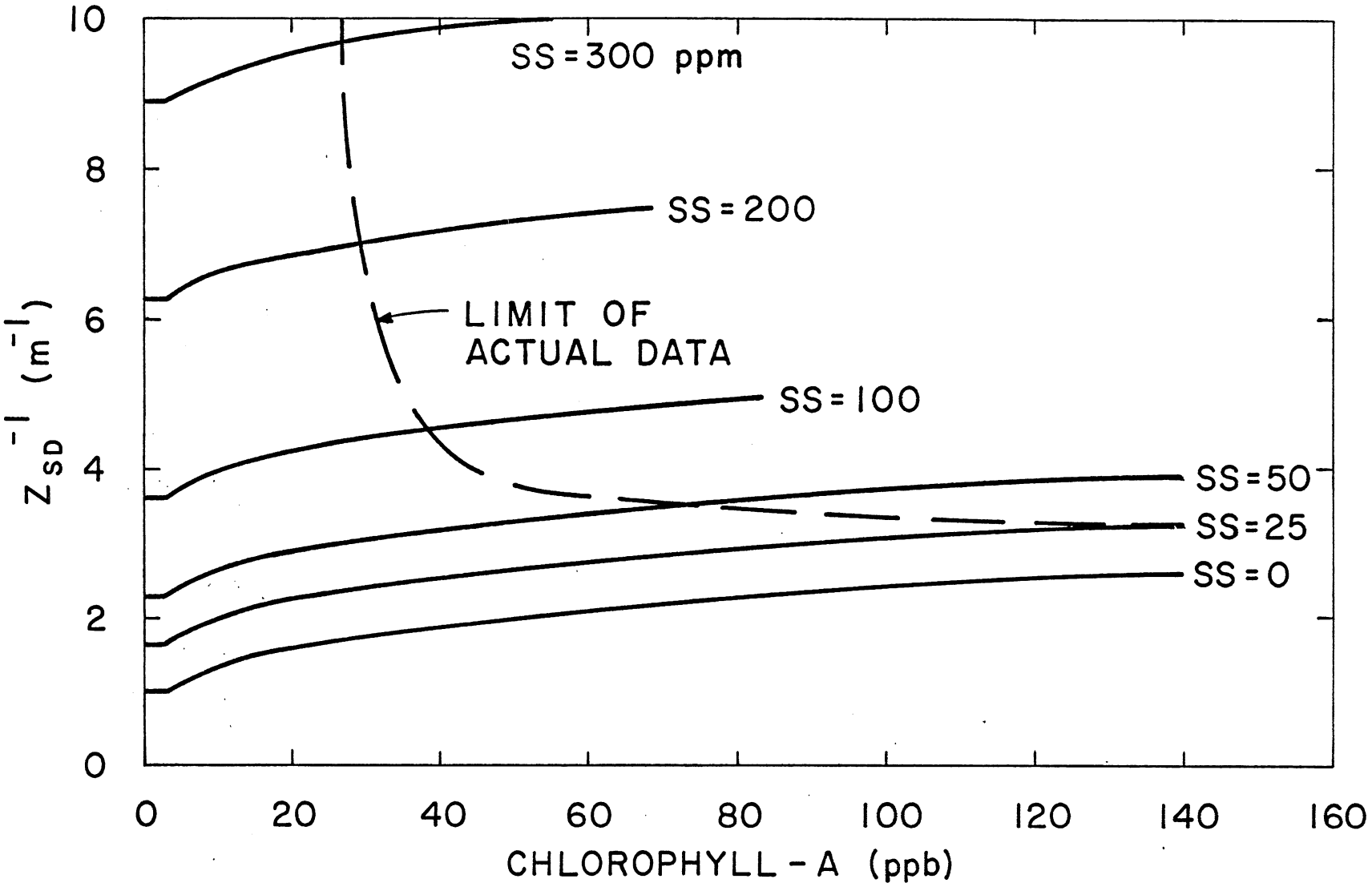

Fig. IX-5. Inverse of Secchi depth versus chlorophyll-a and suspended sediment concentration, proposed composite relationship for Lake Chicot.

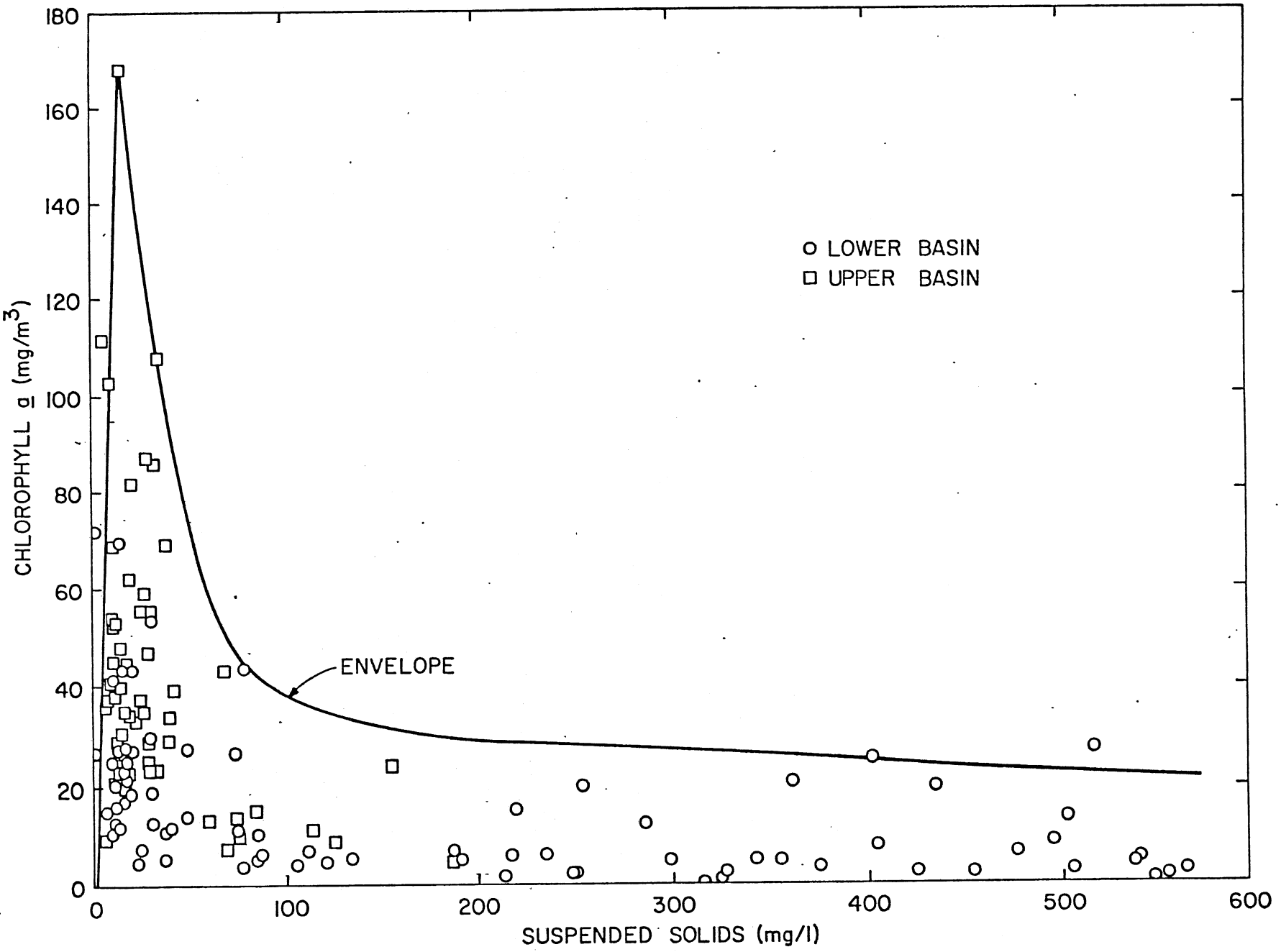

Fig. IX-6. Chlorophyll-a versus suspended solids in upper and lower Lake Chicot. USDA Stations 7 and 4.

X. COMPUTER PROGRAM RESQUAL II

A. Organization

The submodels identified in Fig. II-2 and described in the preceding section are incorporated in computer program RESQUAL II. A detailed description of the program was prepared by Fu (1982). Among the main submodels describing physical/chemical biological processes are:

CHLORO = Chlorophyll growth
DCFLOW = Density current
HEBUG = Heat budget
DISOLID = Dissolved solids and available phosphorus
RESSETL = Suspended sediments and non-available phosphorus
WINMIX = Mixed layer depth

There is a total of 53 subroutines in RESQUAL II. A complete alphabetical listing and brief description of each routine was assembled by Fu (1982).

Subroutines to facilitate input, computing options, and output are:

START = Control input and computing options
PRNOUT = Control output

The main program calls the submodels in sequence. By not solving all equations simultaneously, the program is simplified and the computing time is considerably reduced.

The uncoupling of the submodels requires that input data into one submodel be taken from the output of the other submodels in the previous timestep. This is appropriate for three reasons.

First, the model is operated in a timestep (1 day) over which changes in the computed parameters are small. The error introduced in using e.g. suspended sediment concentration from the previous day instead of the current day affects results to a lesser degree (as was verified by adding additional iteration steps to the program) than the uncertainties in estimating model input parameters, e.g. settling velocity of particles and entrainment coefficient of density inflow, surface heat exchange coefficients, albedo, etc.

Second, the coupling between the main submodels in RESQUAL is actually very weak. Most of the inflow into Lake Chicot occurs during the two months just prior to the summer stratification period. Outflow is always

from the surface mixed layer. Suspended sediment concentration affects mainly the radiation balance of the mixed layer and suspended sediment concentration in the mixed layer changes only slowly. Dissolved solids concentrations do not control density stratification to any appreciable degree.

Third, the input variables which drive the model most strongly are runoff and weather related. The latter are highly variable in time and have to be obtained from measuring stations remote from the lake. Because of that variability, lake temperatures and mixing "tend" towards constantly changing equilibrium or ultimate temperatures. Therefore, prediction errors are not cumulative.

B. Numerical Solutions

The partial differential equations (advection/diffusion equations) for T, SS, Ch&a, P_a and P_n are solved by implicit methods.

1. Water Temperature Eq. V-1

In the formation of a finite difference scheme, stability and accuracy are of main concern. For the water temperature Eq. V-1, a fully implicit central difference scheme was selected. The scheme was formulated for variable layer thickness $\Delta z(i)$. The resulting finite difference equation is of the form

$$T(i,j+1) - T(i,j) = - D^*(i-1/2)\,[T(i,j+1) - T(i-1,j+1)]$$

$$+ D^*(i+1/2)\,[T(i+1,j+1) - T(i,j+1)] + S^*\Delta t \qquad (X\text{-}1)$$

where i = number of layer counted from the surface

j = timestep (day)

$$D^*(i-1/2) = \frac{2\Delta t\, D(i-1/2)}{\Delta z(i)\,[\Delta z(i) + \Delta z(i-1)]}$$

$$D^*(i+1/2) = \frac{2\Delta t\, D(i+1/2)}{\Delta z(i)\,[\Delta z(i) + \Delta z(i+1)]}$$

and $$S^* = \frac{S}{\rho c V(i)}$$

The above equation may be rewritten as

$$aT(i-1,j+1) - bT(i,j+1) + cT(i+1,j+1) + d = 0 \qquad \text{(X-2)}$$

where $a = D^*(i-1/2)$

$c = D^*(i+1/2)$

$b = 1 + a + c$

$d = T(i,j) + S^*\Delta t$

To compute D(i-1/2) and D(i+1/2), a harmonic mean is used

$$D(i+1/2) = \frac{2D(i)\ D(i+1)}{D(i) + D(i+1)} \qquad \text{(X-3)}$$

$$D(i-1/2) = \frac{2D(i)\ D(i-1)}{D(i) + D(i-1)} \qquad \text{(X-4)}$$

Equation X-2 was solved by a tri-diagonal matrix algorithm. The boundary conditions applied are:

(i) no heat flux to and from the sediment or T(j+1,N) = T(j+1,N+1), where N+1 refers to a dummy layer below the bottom layer of the reservoir.

(ii) No diffusive heat flux between the surface mixed layer and the hypolimnion

$$\left[D\,\frac{\partial T}{\partial z}\right]_{m+1/2} = 0$$

where m = number of last layer in surface mixed layer.

After introduction of the boundary conditions and algebraic manipulation, the coefficients in Eq. X-2 become

$$a_i = D^*(i-1)$$

$$c_i = D^*(i)$$

For the topmost layer (1): $a_1 = 0$ and $c_1 = D^*(1)$

for the bottom layer (N): $a_N = D^*(N-1)$ and $d_N = T(N,j) + S(N)\ \Delta t$

This gives for the bottom layer

$$T(N,j+1) = g_N \tag{X-5}$$

$$g_N = \frac{a_N\ g_{N-1} + d_N}{1 + a_N(1 + w_{N-1})}$$

$$T(i,j+1) = g_i - w_i\ T(i+1,j+1) \tag{X-6}$$

where $$g_i = \frac{a_i\ g_{i-1} + d_i}{b_i + w_{i-1} + a_i}$$

and $$w_i = \frac{-c_i}{b_i + w_{i-1}\ a_i}$$

Equation X-6 can be solved from N on backwards.

The numerical solution of the diffusion equation for heat necessary to predict water temprature stratification is accomplished as part of subroutine HEBUG.

2. Suspended Sediment Eq. VI-1

The subroutine which solves the suspended sediment Eq. VI-1 is RESSETL. An implicit, hybrid finite difference scheme was developed to solve the suspended sediment equation. That scheme has been described in detail by Dhamotharan et al. (1981). It is stable for various combinations of vertical turbulent diffusivities and particle fall velocities.

3. Chlorophyll-a Eq. VII-1

CHLORO is a modified version of the subroutine RESSETL contained in the RESQUAL model. This subroutine will solve Eq. VII-1 for all layers of the lake by using an implicit finite difference scheme. The numerical method used to solve this equation is described by Dhamotharan et al. (1981). The modification of RESSETL is required to account for the additional source and sink terms that are contained in the chlorophyll-a model.

C. Computational Options

One need not use all available submodels each time. Three options are available to select submodels by setting the elements of the integer array MODEL(I) to either 1 or 0. (Zero means a submodel will not be used; one means it will be used.) If all elements of MODEL(I) are set to zero, only the water temperature, suspended solids, and dissolved solids submodels will be selected. If MODEL(1) is set to one and all others zero, the light-limited chlorphyll-a submodel will be selected in addition to the water temperature, suspended solids and dissolved solids submodels. If MODEL(2) is set to one and all others zero, all the submodels will be selected.

D. Model Input

MODEL RESQUAL II requires four types of input data:

- initial conditions
- morphometric lake and channel data
- inflow data
- weather data

The details of these requirements are given in the instruction manual prepared by Fu (1982). Some of the main points shall be given here.

Initial Conditions

The initial conditions which need to be specified include:

(a) the initial number N of layer in the lake typically 20
(b) T(i,1)
(c) SS(i,1)
(d) Chℓa(i,1)
(e) $P_a(i,1)$; $P_n(i,1)$

where the number of layers varies, $1 < i < N$. An initial lake stage is also required.

Lake Morphology

Lake Morphology has been described in Section III. The parameters m and c in Eq. III-3 need to be specified.

Inflow

Inflow has been discussed in Section III-B. Both quantity and quality of inflow need to be specified on a daily basis. Inflow rate is given by specifying an upstream stage elevation S_M and then computing flow rate by Eq. III-4. Inflow water temperature must be specified. Inflow suspended sediment concentration, chlorophyll-a, and phosphorus of the inflow will be estimated by Eq. III-5 to III-8.

Weather

Required weather data comprise daily total solar radiation, daily mean air temperature, dew point temperature, mean wind velocity, daily precipitation, and daily cloud cover.

E. Model Output

Model output is either in the form of tables or graphs as described by Fu (1982).

XI. CALIBRATION

RESQUAL II contains submodels which simulate water temperature, suspended solids, dissolved solids, chlorophyll-a, available ortho-dissolved phosphorus, non-available phosphorus, total phosphorus, and Secchi depth. Coefficients in each of these submodels have to be assigned numerical values. Some of these are physical constants, others are known from previous investigations or can be derived from Lake Chicot data with good reliability. For some coefficients, only order of magnitude estimates or ranges of numerical values are known. More precise values of these coefficients applicable only to Lake Chicot are established by model calibration, i.e. comparison of simulated and observed results.

The calibration was made with data collected during water year 1977 (Oct. 1, 1976 - Sept. 30, 1977). The data were collected by the USDA/ARS mostly at biweekly intervals. Calibrations were made in the major submodels successively and in the order in which they are listed in Table XI-1.

The mass flow and temperature stratification models were calibrated first. The two parameters which were the least well established and had to be calibrated were vertical turbulent exchange coefficient K_z and initial dilution at the plunge point γ_{in}.

The temperature model was at first calibrated for mean annual values of K_z = 400 m^2/day in the surface mixed layer and K_z = 1 m^2/day in the hypolimnion, respectively. (See Dhamotharan, 1979). Then, coefficients a_m = 28 for the mixed layer, a_h = 0.1 for the hypolimnion, and b = 1.3 in Eq. V-21 were determined by using a mean annual wind in these equations.

In the suspended sediment model a particle size on the order of 1 μ as determined by sediment analysis had to be used. The complete size distribution of particles was never obtained. Calibration confirmed that 1 μ gave loss rates by settling in agreement with measurements.

The chlorophyll submodel required several coefficients. Literature and Lake Chicot field values of these coefficients are given in Table VIII-1. The range of values tested in the model and the calibrated value are given in Table XI-1.

The phosphorus model had several coefficients to be calibrated. Ranges and values are shown in Tables XI-1 and VIII-1. Simulated results and calibration data are shown in Figs. XI-1 through XI-7.

RESQUAL II has been calibrated by comparing the computed values with available measurements. The root mean square calibration error (ε) for

each water quality parameter is computed in the plotting program RESPLT and printed on the output plot. The root mean square calibration error ε is defined as

$$\varepsilon = \sqrt{\frac{\sum_{i=1}^{n} (C_{ic} - C_{im})^2}{n}} \qquad \text{(XI-1)}$$

where C_{ic}= computed water quality parameter on the ith day

C_{im} = measured water quality parameter on the same day

n = number of measurements

Calibration coefficients were changed until the value of ε could not be further reduced.

More systematic schemes to calibrate RESQUAL II such as the least-squares optimization adopted by Norton (1974) in calibrating the RMA-12 model were not used because of the large computing cost which would have been involved.

TABLE XI-1. COEFFICIENTS OF SUBMODELS

Submodel	Symbol	Coefficient	Range of Value Tested	Value Used
1. Temperature	a_m	Wind dependent vertical diffusion coeff.	28.0	28.0
	b	exponent in the wind dependent vertical diffusion coeff.	1.3	1.3
	a_h	wind dependent vertical diffusion coeff.	0.1	0.1
	γ_{in}	Plunging entrainment coefficient ( )	1.8 - 5.0	mixed layer
2. Suspended Sediment		FRAC = fraction of inflow suspended sediment deposited instantly at Lake inlet	0.3 - 0.65 (Before Mar. 10) 0.8 - 1.0 (after Mar. 10)	0.35 before March 10 and 1.0 after Mar 10
		Particle diameter (DS)	0.8μ - 4.0μ	1.0μ
3. Chlorophyll-a	W_c	Fall velocity (FVCHLA)	0.03 m/day - 1.0 m/day	0.04 m/day
	ϕ	Carbon chlorphyll ratio (YCCHLA)	25 - 60	30
	K_I	Half saturation coeff. for light (HSC)	75 $\mu E/m^2$-sec to 100$\mu E/m^2$-sec	100 $\mu E/m^2$-sec
	--	Threshold concentration value of chlorophyll-a	1 ppb - 5 ppb	3 ppb
	K_2	Respiration/loss coeff.	0.003 - 0.006/°C-day	0.005 °C day
4. Dissolved ortho-phosphorus (Avail. Phosph.)	K_p	Half saturation coeff. for available phosphorus (HSCPA)	0.01 ppm - 0.02 ppm	0.015 ppm
	r_m	Release fraction of phosphorus (RFM) in the mixed layer	0.6 - 0.8	0.8
	r_h	Phosphorus release fraction of phosphorus in the hypolimnion RFH)	1.0	1.0
	K_r	Bottom release rate (RR)	0	0
	Y_{ca}	Chlorophyll to phosphorus ratio (YCA)	300 - 700	600 (ppb/ppm)
	$P_{a,equil}$	Equilibrium conc. of available phosphorus (PAEQ)	0.08 ppm - 0.10 ppm	0.08 ppm
5. Convertible Phosphorus (Non-avail. phosph.)	η	Fraction of convertible phosphorus in particulate (PNFRAC)	0.2 - .25	0.2
	P_{equil}	Equilibrium concentration of available (dissolved ortho phos.)	0.08 - 0.10 ppm	.08 ppm
	K_{rr}	Resuspension rate of non-available (mostly particulate) phosphorus	0	0 g SS/m^2 day

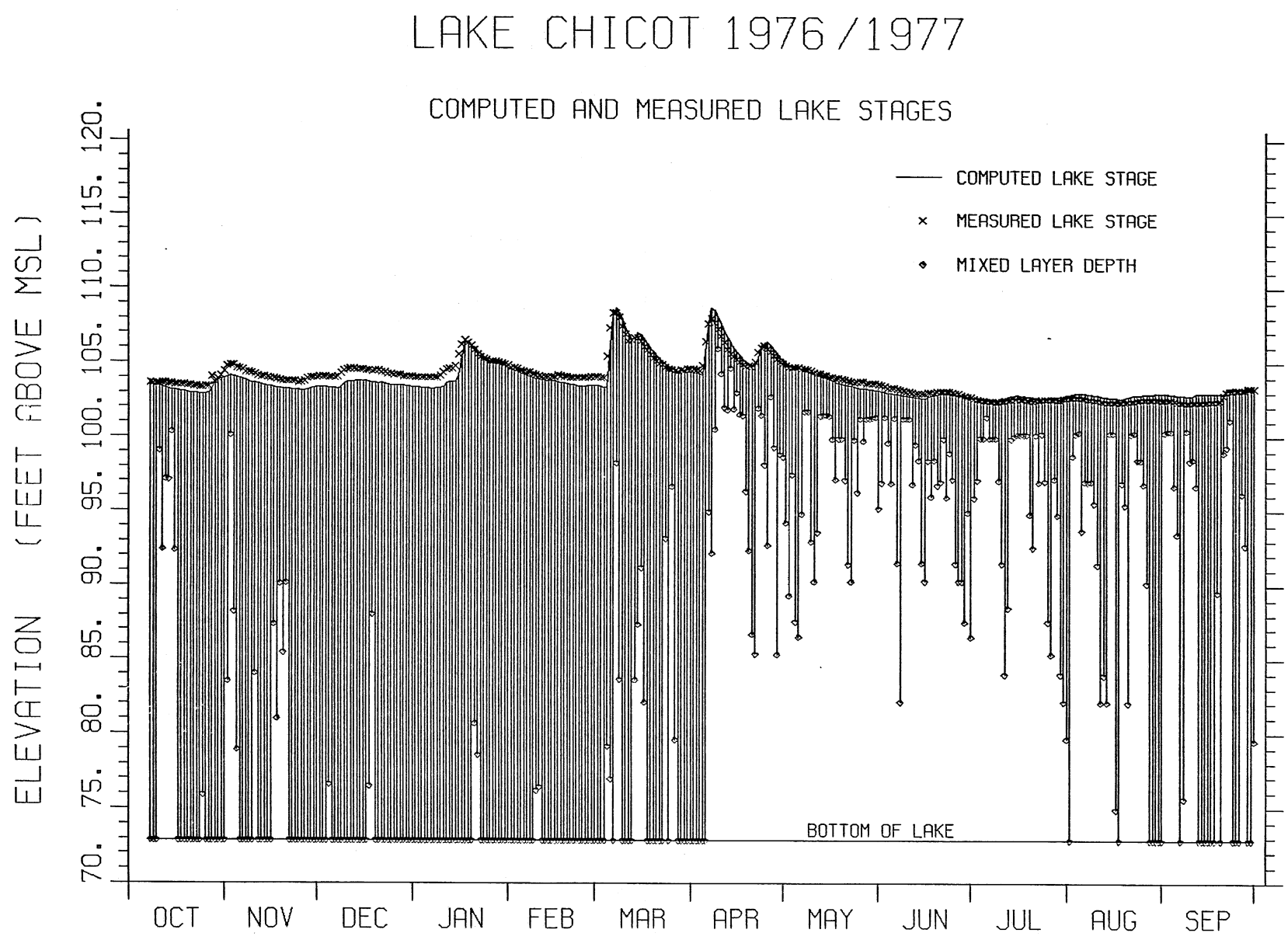
LAKE CHICOT 1976/1977
COMPUTED AND MEASURED LAKE STAGES
COMPUTED LAKE STAGE
MEASURED LAKE STAGE
MIXED LAYER DEPTH
ELEVATION (FEET ABOVE MSL)
70. 75. 80. 85. 90. 95. 100. 105. 110. 115. 120.
BOTTOM OF LAKE
OCT NOV DEC JAN FEB MAR APR MAY JUN JUL AUG SEP

FIGURE XI-1

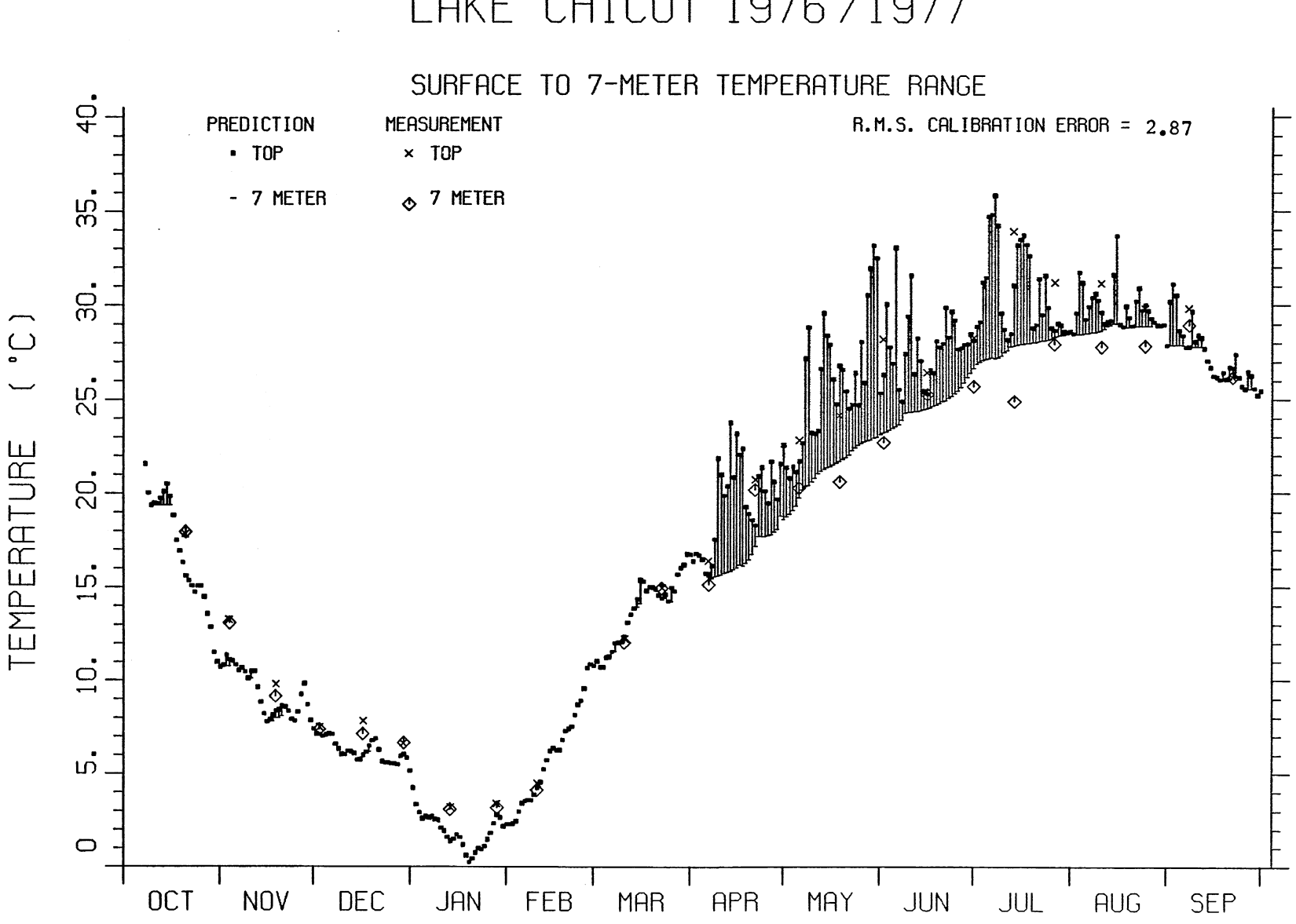
LAKE CHICOT 1976/1977
SURFACE TO 7-METER TEMPERATURE RANGE
PREDICTION
• TOP
- 7 METER
MEASUREMENT
× TOP
◇ 7 METER
R.M.S. CALIBRATION ERROR = 2.87
TEMPERATURE (°C)
0
5.
10.
15.
20.
25.
30.
35.
40.
OCT
NOV
DEC
JAN
FEB
MAR
APR
MAY
JUN
JUL
AUG
SEP

FIGURE XI-2

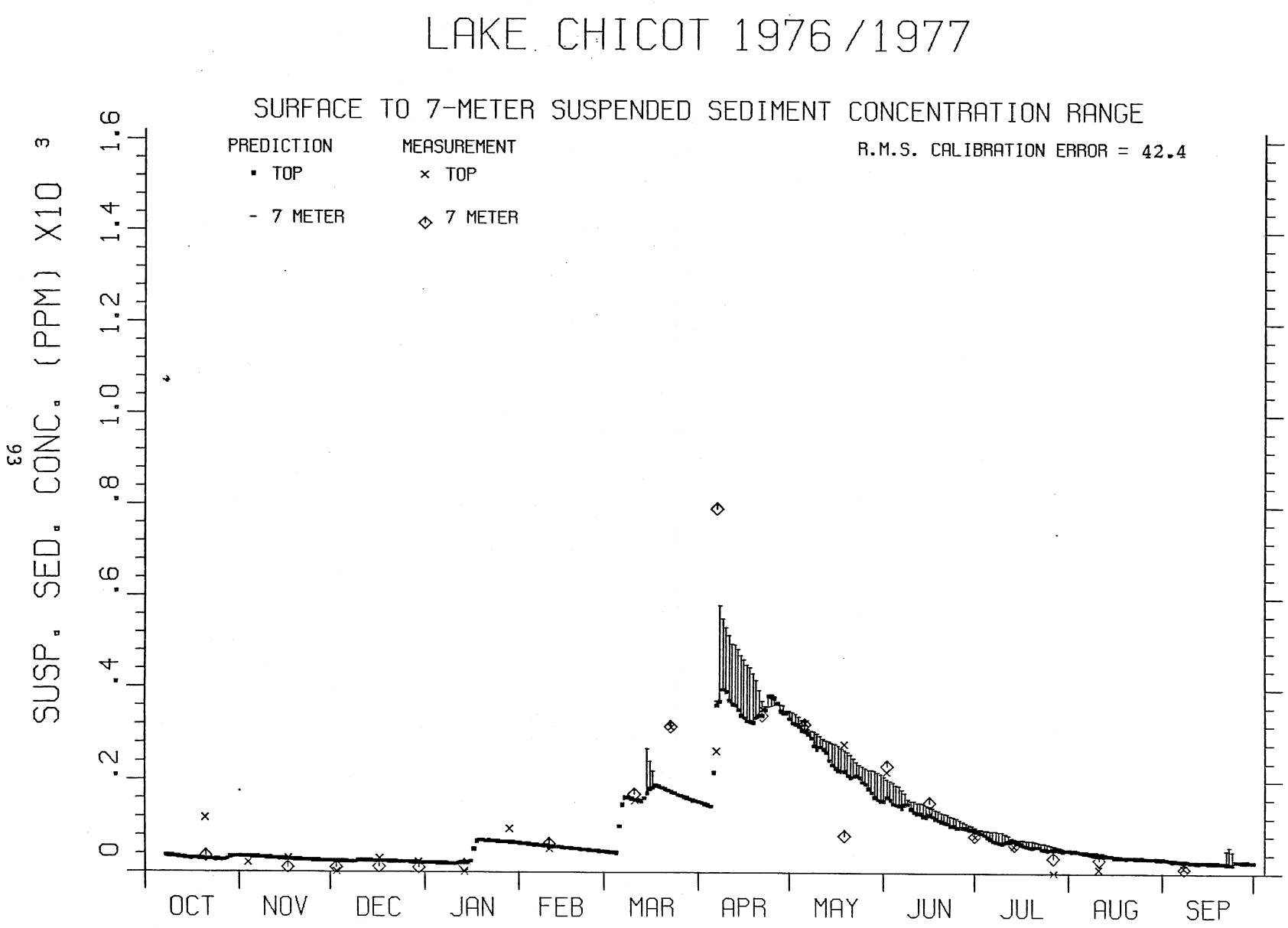
LAKE CHICOT 1976/1977
SURFACE TO 7-METER SUSPENDED SEDIMENT CONCENTRATION RANGE
PREDICTION
TOP
7 METER
MEASUREMENT
TOP
7 METER
R.M.S. CALIBRATION ERROR = 42.4
SUSP. SED. CONC. (PPM) X10 3
0
.2
.4
.6
.8
1.0
1.2
1.4
1.6
OCT
NOV
DEC
JAN
FEB
MAR
APR
MAY
JUN
JUL
AUG
SEP

FIGURE XI-3

LAKE CHICOT 1976/1977

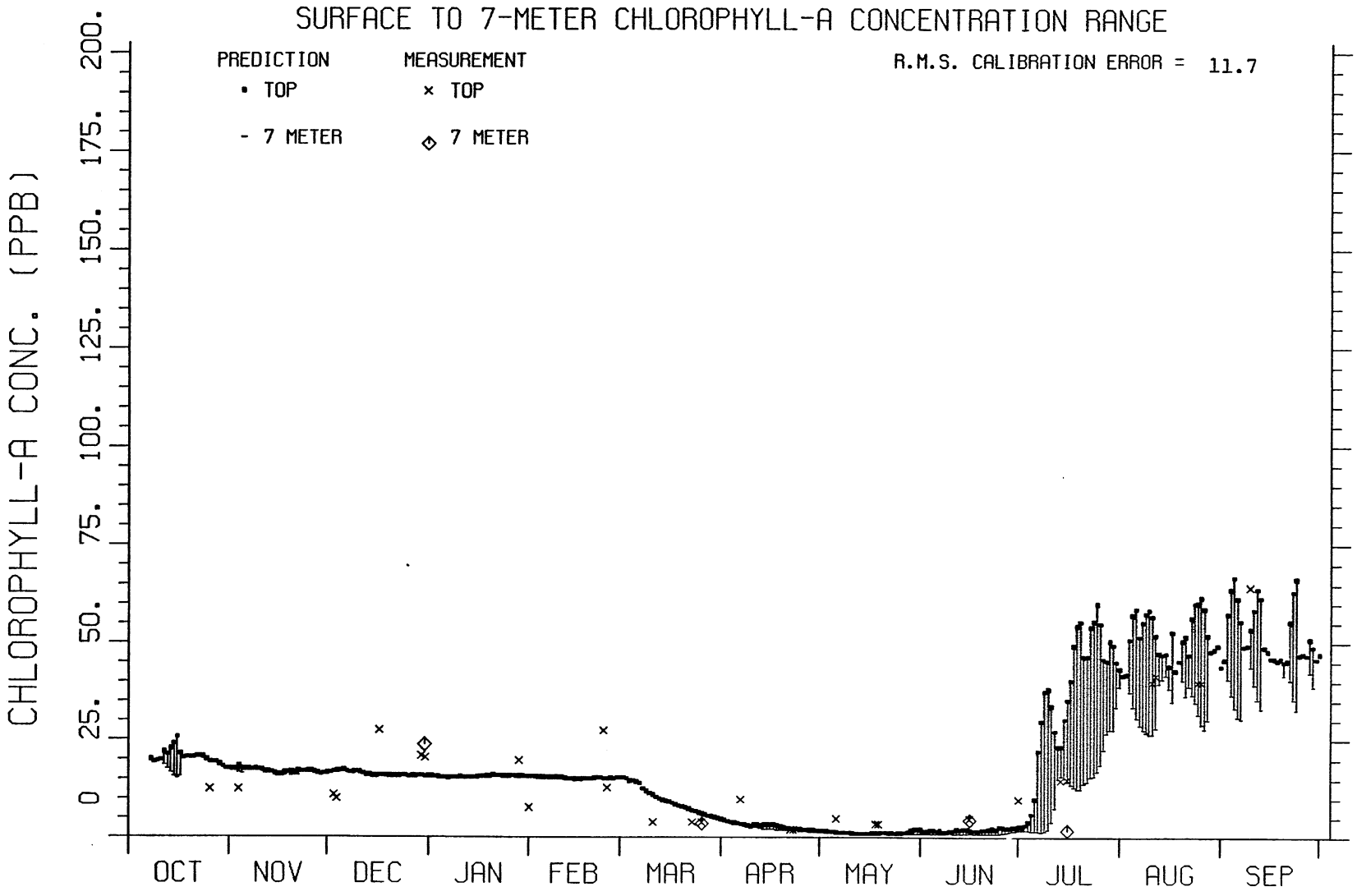

FIGURE XI-4

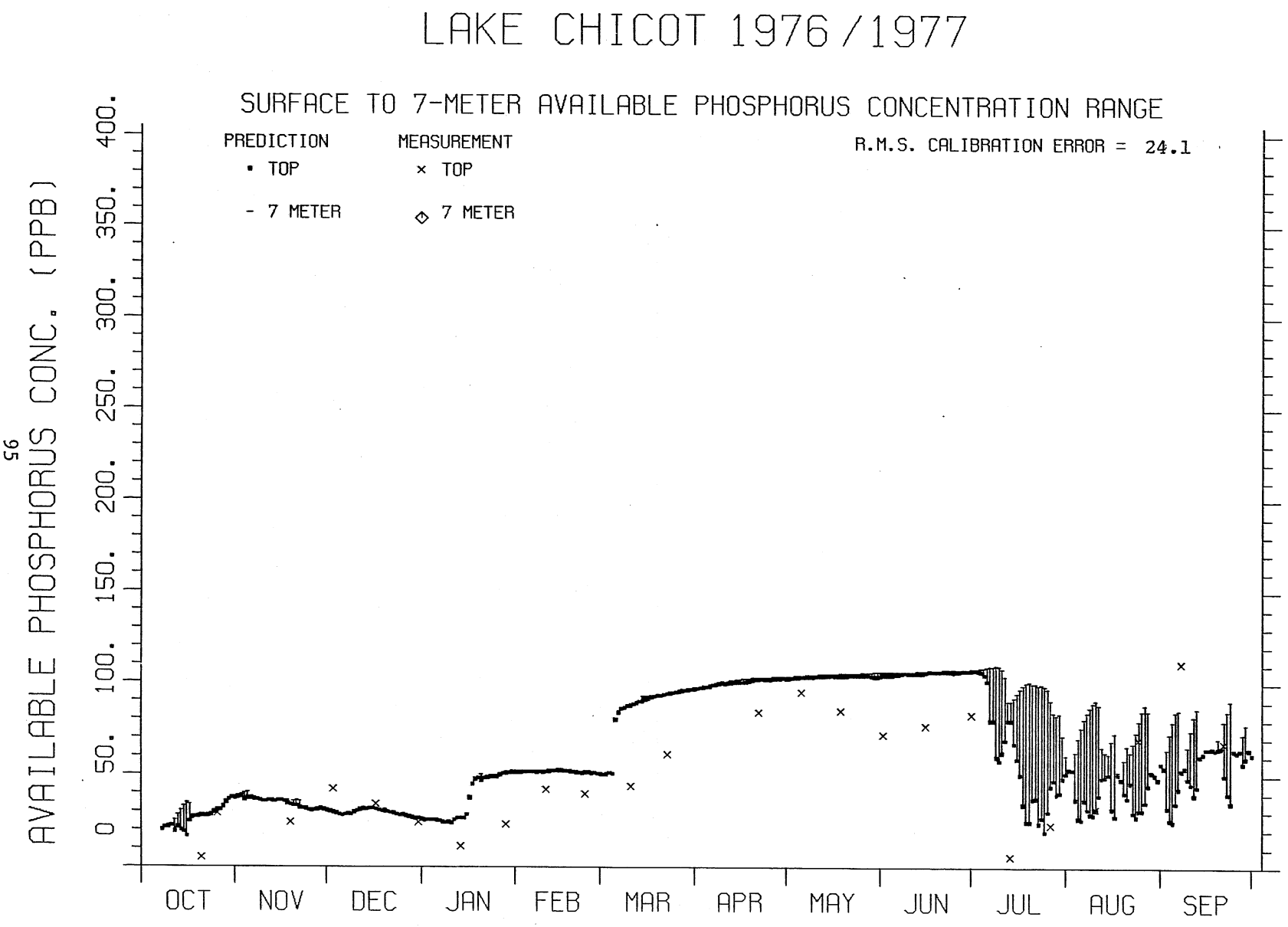
LAKE CHICOT 1976/1977
SURFACE TO 7-METER AVAILABLE PHOSPHORUS CONCENTRATION RANGE
PREDICTION
• TOP
- 7 METER
MEASUREMENT
× TOP
◇ 7 METER
R.M.S. CALIBRATION ERROR = 24.1
AVAILABLE PHOSPHORUS CONC. (PPB)
0
50.
100.
150.
200.
250.
300.
350.
400.
OCT
NOV
DEC
JAN
FEB
MAR
APR
MAY
JUN
JUL
AUG
SEP

FIGURE XI-5

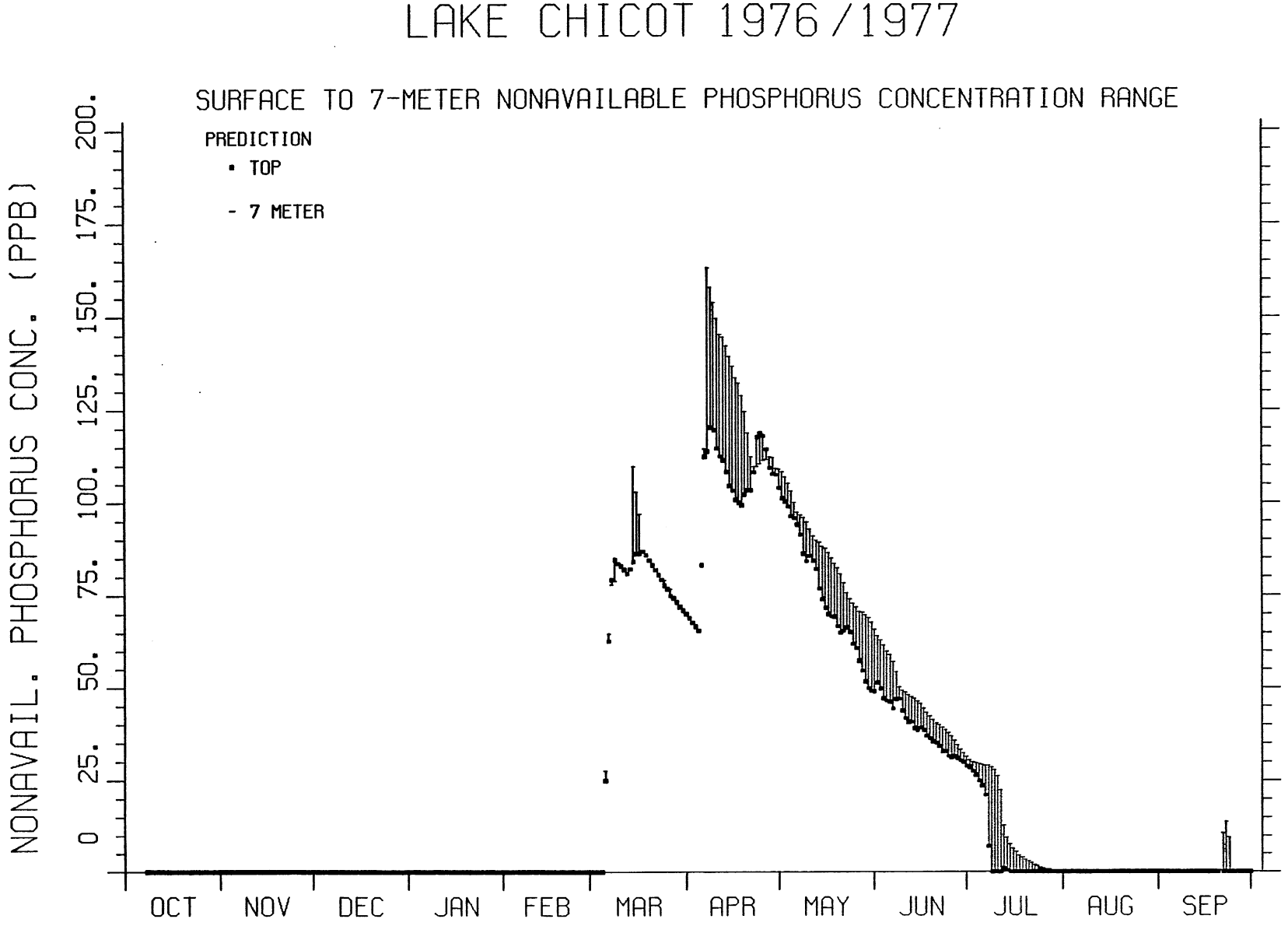
LAKE CHICOT 1976/1977
SURFACE TO 7-METER NONAVAILABLE PHOSPHORUS CONCENTRATION RANGE
PREDICTION
• TOP
- 7 METER
NONAVAIL. PHOSPHORUS CONC. (PPB)
0
25.
50.
75.
100.
125.
150.
175.
200.
OCT
NOV
DEC
JAN
FEB
MAR
APR
MAY
JUN
JUL
AUG
SEP

FIGURE XI-6

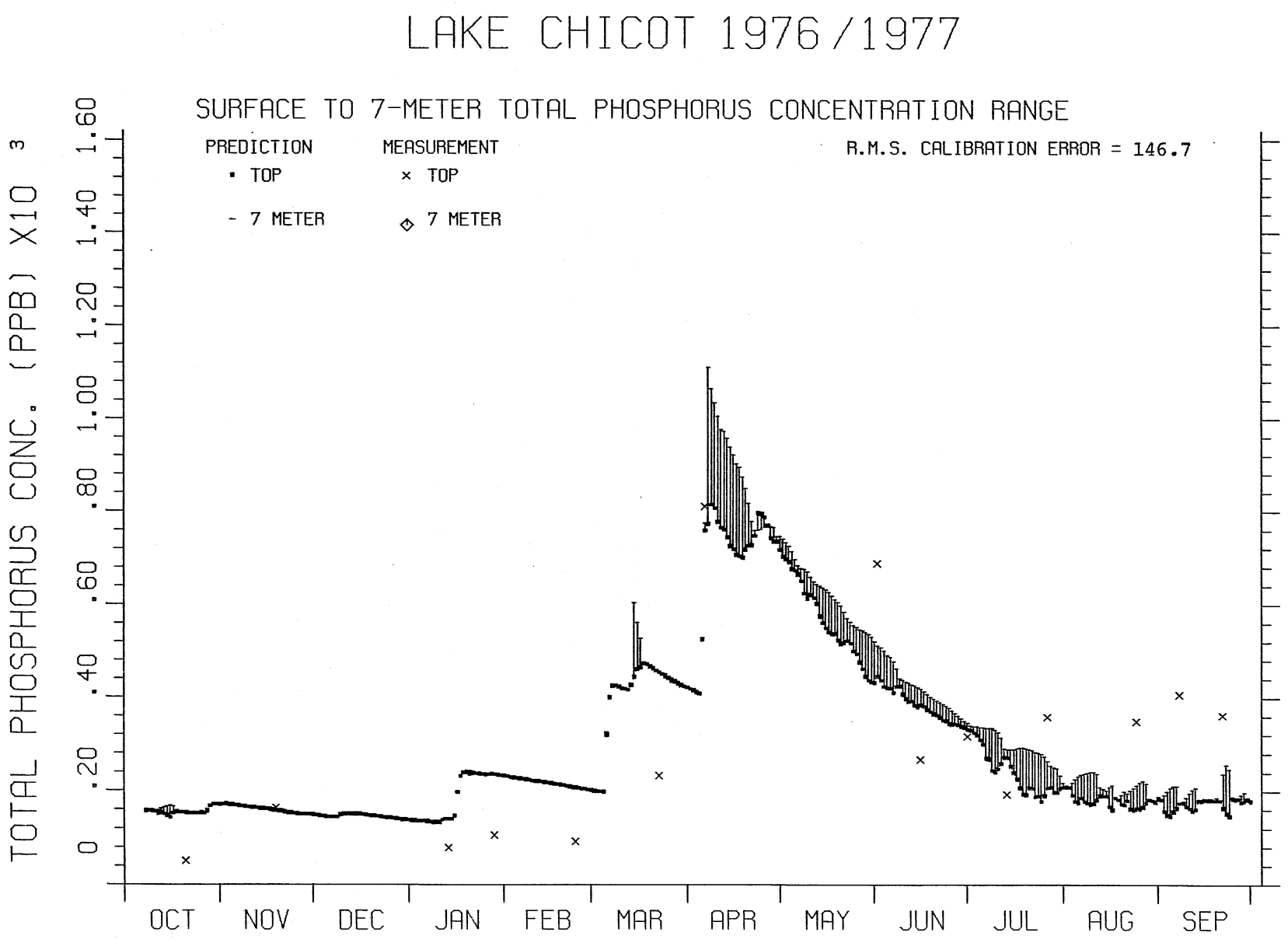
LAKE CHICOT 1976/1977
SURFACE TO 7-METER TOTAL PHOSPHORUS CONCENTRATION RANGE
PREDICTION
▪ TOP
- 7 METER
MEASUREMENT
× TOP
◇ 7 METER
R.M.S. CALIBRATION ERROR = 146.7
TOTAL PHOSPHORUS CONC. (PPB) X10 3
0
.20
.40
.60
.80
1.00
1.20
1.40
1.60
OCT
NOV
DEC
JAN
FEB
MAR
APR
MAY
JUN
JUL
AUG
SEP

FIGURE XI-7

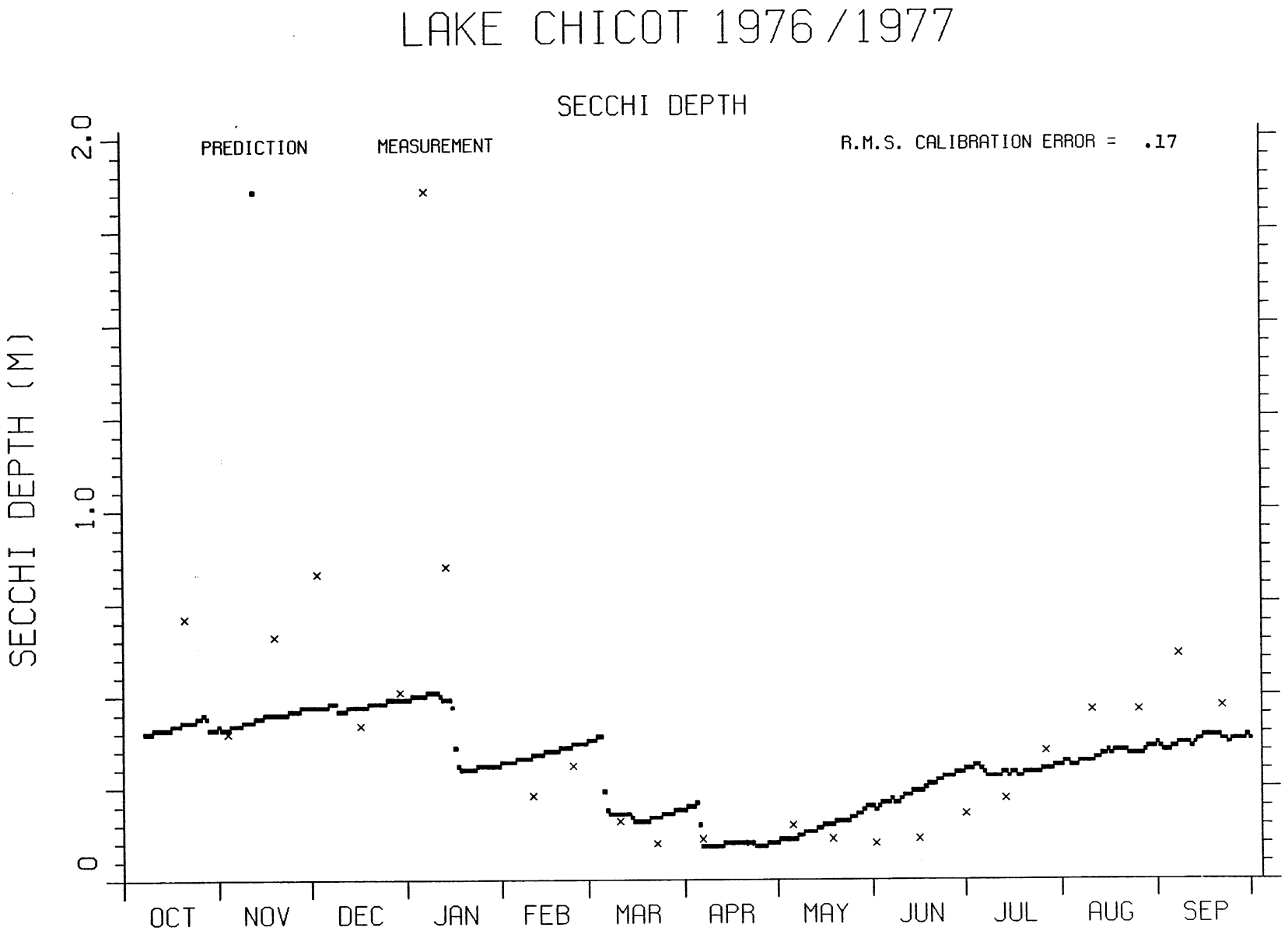
LAKE CHICOT 1976/1977
SECCHI DEPTH
PREDICTION
MEASUREMENT
R.M.S. CALIBRATION ERROR = .17
SECCHI DEPTH (M)
2.0
1.0
0
OCT
NOV
DEC
JAN
FEB
MAR
APR
MAY
JUN
JUL
AUG
SEP

FIGURE XI-8

XII. MODEL VERIFICATION

Water quality data sets measured during the water years 1977/78 and 1978/79 were used for model verification. A comparison between predictions and data is shown in Figs. XII-1 through XII-14. The root mean square error between predictions and measurements is again shown on the graphs. The degree of agreement between predictions and measurements shown in Figs. XII-1 through XII-14 makes possible the conclusion that the model is sufficiently verified for application to the exploration of some management alternatives for Lake Chicot.

Major limitations in the available data are with reference to the inaccuracies in inflow rates (Fig. III-3) and the weak correlation between inflow, water quality, and inflow rate (see e.g. Figs. VII-5 and III-6) which had to be used in the simulation. The greatest limitation in the model formulation itself is believed to be in the phosphorus model with its many coefficients and exchange processes between different forms of phosphorus.

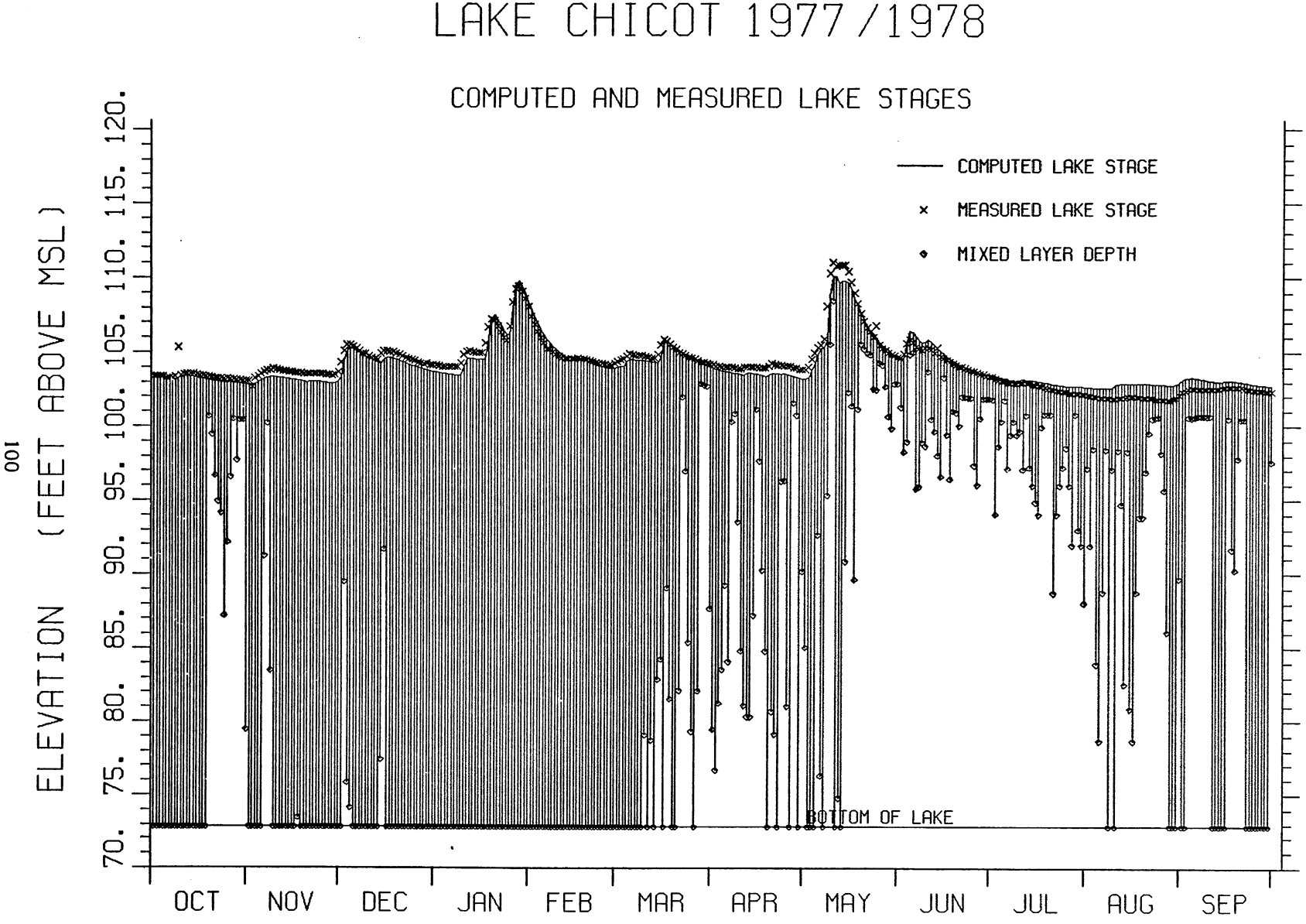
LAKE CHICOT 1977/1978
COMPUTED AND MEASURED LAKE STAGES
COMPUTED LAKE STAGE
MEASURED LAKE STAGE
MIXED LAYER DEPTH
BOTTOM OF LAKE
ELEVATION (FEET ABOVE MSL)
100
70. 75. 80. 85. 90. 95. 100. 105. 110. 115. 120.
OCT NOV DEC JAN FEB MAR APR MAY JUN JUL AUG SEP

FIGURE XII-1

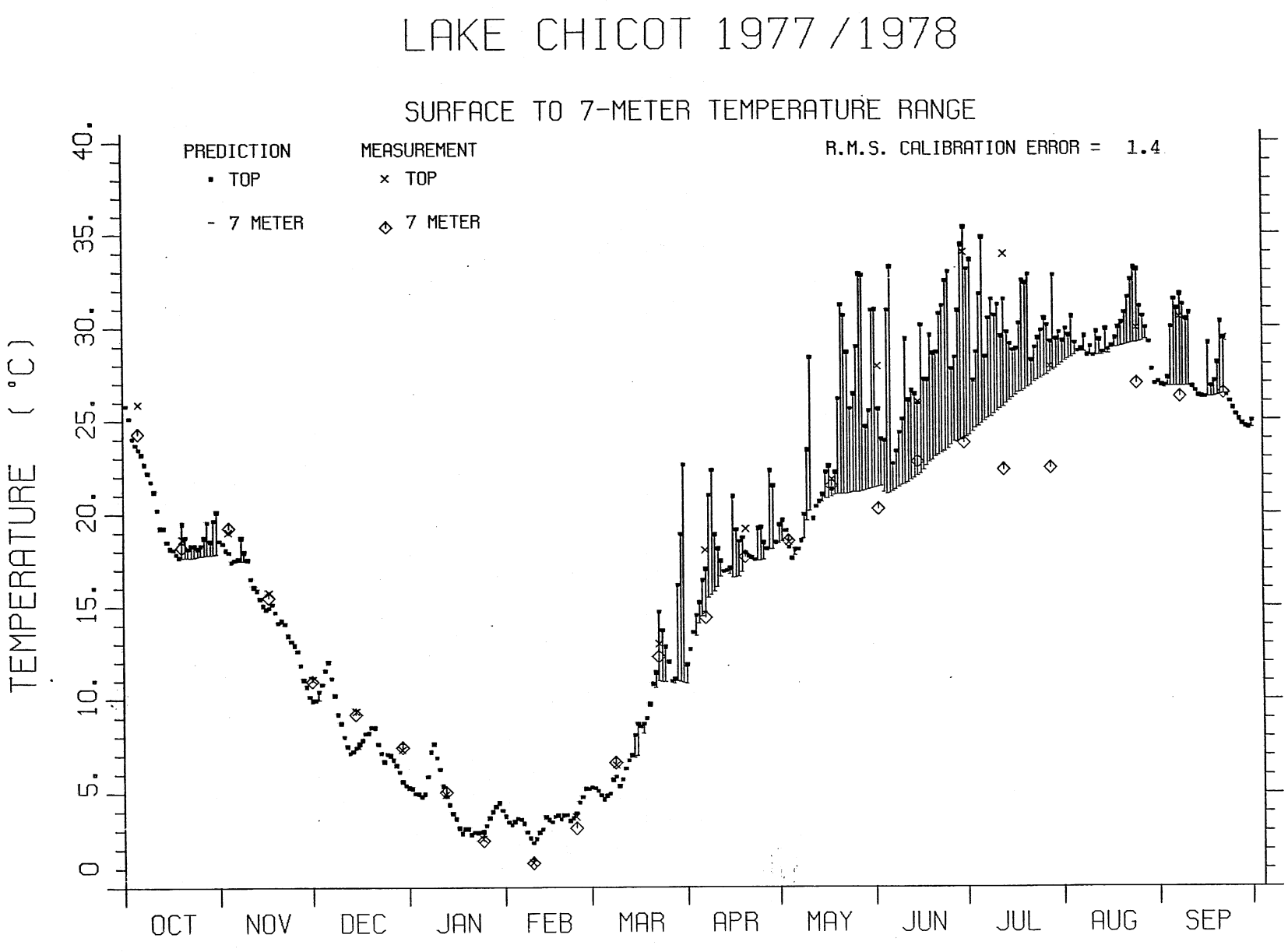
LAKE CHICOT 1977/1978
SURFACE TO 7-METER TEMPERATURE RANGE
PREDICTION
TOP
7 METER
MEASUREMENT
TOP
7 METER
R.M.S. CALIBRATION ERROR = 1.4
TEMPERATURE (°C)
0
5.
10.
15.
20.
25.
30.
35.
40.
OCT
NOV
DEC
JAN
FEB
MAR
APR
MAY
JUN
JUL
AUG
SEP

FIGURE XII-2

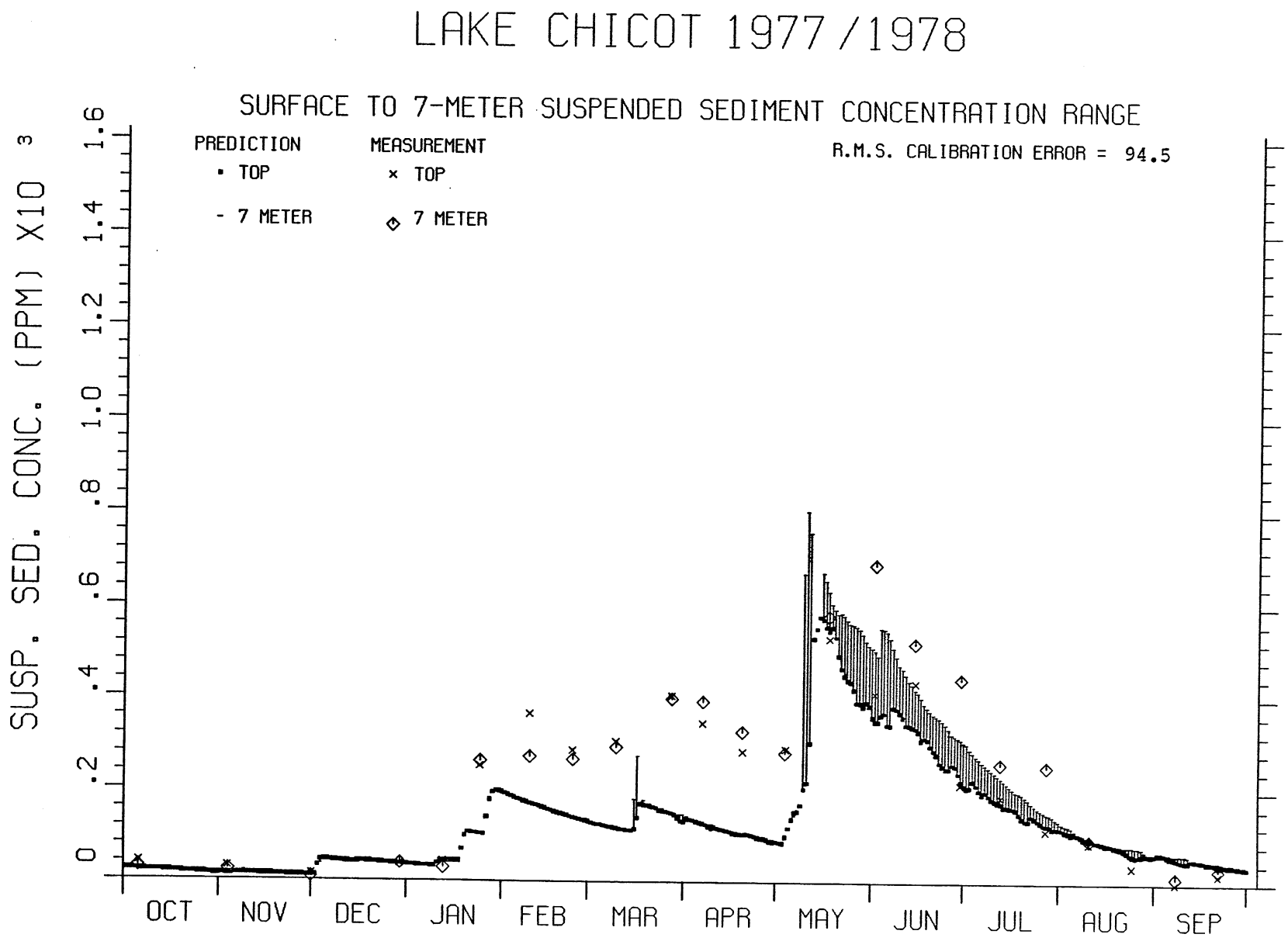
LAKE CHICOT 1977/1978
SURFACE TO 7-METER SUSPENDED SEDIMENT CONCENTRATION RANGE
PREDICTION
• TOP
- 7 METER
MEASUREMENT
× TOP
◇ 7 METER
R.M.S. CALIBRATION ERROR = 94.5
SUSP. SED. CONC. (PPM) X10 3
0
.2
.4
.6
.8
1.0
1.2
1.4
1.6
OCT
NOV
DEC
JAN
FEB
MAR
APR
MAY
JUN
JUL
AUG
SEP

FIGURE XII-3

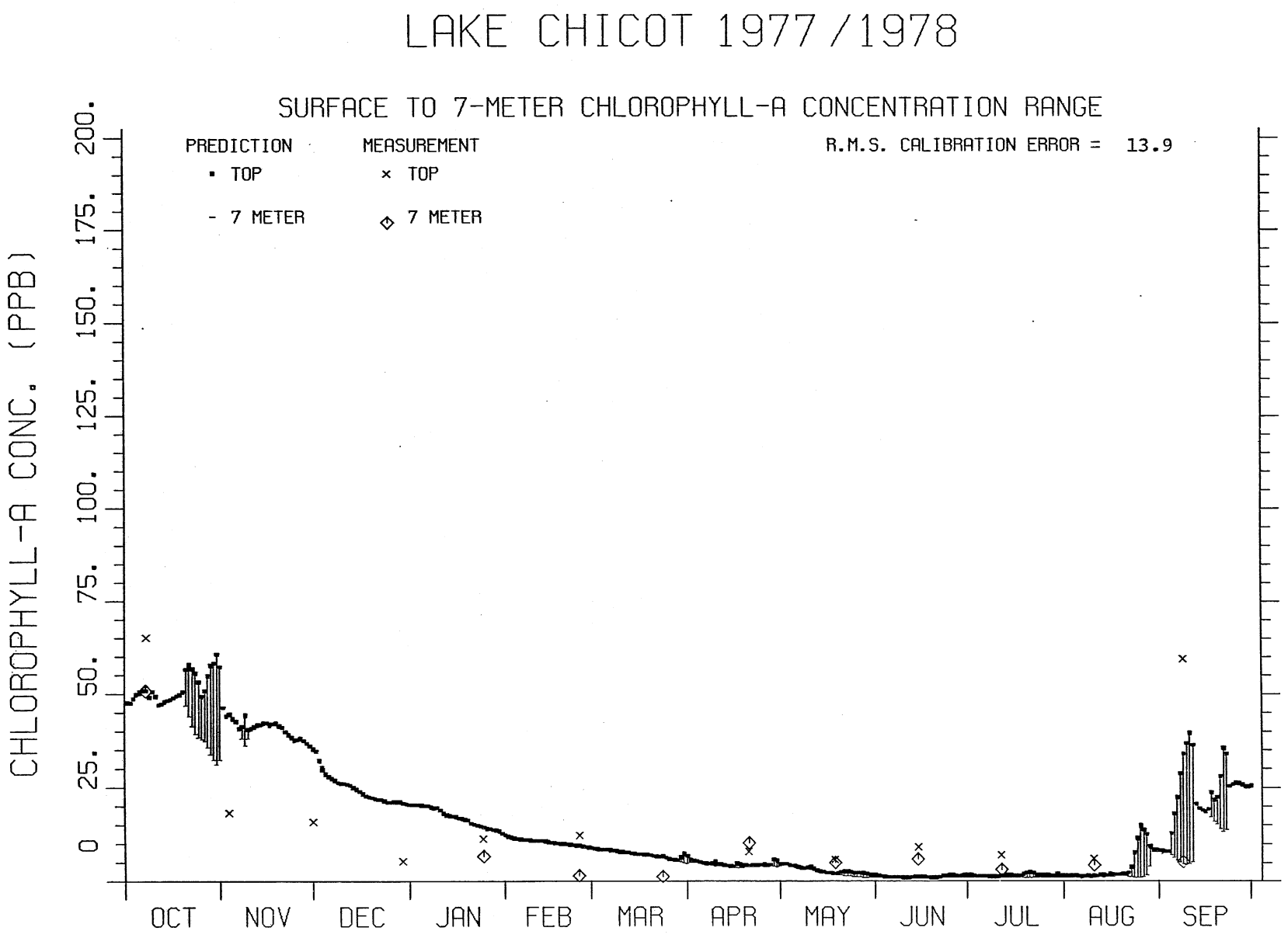
LAKE CHICOT 1977/1978
SURFACE TO 7-METER CHLOROPHYLL-A CONCENTRATION RANGE
PREDICTION
MEASUREMENT
R.M.S. CALIBRATION ERROR = 13.9
TOP
TOP
7 METER
7 METER
CHLOROPHYLL-A CONC. (PPB)
0
25.
50.
75.
100.
125.
150.
175.
200.
OCT
NOV
DEC
JAN
FEB
MAR
APR
MAY
JUN
JUL
AUG
SEP

FIGURE XII-4

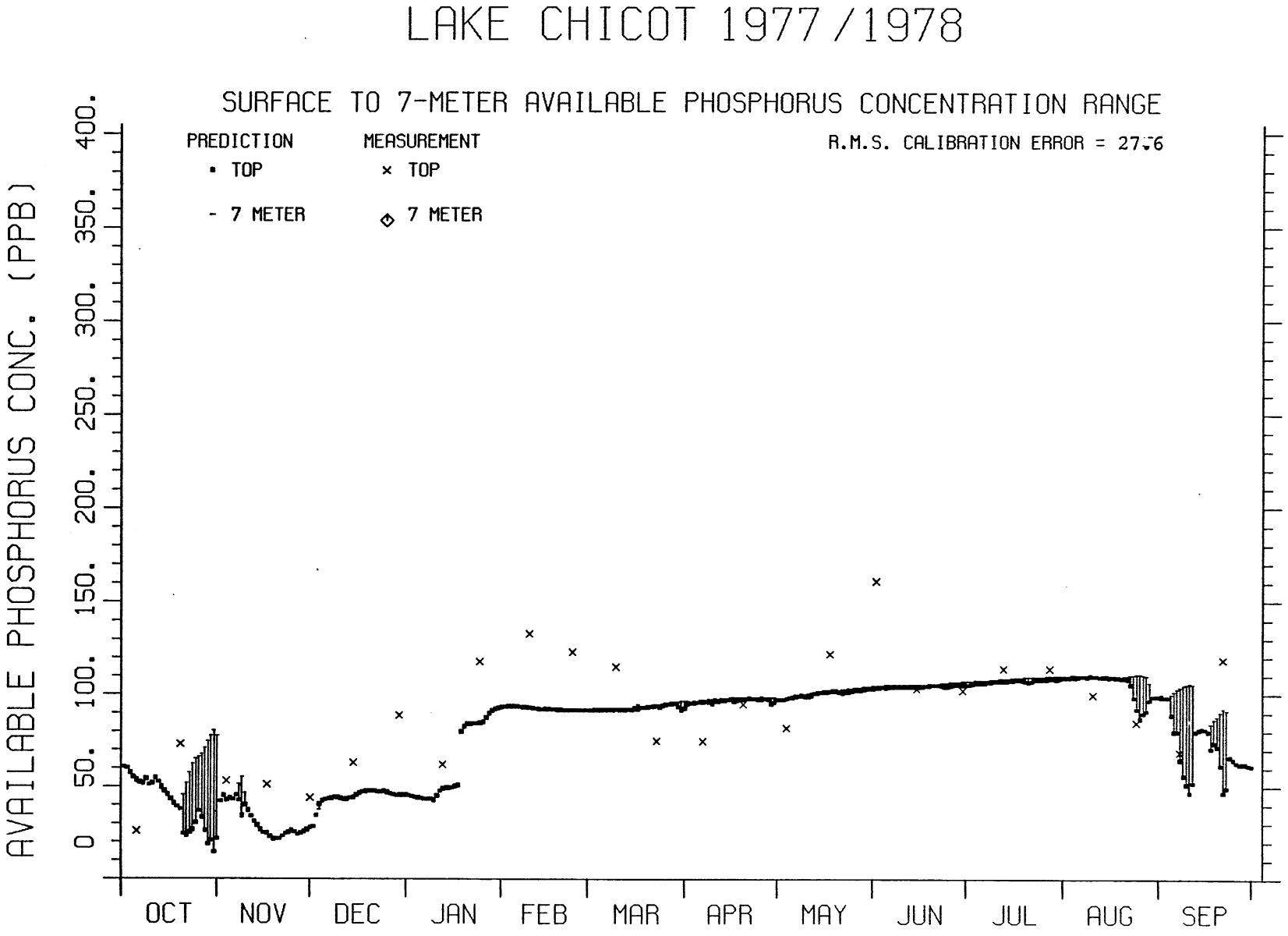
LAKE CHICOT 1977/1978
SURFACE TO 7-METER AVAILABLE PHOSPHORUS CONCENTRATION RANGE
PREDICTION
• TOP
- 7 METER
MEASUREMENT
× TOP
◇ 7 METER
R.M.S. CALIBRATION ERROR = 27.6
AVAILABLE PHOSPHORUS CONC. (PPB)
0
50.
100.
150.
200.
250.
300.
350.
400.
OCT
NOV
DEC
JAN
FEB
MAR
APR
MAY
JUN
JUL
AUG
SEP

FIGURE XII-5

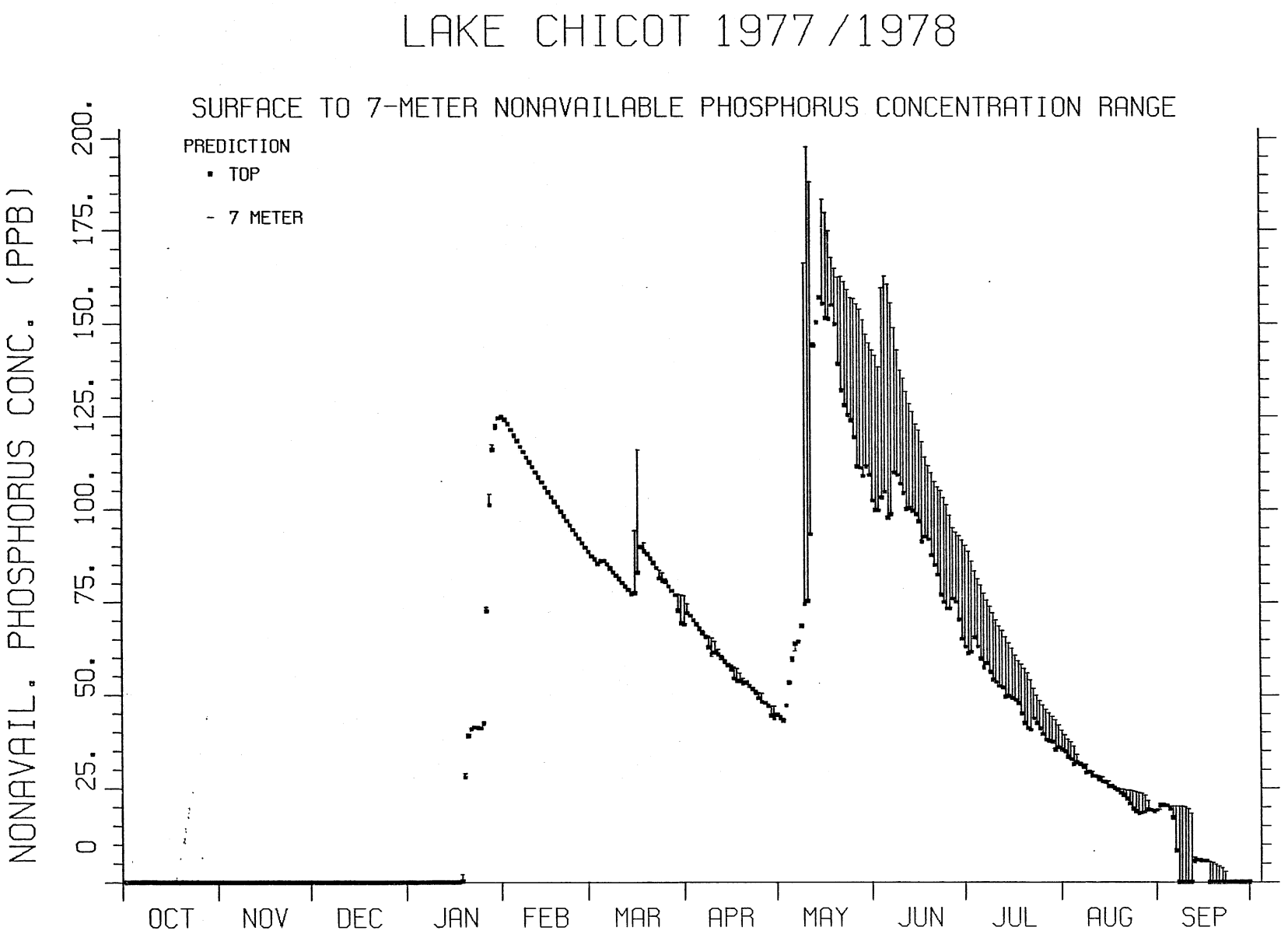
LAKE CHICOT 1977/1978
SURFACE TO 7-METER NONAVAILABLE PHOSPHORUS CONCENTRATION RANGE
PREDICTION
▪ TOP
- 7 METER
NONAVAIL. PHOSPHORUS CONC. (PPB)
0
25.
50.
75.
100.
125.
150.
175.
200.
OCT
NOV
DEC
JAN
FEB
MAR
APR
MAY
JUN
JUL
AUG
SEP

FIGURE XII-6

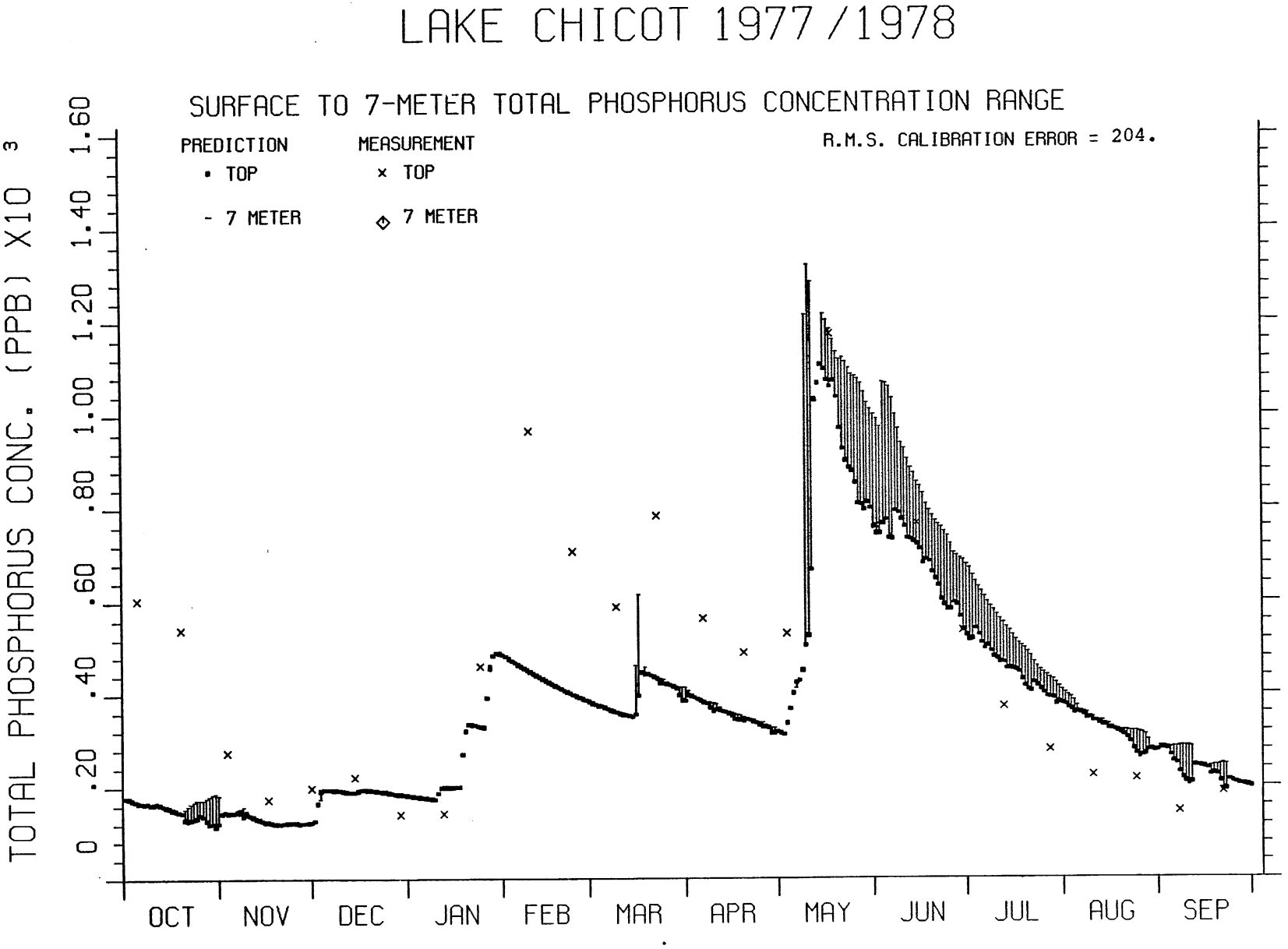
LAKE CHICOT 1977/1978
SURFACE TO 7-METER TOTAL PHOSPHORUS CONCENTRATION RANGE
PREDICTION
• TOP
- 7 METER
MEASUREMENT
× TOP
◇ 7 METER
R.M.S. CALIBRATION ERROR = 204.
TOTAL PHOSPHORUS CONC. (PPB) X10 3
0
.20
.40
.60
.80
1.00
1.20
1.40
1.60
OCT
NOV
DEC
JAN
FEB
MAR
APR
MAY
JUN
JUL
AUG
SEP

FIGURE XII-7

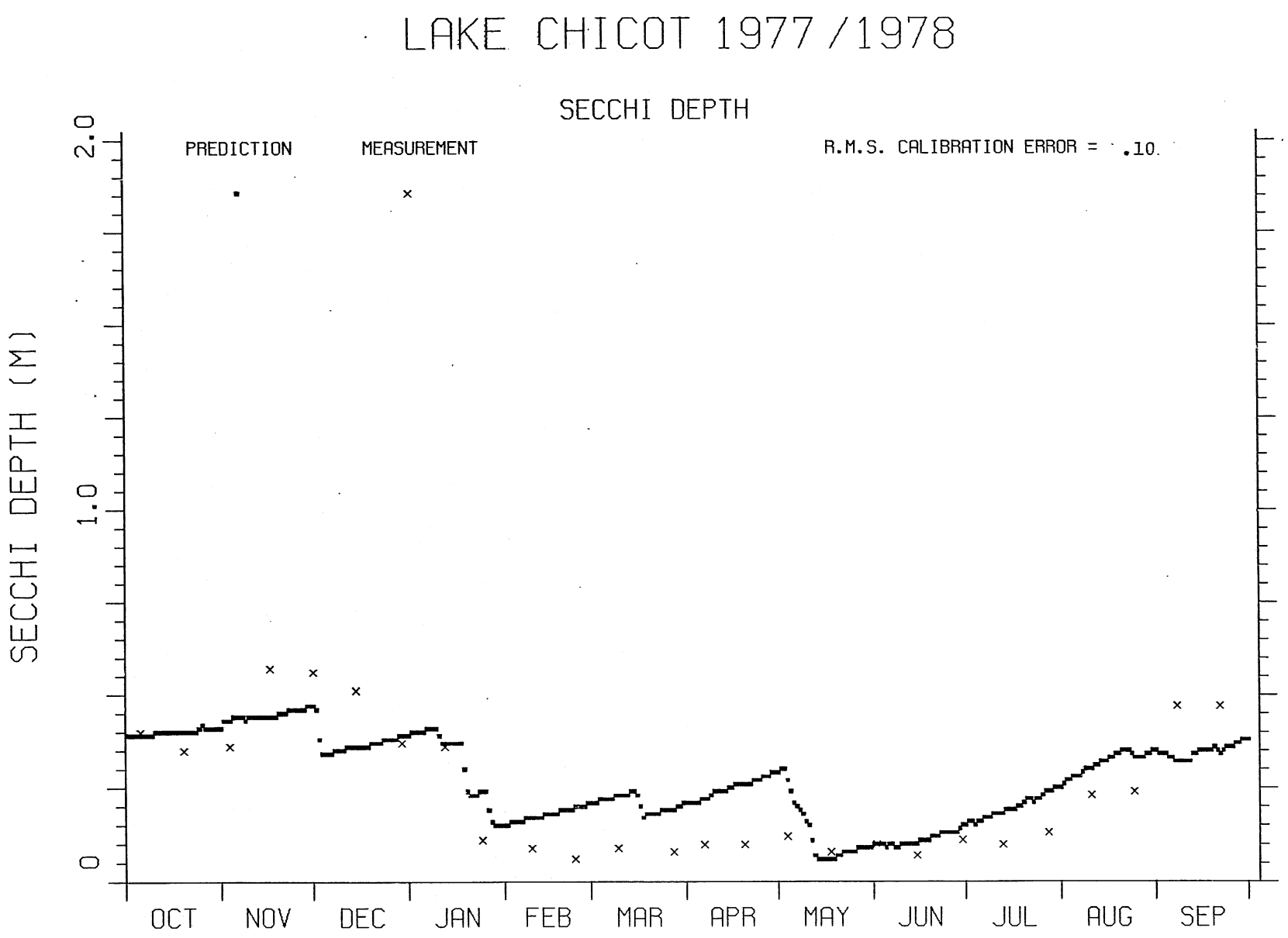
LAKE CHICOT 1977/1978
SECCHI DEPTH
PREDICTION
MEASUREMENT
R.M.S. CALIBRATION ERROR = .10
SECCHI DEPTH (M)
2.0
1.0
0
OCT
NOV
DEC
JAN
FEB
MAR
APR
MAY
JUN
JUL
AUG
SEP

FIGURE XII-8

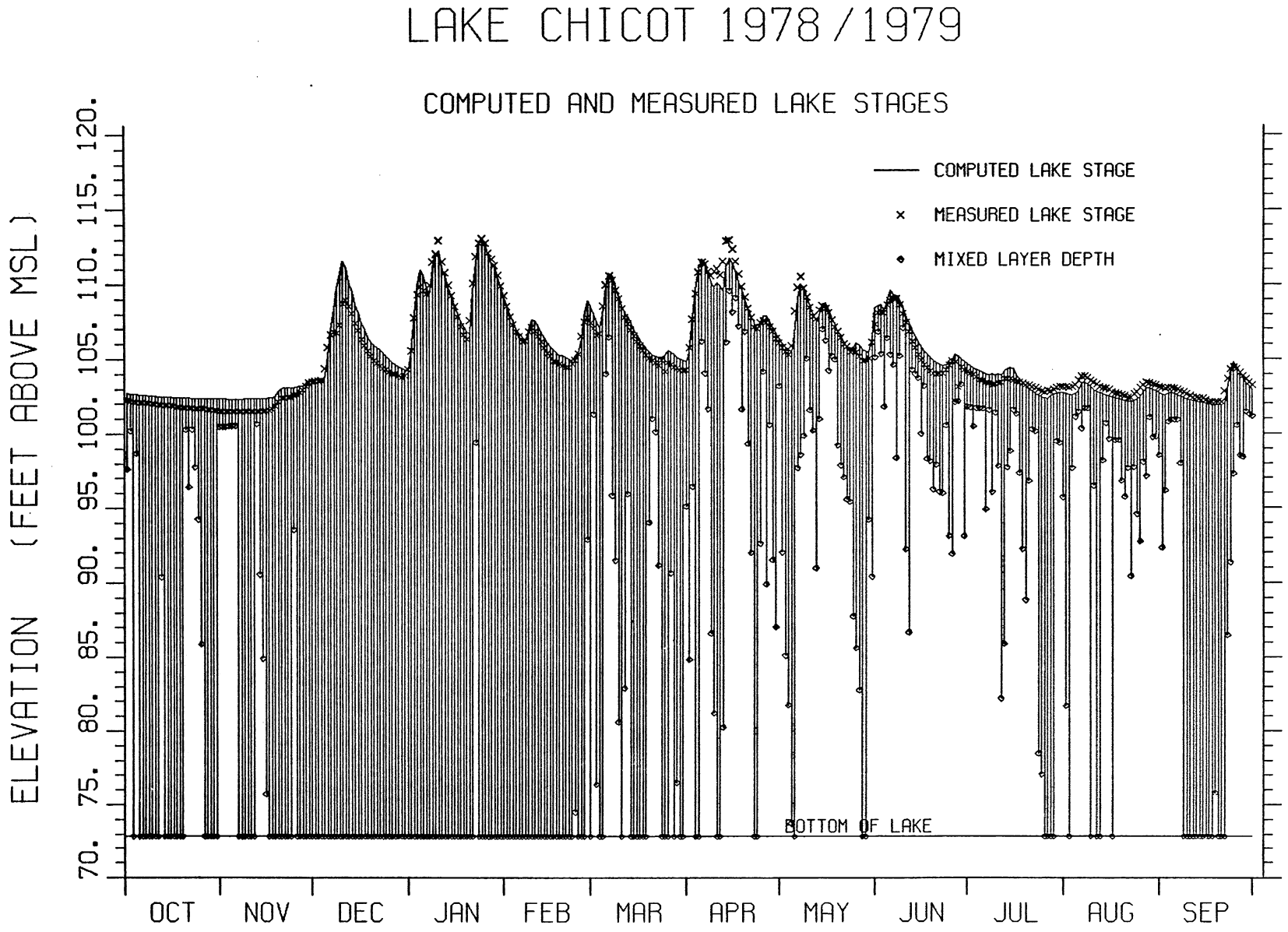
LAKE CHICOT 1978/1979
COMPUTED AND MEASURED LAKE STAGES
COMPUTED LAKE STAGE
MEASURED LAKE STAGE
MIXED LAYER DEPTH
ELEVATION (FEET ABOVE MSL)
70. 75. 80. 85. 90. 95. 100. 105. 110. 115. 120.
BOTTOM OF LAKE
OCT NOV DEC JAN FEB MAR APR MAY JUN JUL AUG SEP

FIGURE XII-9

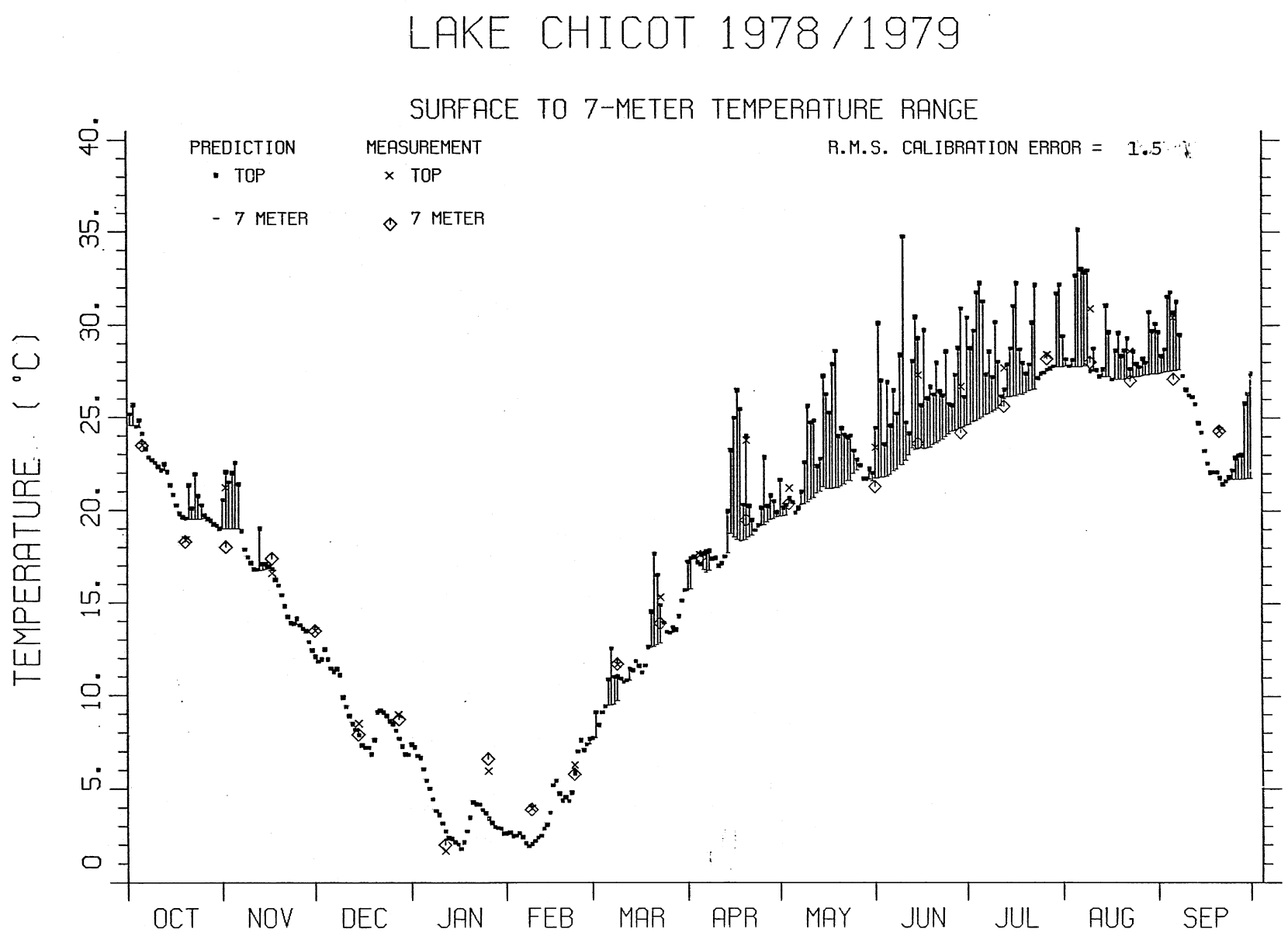

FIGURE XII-10

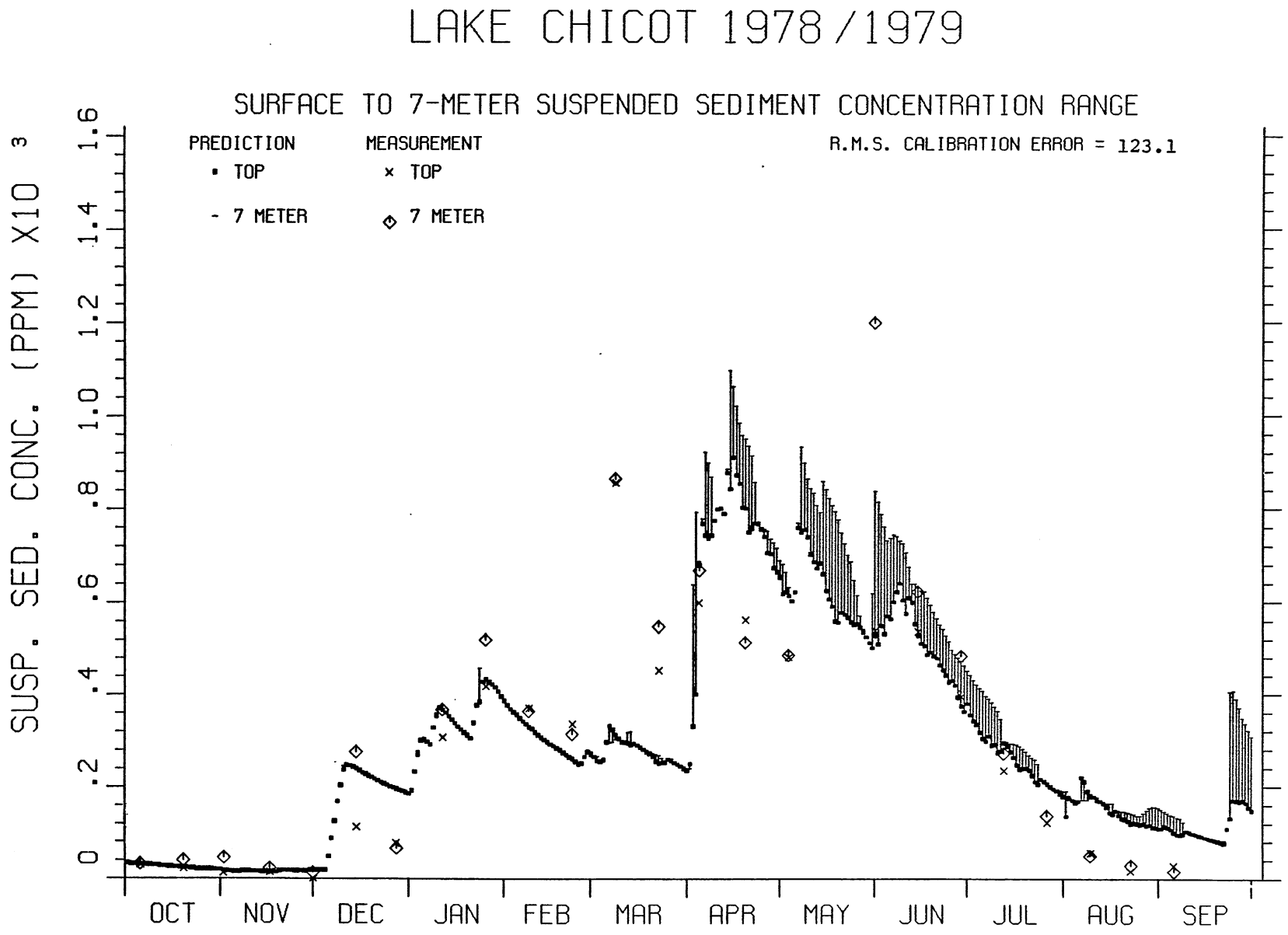

FIGURE XII-11

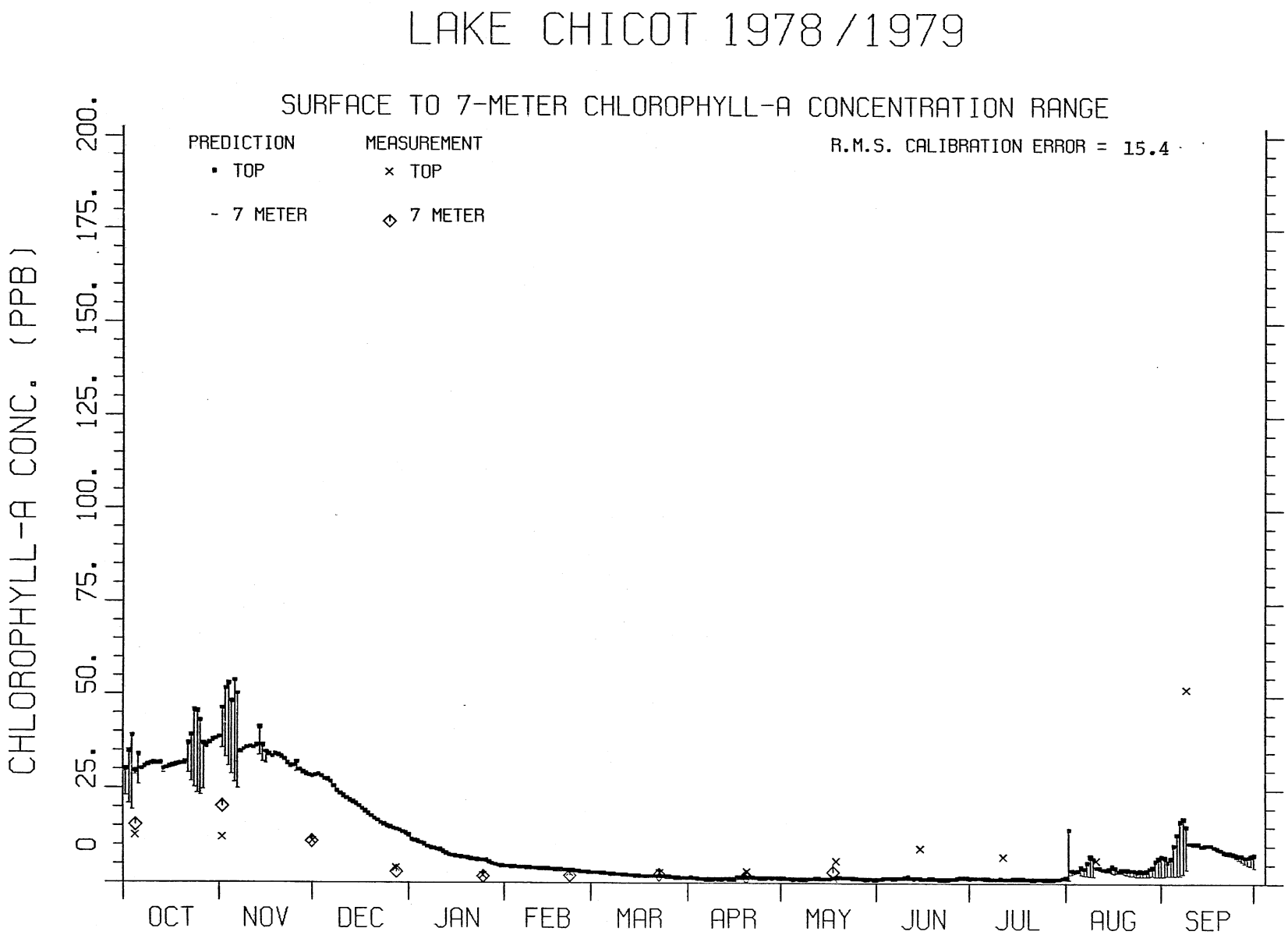

FIGURE XII-12

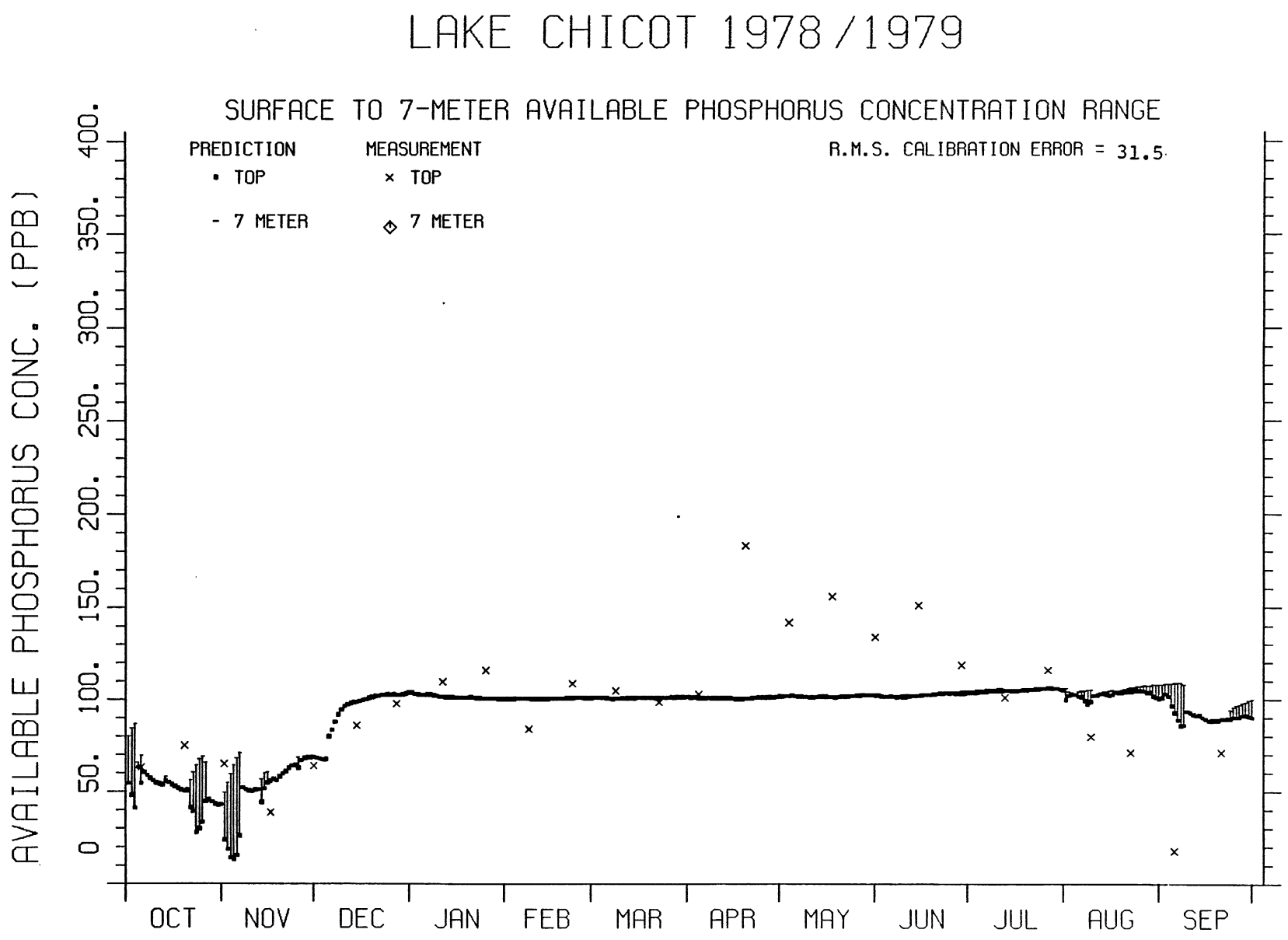

FIGURE XII-13

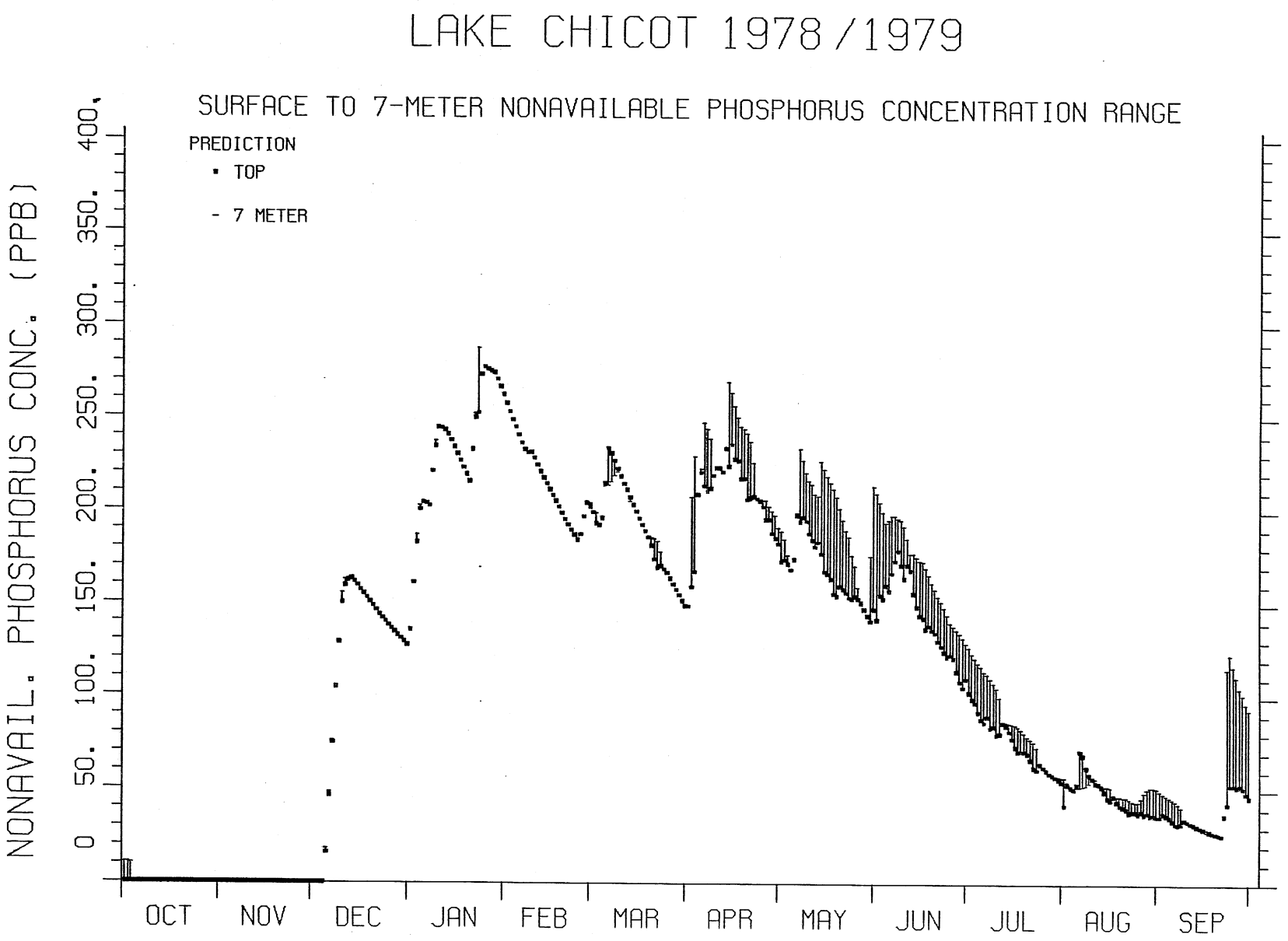

FIGURE XII-14

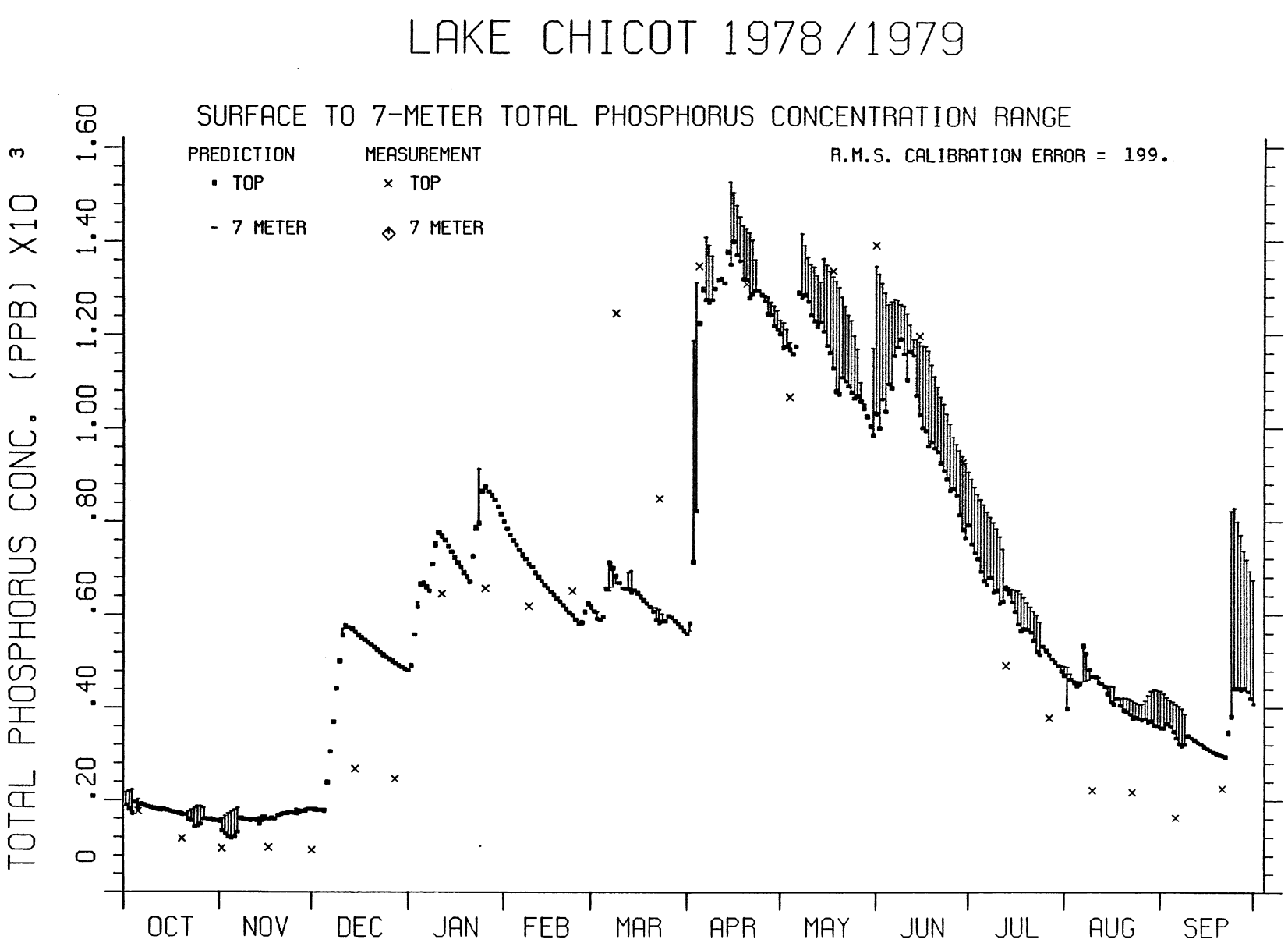

FIGURE XII-15

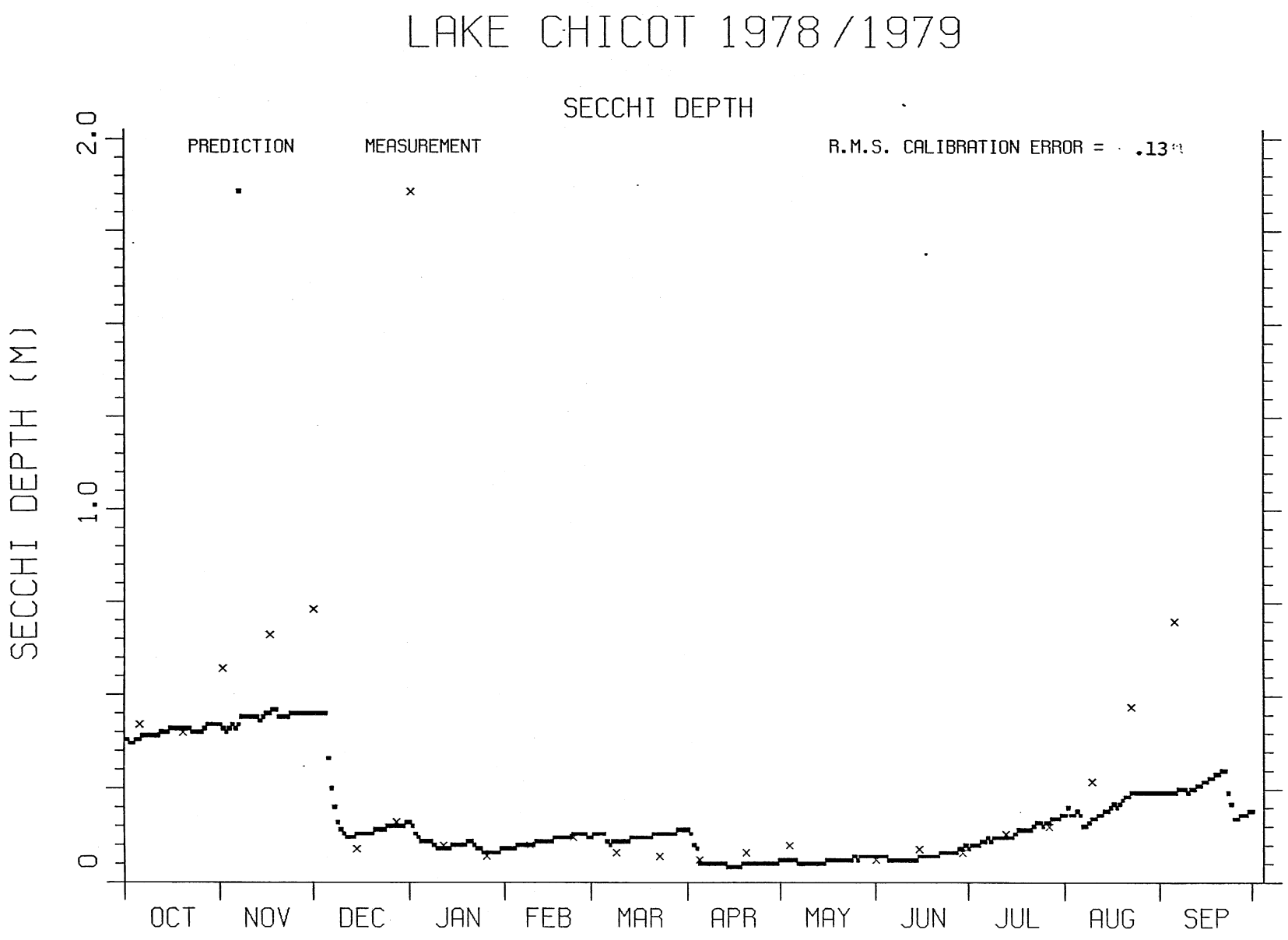

FIGURE XII-16

XIII. MODEL APPLICATION

As an example for the anticipated use of the model, simulations with reduced inflow rates into Lake Chicot have been made. In anticipation of the operation of the new pumping station at Macon Lake, inflow rates have been truncated at 0.005 cfs, 5 cfs, 50 cfs, 100 cfs, 250 cfs, and 500 cfs. Flows above these values are diverted to the Mississippi River. The predicted water quality under the weather conditions encountered in 1976/77, 1977/78, and 1978/79 are shown in Figs. XIII-1 through XIII-12. The effect of inflow diversion on lake stages is obvious in Figs. XIII-1, XIII-2, and XIII-3 and would be the same in every year. The suspended sediment concentration, and hence turbidity of the lake, is very much a factor of inflow; the recovery of the lake from a suspended sediment problem over a three-year period and for six rates of diversion is shown in Figs. XIII-4, XIII-5, and XIII-6. As lessened turbidity of the lake permits an increase in light penetration, phytoplankton growth increases as shown in Figs. XIII-7, XIII-8, and XIII-9.

An estimate of the clarity of the lake under the various diversions is given in terms of predicted Secchi depths in Figs. XIII-10, XIII-11, and XIII-12.

TABLE XIII-1. SUMMARY OF SUSPENDED SEDIMENT TRAP EFFICIENCIES

Water Year	Maximum Inflow (cfs)	Computed Apparent Trap Efficiency (%)	Observed (Estimated) Trap Eff.
1976-77	Actual	70.2	68
	50	90.2	
	100	89.2	
	250	86.3	
	500	83.5	
1977-78	Actual	59.9	56
	5	97.5	
	50	92.8	
	100	89.9	
	250	85.0	
	500	80.0	
1978-79	Actual	53.6	62
	5	96.3	
	50	91.2	
	100	87.2	
	250	79.7	
	500	72.6	

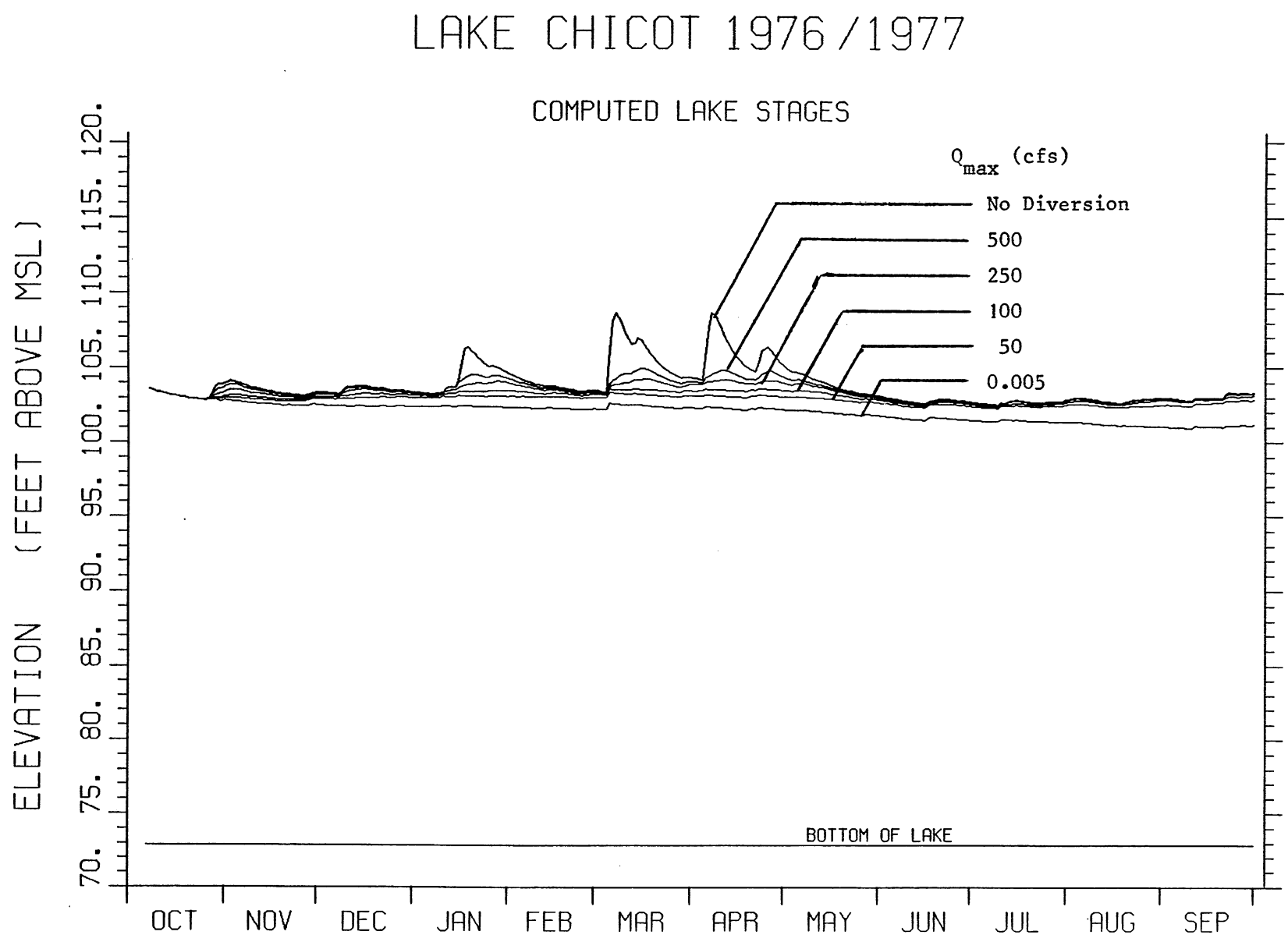

FIGURE XIII-1

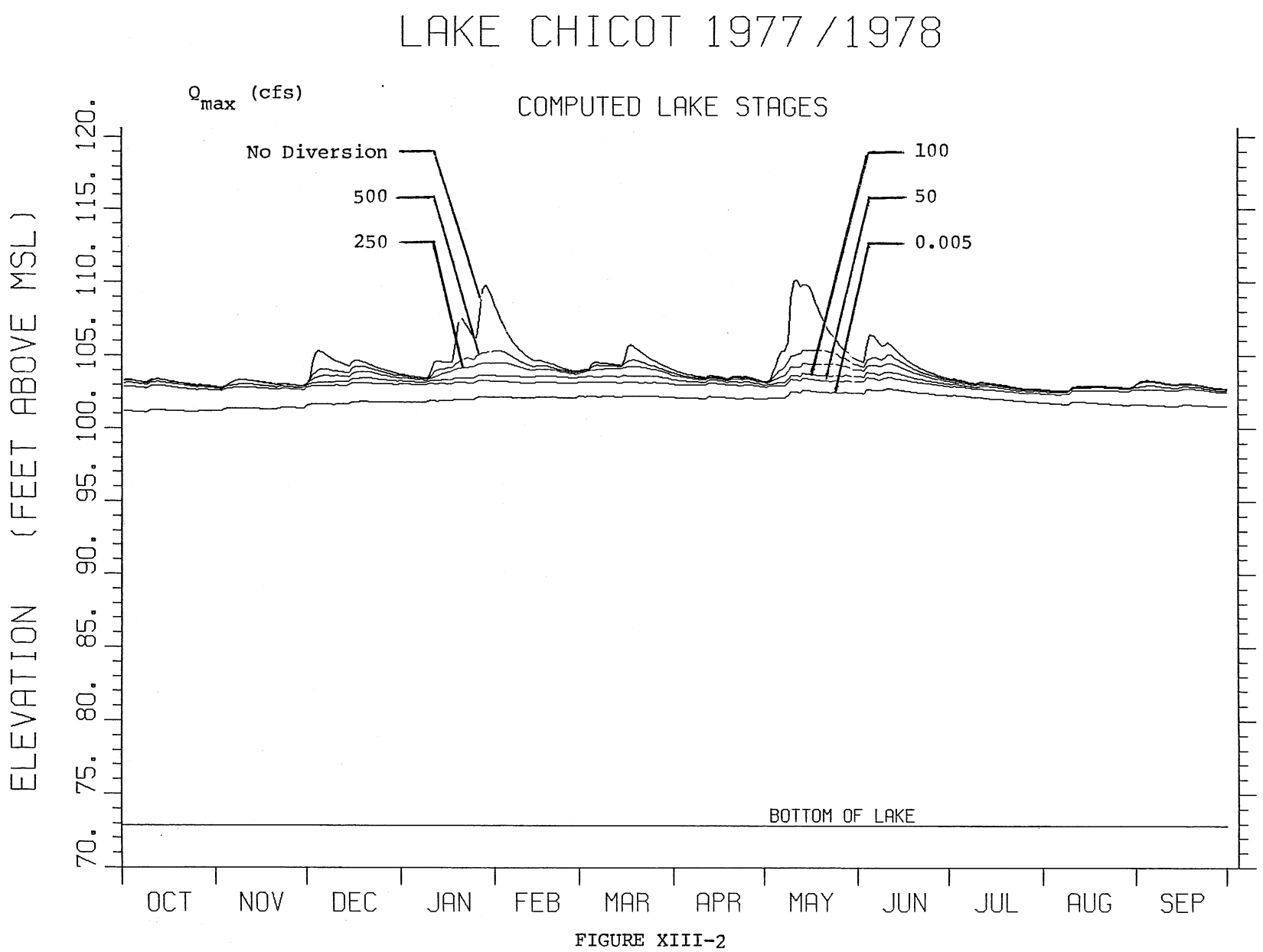

FIGURE XIII-2

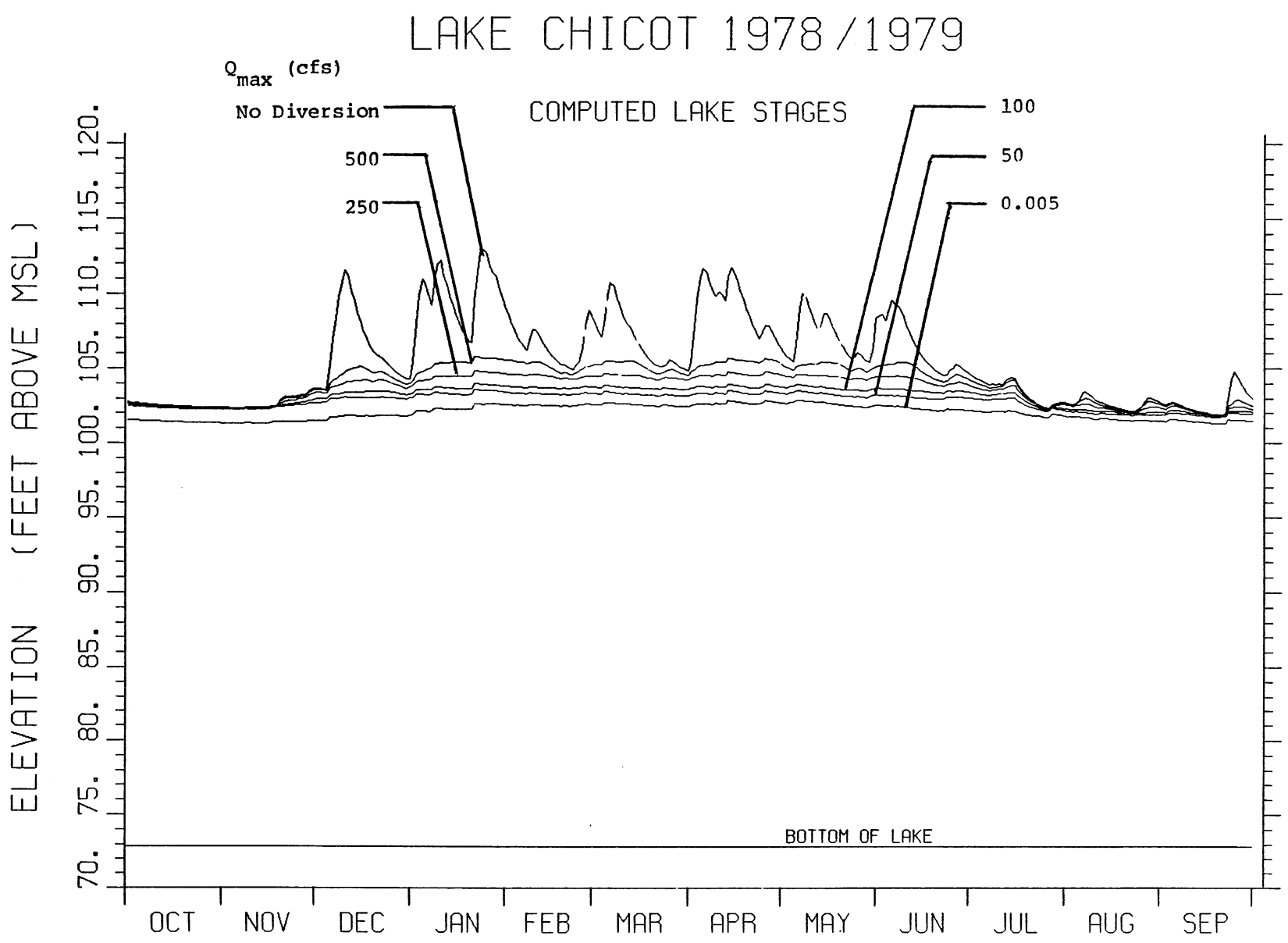

FIGURE XIII-3

LAKE CHICOT 1976/1977

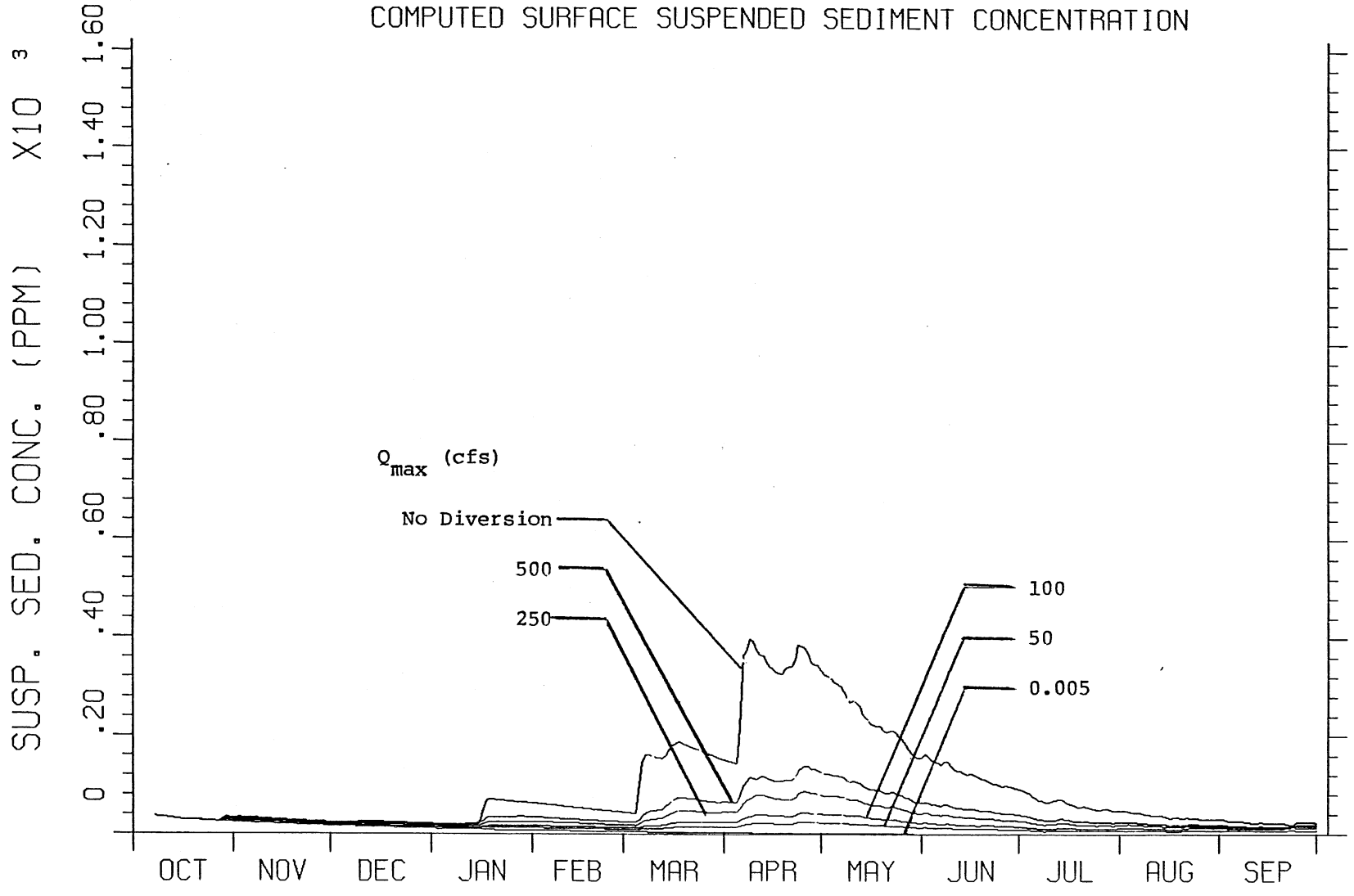

FIGURE XIII-4

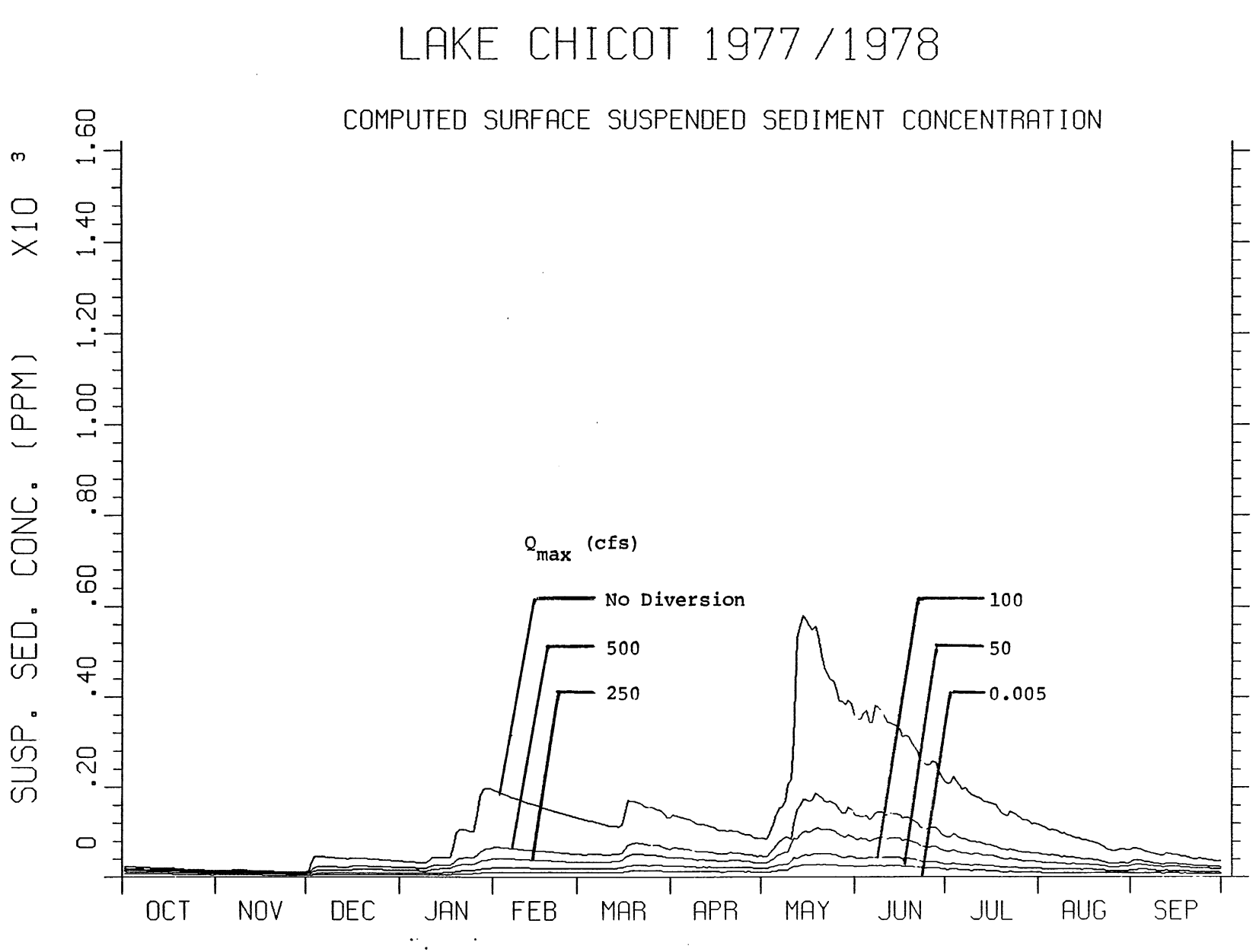

FIGURE XIII-5

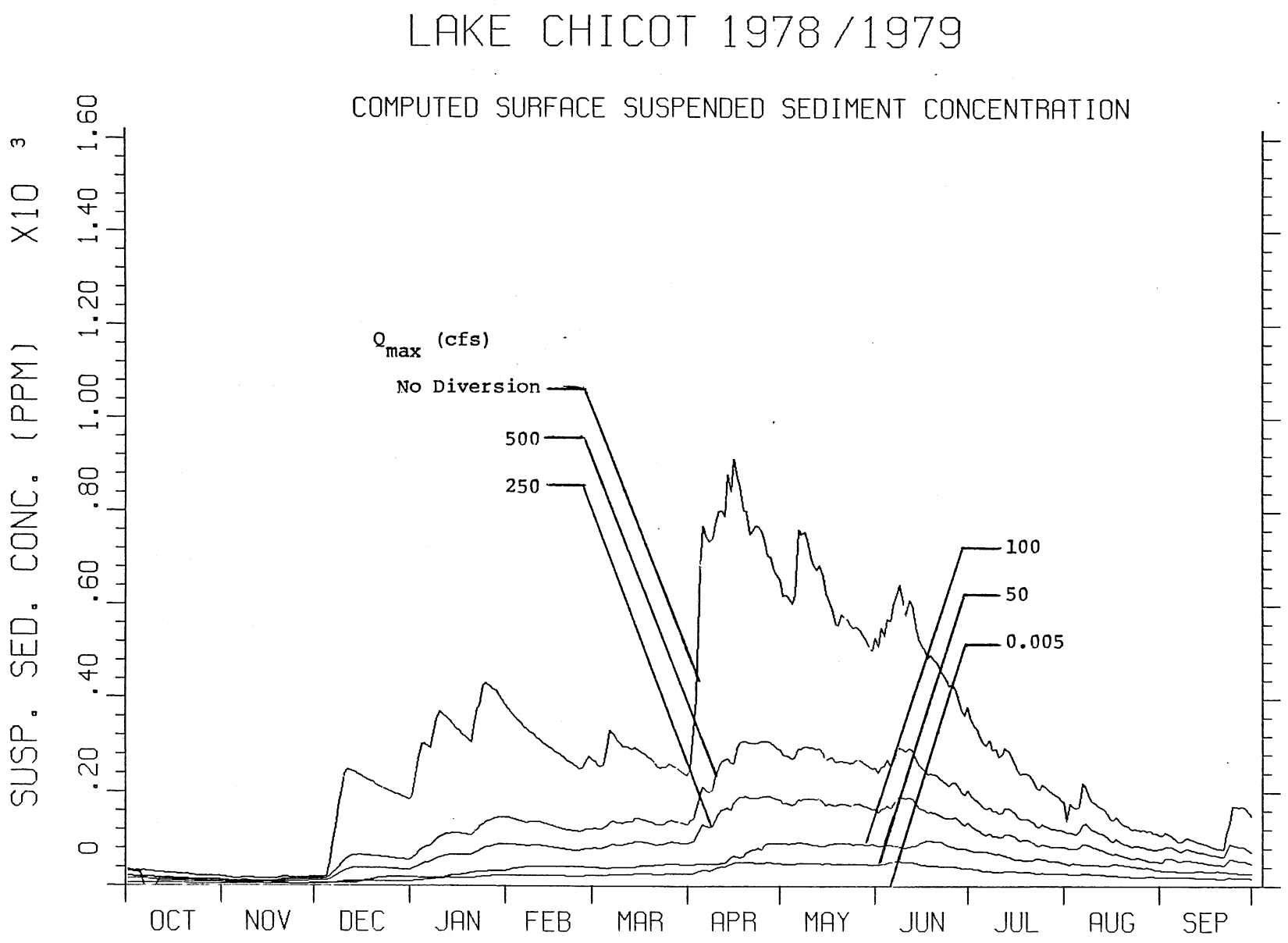

FIGURE XIII-6

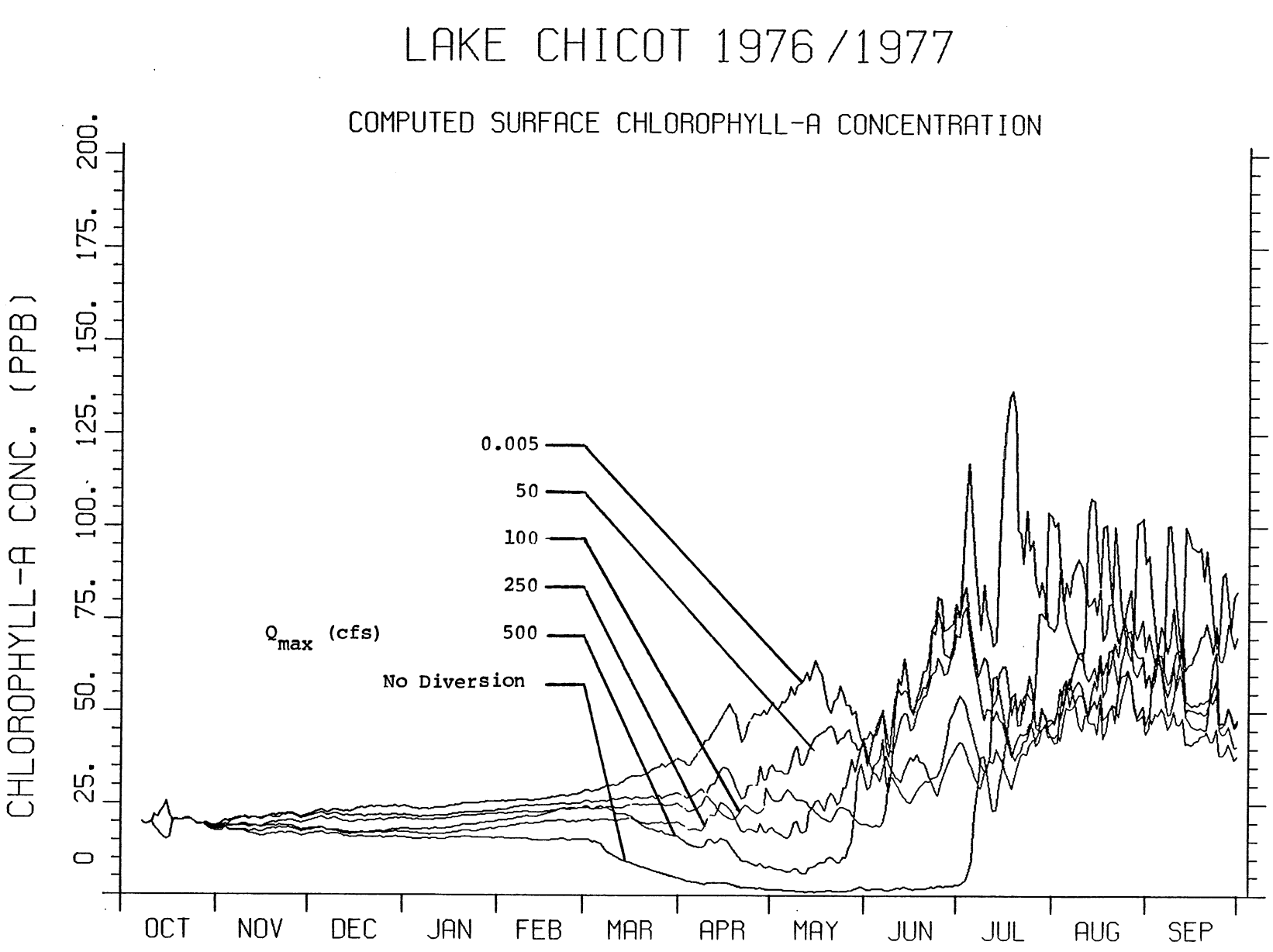

FIGURE XIII-7

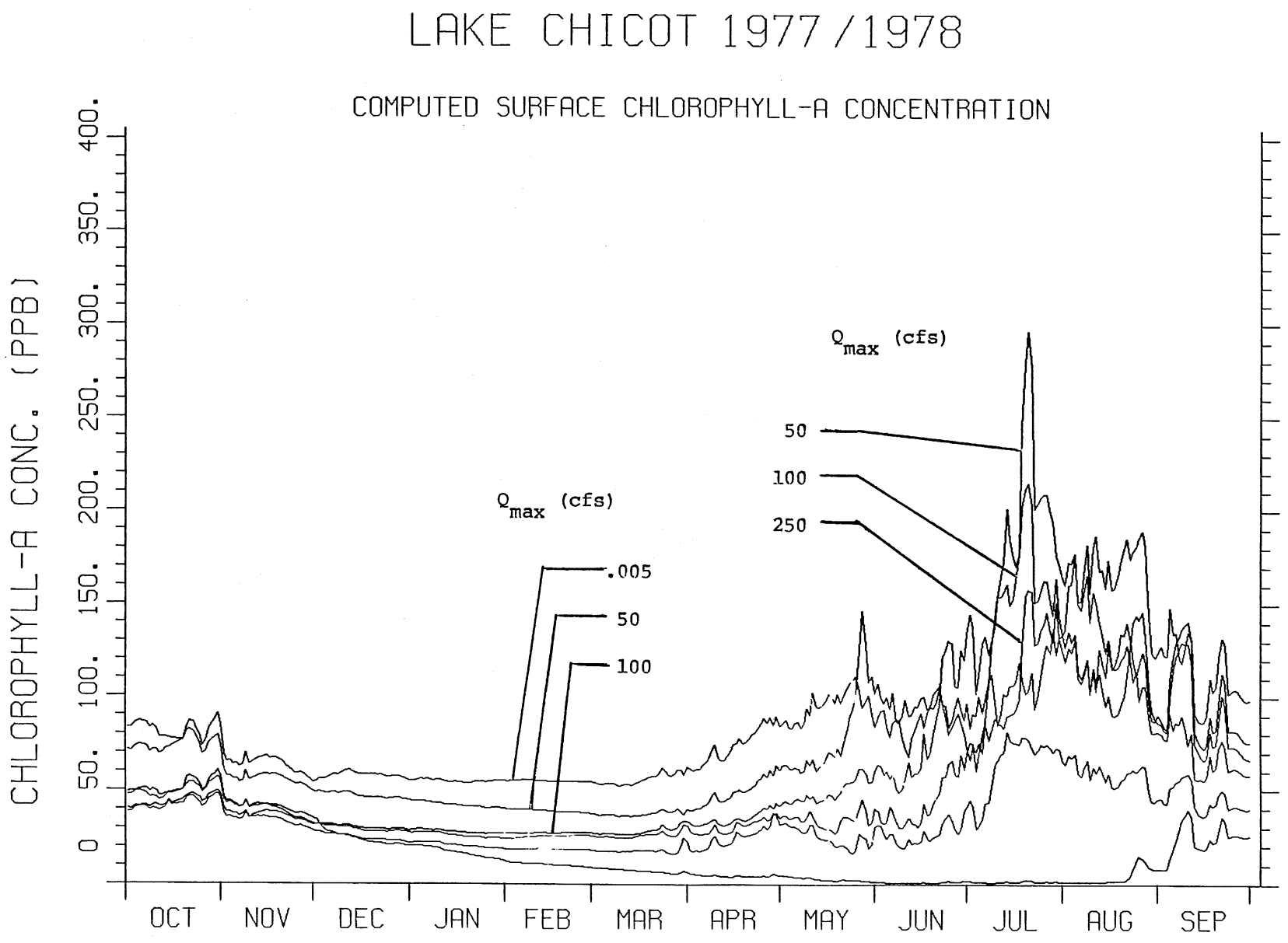

FIGURE XIII-8

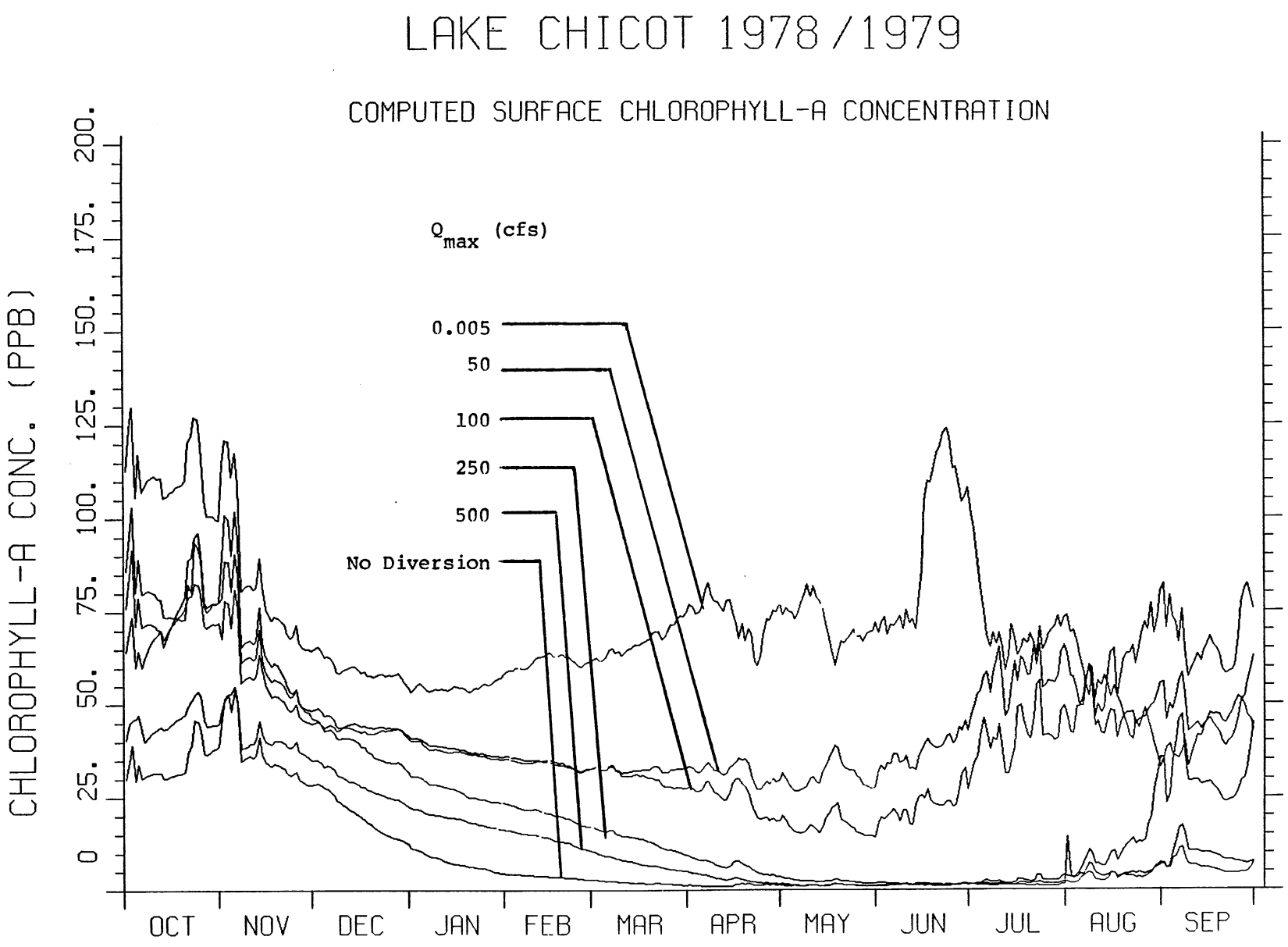

FIGURE XIII-9

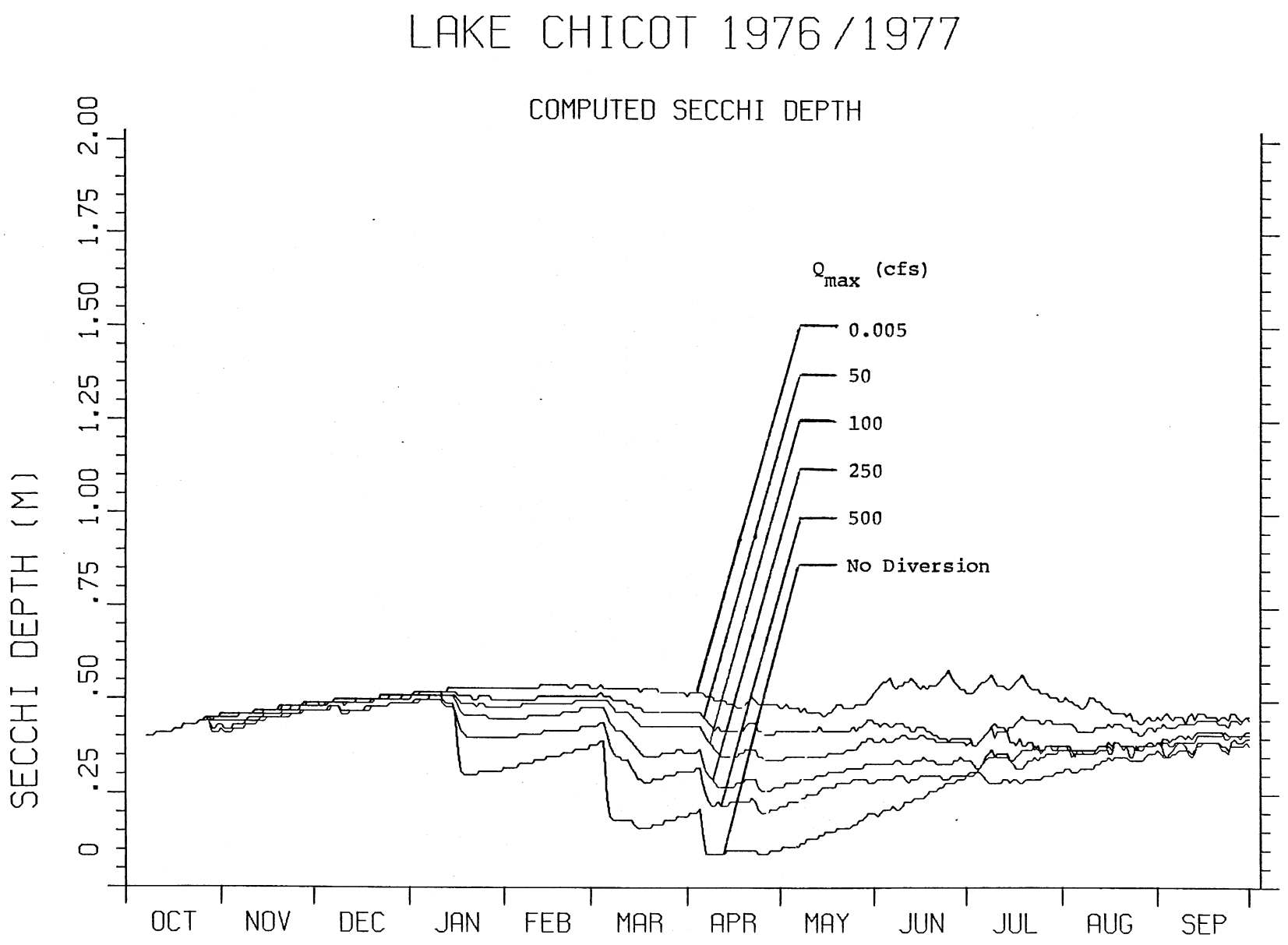

FIGURE XIII-10

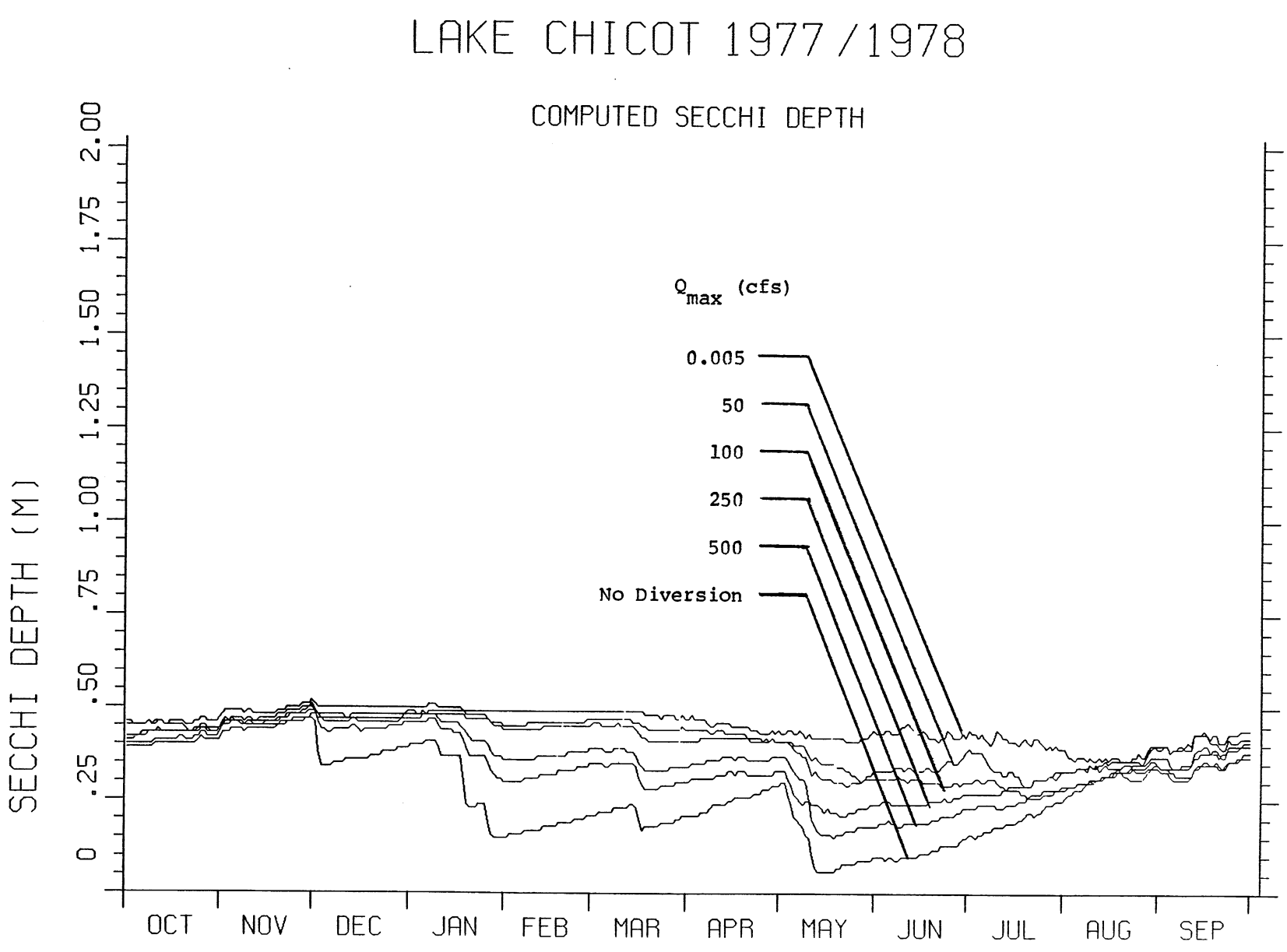

FIGURE XIII-11

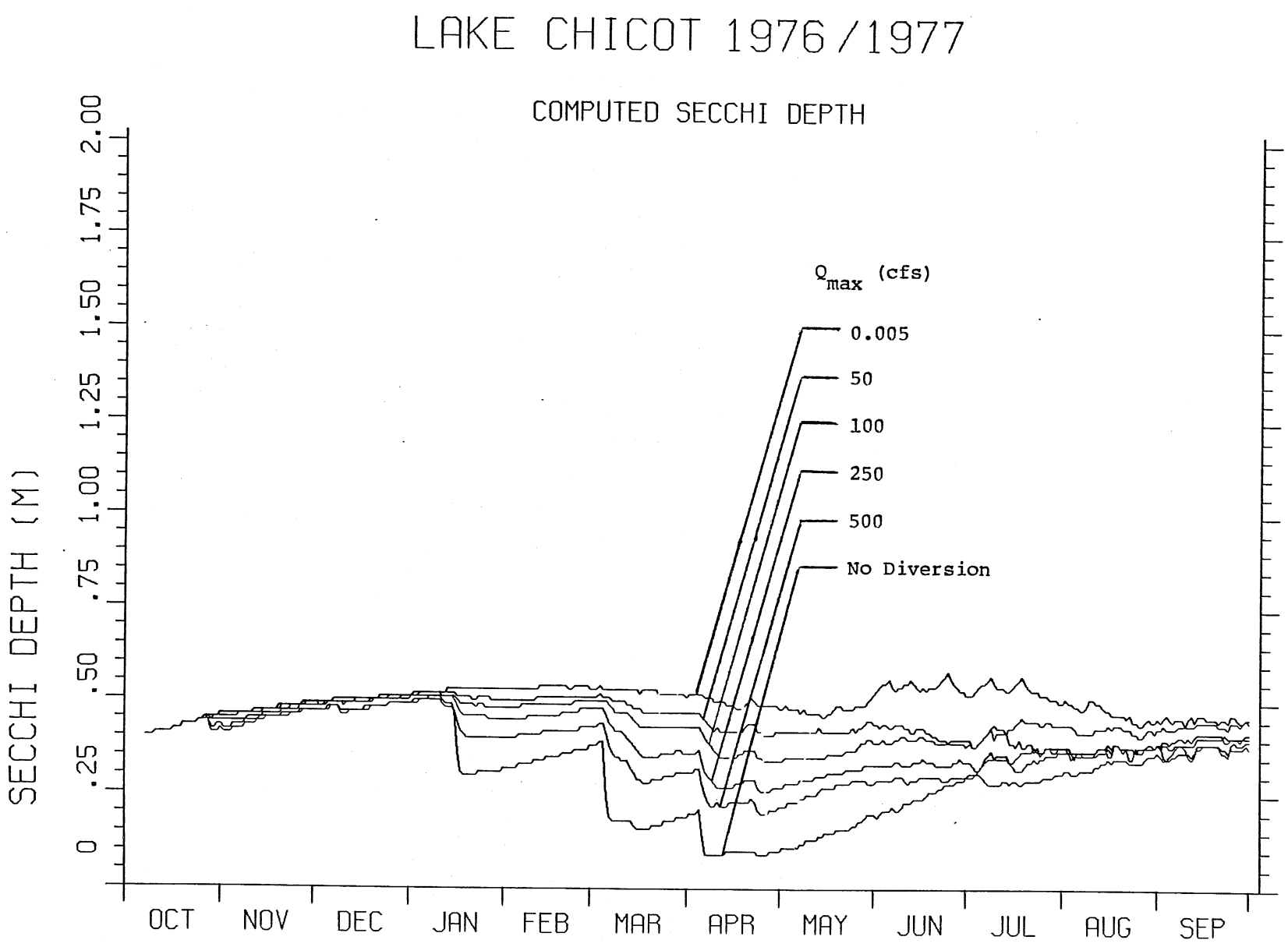

FIGURE XIII-10

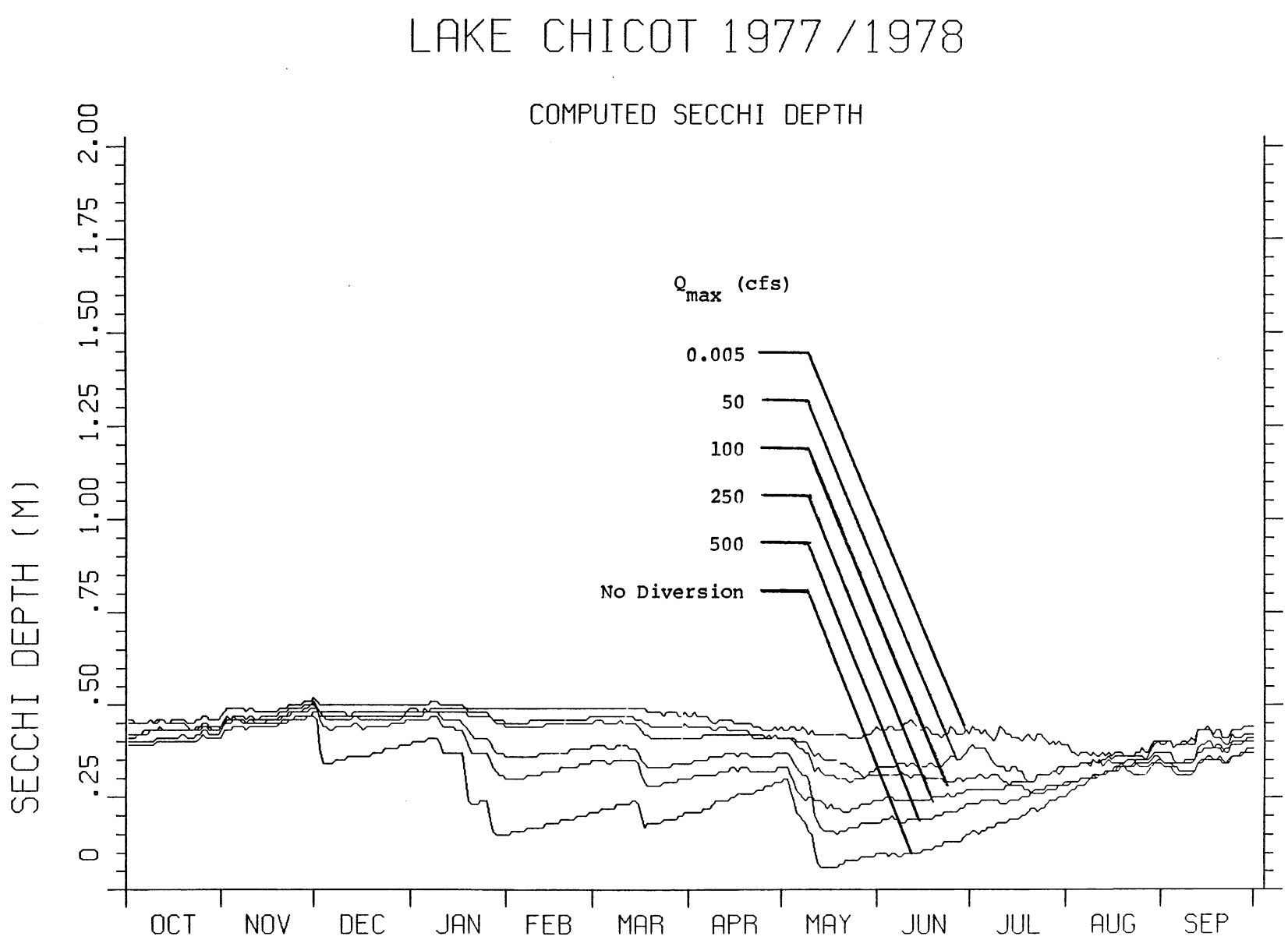

FIGURE XIII-11

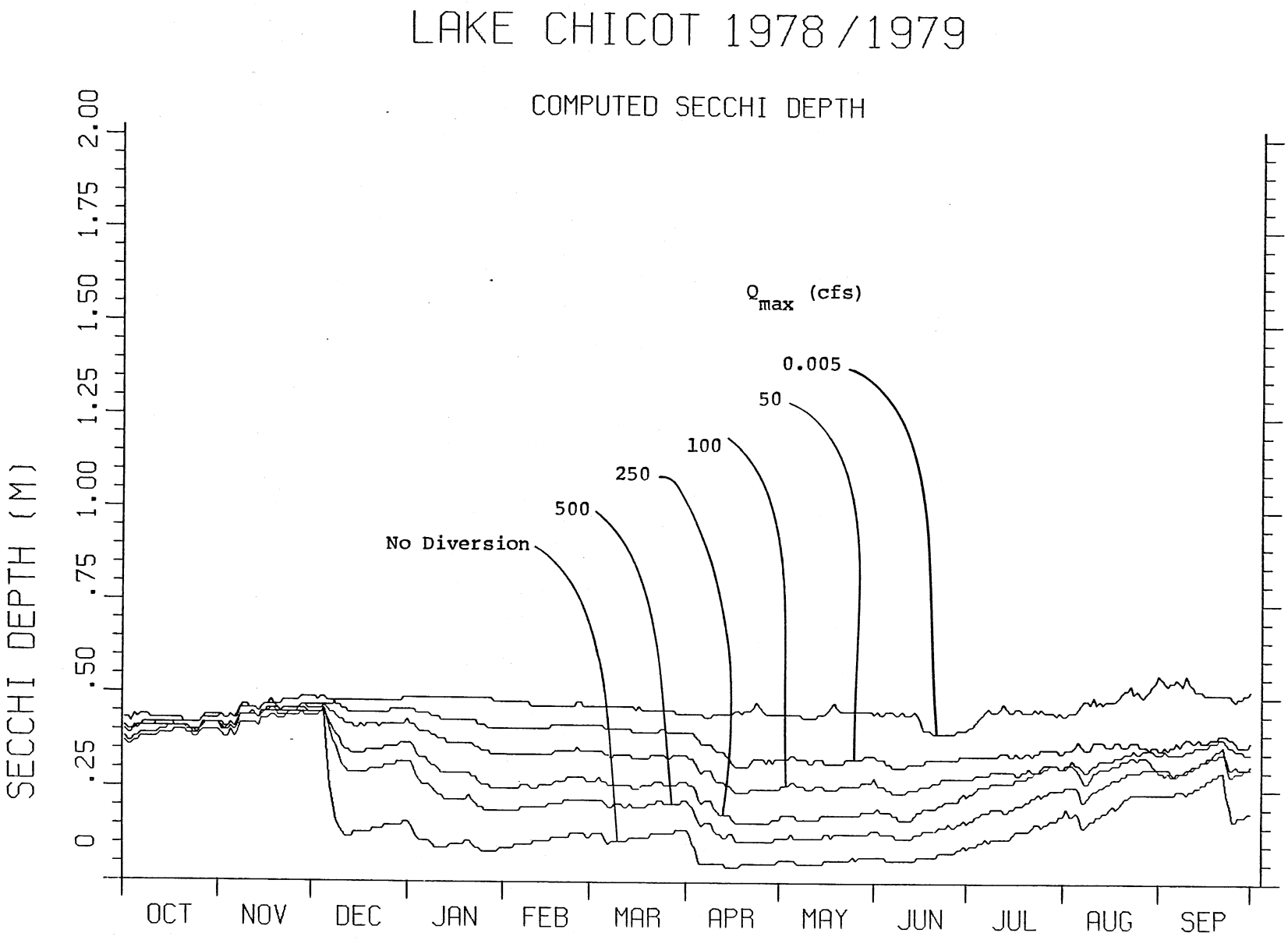

FIGURE XIII-12

XVI. BIBLIOGRAPHY

1. Akiyama, J. and Stefan, H. G., "Theory of Plunging Flow into a Reservoir," University of Minnesota, St. Anthony Falls Hydraulic Laboratory, Internal Memorandum No. IM-97, 83 pp., Dec., 1981.

2. Bacon, E. J., "Primary Productivity, Water Quality, and Limiting Factors in Lake Chicot," Arkansas Water Resources Research Center, Fayetteville, AR. Publ. No. 56, 1978.

3. Bacon E. J., "Primary Productivity in Lake Chicot, Chicot County, Arkansas, Quarterly Progress Reports, University of Arkansas, Monticello, AR, Oct. 1977-Sept. 1980.

4. Baker, L. "Concepts of a Nitrogen Cycling Model of Lake Chicot, Arkansas," University of Minnesota, St. Anthony Falls Hydraulic Laboratory, Internal Memorandum No. 99, July, 1982.

5. Burns, N.M. and Rosa, F., "In Situ Measurement of the Settling Velocity of Organic Carbon Particles and 10 Species of Phytoplankton," Limnol. Oceanogr., 25(5), 1980.

6. Bowen, I.S. "The Ratio of Heat Loss by Construction and by Evaporation from Any Water Surface," Phys. Review, Vol. 27, pp. 779-787, 1926.

7. Brezonik, P. L., "Effect of organic color and turbidity on Secchi disk transparency," Jour. Fish Res. Board, Canada, 35:1410-1416, 1978.

8. Canale, R. P. and Vogel, A. H., "Effects of Temperature on Phytoplankton Growth," ASCE, Jour. Env. Engr. Div., Vol. 100, EE1, pp. 231-241, 1974.

9. Cardoni, J. J. and Hanson, M. J., "Lake Chicot Intensive Field Investigations, June 30 to July 10, 1981," University of Minnesota, St. Anthony Falls Hydraulic Laboratory, External Memorandum No. 176, 92 pp., Dec., 1981.

10. Cardoni, J. J. and Stefan, H. G., "A Model for Light and Temperature Limited Primary Productivity in Lake Chicot," University of Minnesota, St. Anthony Falls Hydraulic Laboratory External Memorandum M-177, 46 pp., May, 1982a.

11. Cardoni, J. J., Hanson, Mark J., and Stefan, H. G., "A Model of Phosphorus Available for Phytoplankton Growth in Lake Chicot, University of Minnesota, St. Anthony Falls Hydraulic Laboratory External Memorandum M-178, July, 1982.

12. Chen, C. W., "Concepts and Utilities of Ecological Model," ASCE, Jour. Sanitary Engr. Div., Vol. 96, pp. 1085-97, Oct., 1970.

13. Combs, W. S., "The Measurement and Prediction of Irradiance Available for Photosynthesis by Phytoplankton in Lakes," Ph. D. thesis, Universityof Minnesota, Minneapolis, 1977.

14. Cooper, C. M. and Bacon, E. J., "Effects of Suspended Sediments on Primary Productivity in Lake Chicot, Arkansas," Proc., Sym. on Surface Water Impoundments, June, 1980, Minneapolis, Minnesota, publ. by American Society of Civil Engineers, Oct., 1981.

15. Dake, J.M.K., "Evaporative Cooling of a Body of Water," Water Resources Research, Vol. 8, No. 4, Aug., 1972.

16. Dake, J.M.K. and Harleman, D.R.F., "Thermal Stratification in Lakes: Analytical and Laboratory Studies," Water Resources Research, Vol. 5, No. 2, pp. 404-495, 1969.

17. Dhamotharan, S., "A Mathematical Model for Temperature and Turbidity Stratification Dynamics in Shallow Reservoirs," Ph. D. Thesis, University of Minnesota, 319 pp., March, 1979.

18. Dhamotharan, S., Gulliver, J., and Stefan, H., "Unsteady One-Dimensional Setling of Suspended Sediment," Water Resources Research, Vol. 17, No. 4, pp. 1125-1132, Aug., 1981.

19. Dhamotharan, S., Stefan, H. G., and Schiebe, F. R., "Turbid Reservoir Stratification Modelling," Proceedings, 26th Annual Hydraulic Div. Specialty Conf., ASCE, Univ. of Maryland, College Park, Maryland, Aug., 1978.

20. DiGiano, F. A., Lijklema, L., and Van Stratan, G., "Wind Induced Dispersion and Algal Growth in Shallow Lakes," Ecological Modelling, Vol. 4, pp. 237-252, 1978.

21. DiToro, D. D., "Applicability of Cellular Equilibrium and Monod Theory to Phytoplankton Growth Kinetics," Ecol. Modelling, Vol. 8, 1980, pp. 201-218.

22. Environmental Protection Agency, Report on "Chicot Lake, Chicot County, Arkansas, EPA Region VI." National Eutrophication Survey, Environmental Monitoring and Support Laboratory, Las Vegas, NV and Corvallis Environmental Research Laboratory, Corvallis, OR. Working Paper No. 484, 17 pp., 1977.

23. Eppley, R. W., "Temperature and Phytoplankton Growth in the Sea," Fish. Bull., 70:1063-1085, 1972.

24. Field, S. D. and Effler, S. W. Photosynthesis-Light Mathematical Formulations, Jour. Env. Engr. Div., ASCE, Vol. 108, EE1, pp. 199-203, 1982.

25. Filatov, N. N., Rjanzhin, S.V., and Zaycev, L. V., "Investigation of Turbulence and Langamir Circulation in Lake Ladoga," Jour. of Great Lakes Research, Vol. 17, No. 1, pp. 1-6, 1981.

26. Ford, D. E., "Water Temperature Dynamics of Dimictic Lakes: Analysis and Prediction Using Integral Energy Concepts," Ph. D. thesis, University of Minnesota, June, 1976.

27. Ford, D. E. and Stefan, H., "Thermal Prediction Using Integral Energy Model," ASCE, Jour. of the Hydraulics Division, Vol. 106, HY1, pp. 39-55, Jan., 1980.

28. Fu, Alec, "User Instructions for RESQUAL II, A Dynamic Water Quality Simulation Model for a Shallow Stratified Lake or Reservoir," University of Minnesota, St. Anthony Falls Hydraulic Laboratory, External Memorandum No. 179, July, 1982.

29. Garges, E., "A Manual for PHytoplankton. Primary Production Studies in the Baltic," Baltic Marine Biologists in Cooperation with the Danish Agency of Environmental Protection, Copenhagen, 88 pp., 1975.

30. Gibbs, R. J., Mathews, M. D., and Link, D. A., "The Relationship Between Sphere Size and Settling Velocity," Jour. of Sedimentary Petrology, Vol. 41, No. 1, March, 1971.

31. Goldman, J. C. and Carpenter, E. J., "A Kinetic Approach to the Effect of Temperature on Algae Growth, Limnol. Oceanogr., 19:756-766, 1974.

32. Idso, S. B. and Jackson, R. D., "Termal Radiation from the Atmosphere," Jour. of Geophysical Research, Vol. 74, No. 23, Oct., 1969.

33. Imboden, D. M. and Gachter, R., "A Dynamic Lake Model for Trophic State Prediction," Ecological Modelling, 4:77-98, 1978.

34. Jassby, A. D. and Platt, T., "Mathematical Formulation of the Relationship Between Photosynthesis and Light for PHytoplankton, Limnol. Oceanogr. 21(4), pp. 540-547, 1976.

35. Jorgensen, S. E., Mejer, H., and Friis, M., "Examination of a Lake Model," Ecological Modelling, 4:253-278, 1978.

36. Jorgensen, S. E., Jorgensen, L. A., Kamp-Nielson, L., and Mejer, H.F., "Parameter Estimation in Eutrophication Modelling," 13:111-129, 1981.

37. Lee, G. F., Rast, W., Jones, R. A., "Eutrophication of Water Bodies: Insights for an Age-Old Problem," Environmental Science and Technology, 12:900-908, Aug., 1978.

38. Lewis, S. and Nir, A., "A Study of Parameter Estimation Procedures of a Model for Lake Phosphorus Dynamics," Ecol. Modelling, Vol. 4, pp. 99-117, 1978.

39. Marciano and Harbeck, "Mass Transfer Studies," Lake Hefner Studies, U. S. Geological Survey Professional Paper No. 267, 1954.

40. McDowell, L. L., Schreiber, J. D., and Pionke, H. B., "Estimating Soluble (PO_4-P) and Labile Phosphorus in Runoff from Croplands," CREAMS: A field-Scale Model for Chemicals, Runoff, and Erosion from Agricultural Management Systems, W. G. Knisel, ed., USDA Conservation Research Report No. 26, pp. 509-533, 1980.

41. Murray, F. W., "On the Computation of Saturation Vapor Pressure, Jour. of Applied Meteorology, Vol. 6, No. 1, 1967.

42. Metropolitan Waste Control Commission, St. Paul, Minnesota. Upper Mississippi River Water Quality Modeling Study, 208 Grant, preliminary copy, 131 pp., Nov., 1978.

43. Norton, W. R., Final Report for the Upper Mississippi River Basin Model Project, Water Resources Engineers, Walnut Creek, Calif. 94596, 1974.

44. Nyholm, N., "A Simulation Model for Phytoplankton Growth and Nutrient Cycling in Eutrophic, Shallow Lakes," Ecological Modelling, 4:279-310, 1978.

45. O'Connor, D. J., Thomann, R. V., and DiToro, D., "Dynamic Water Quality Forecasting and Management," Manhattan College, Bronx, New York, EPA-600/3-73-009, 1973.

46. Pedersen, F. B., "A Monograph on Turbulent Entrainment and Friction in Two-Layer Stratified Flow," Institute of Hydrodynamics and Hydraulic Engineering, Techn. University of Denmark, Lyngby, 1980.

47. Rothwell, Edward D. and Fletcher, Bobby P., "Lake Chicot Pumping Plant Outlet Structure, Arkansas," Tech. Report HL-79-10, U. S. Army Waterways Experiment Station, Vicksburg, Miss., June, 1979.

48. Schiebe, F. R., Personal communication, USDA, Durant, OK, 1980.

49. Schiebe, F. R., Farell, J. O., McHenry, J. R., "Water Quality Improvement of Lake Chicot, Arkansas," Proceedings, Symposium on Surface Water Impoundments, Minneapolis, Minnesota, June, 1980, publ. by ASCE, 1981.

50. Swain, A., "Material Budget of Lake Chicot, Ph. D. disseration, University of Mississippi, Oxford, Miss., 190 pp., 1980.

51. Schnoor, J. L. and DiToro, D.M., "Differential Phytoplankton Sinking and Growth Rates: An Eigenvalue Analysis. Ecological Modelling, 9:233-245, 1980.

52. Shapiro, J., personal communication, 1982.

53. Smith, R.A., 1980. The Theoretical Basis for Estimating Phytoplankton Production and Specific Growth Rate from Chlorophyll, Light and Temperature Data, Ecological Modelling, 10:243-264, 1980.

54. Stefan, H. G., Cardoni, J.J., Schiebe, F. R., and Cooper, C. M., "A Model of Light Penetration in Lake Chicot," University of Minnesota, St. Anthony Falls Hydraulic Laboratory, External Memorandum 174, Feb., 1982a.

55. Stefan, H.G., Dhamotharan, S., Schiebe, F. R., "Temperature/Sediment Model for a Shallow Lake," ASCE, Jour. of the Env. Engr. Div., Vol. 108, No. EE4, Aug, 1982b

56. Stefan, H. and Ford, D., "Temperature Dynamics in Dimictic Lakes," ASCE, Jour. of the Hydraulics Div., Vol. 101, HY1, Jan., 1975.

57. Swain, A., "Material Budgets of Lake Chicot," Ph. D. dissertation, University of Mississippi, Oxford, 190 pp., 1980.

58. Tennessee Valley Authority, "The Water Temperature Regime of Fully Mixed Streams," Water Resources Research Laboratory, Report No. 15, 1968.

59. U. S. Naval Observatory, The Air Almanac, 1977 data.

60. Walters (1980)

61. Winter, J. C., "Numerical Simulation of Steady State Three-Dimensional Groundwater Flow Near Lakes," Water Resources Research, Vol. 14, No. 2, pp. 245-254, April, 1978.